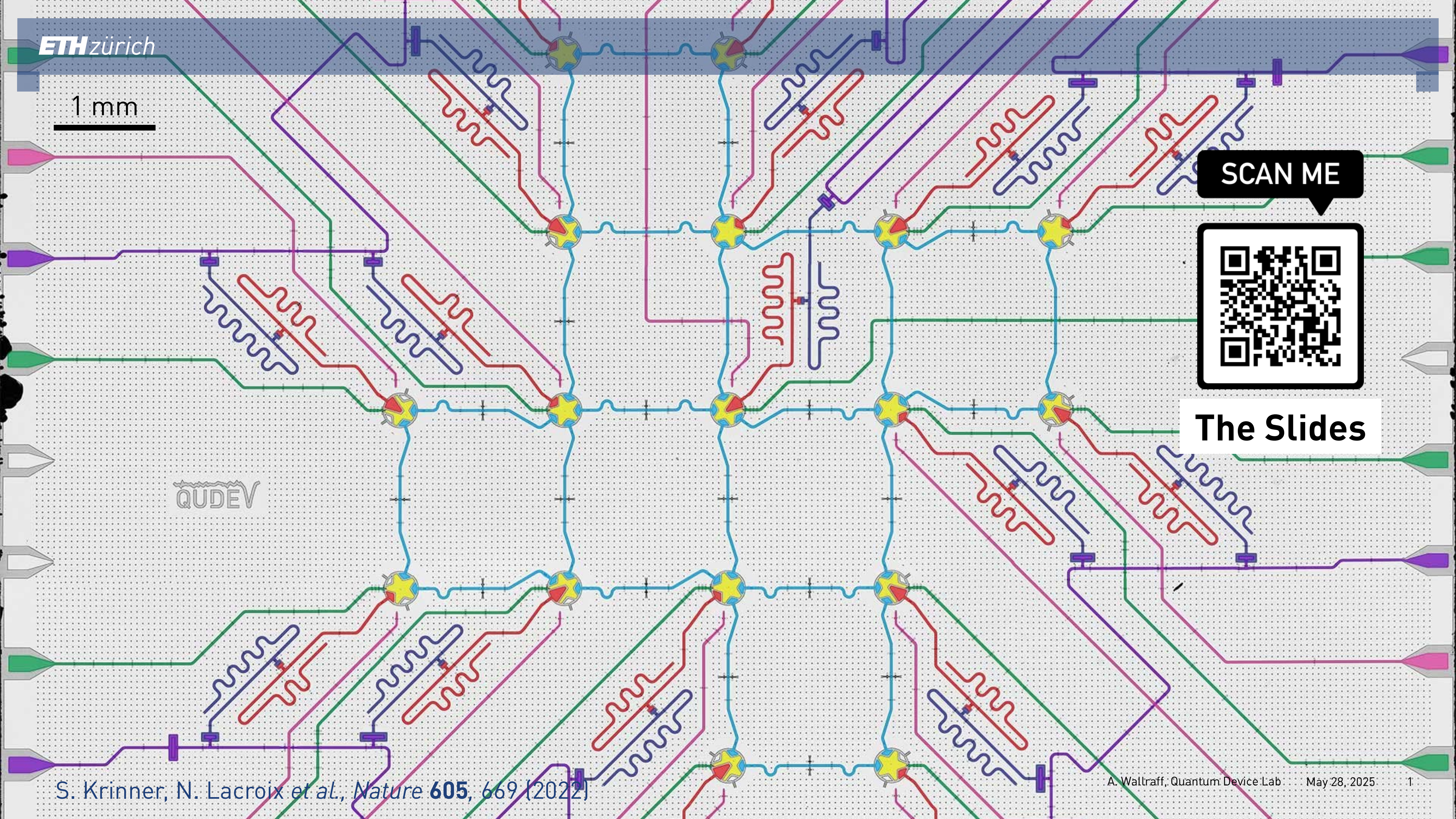

SCAN ME

The Slides

S. Krinner, N. Lacroix *et al.*, *Nature* **605**, 669 (2022)

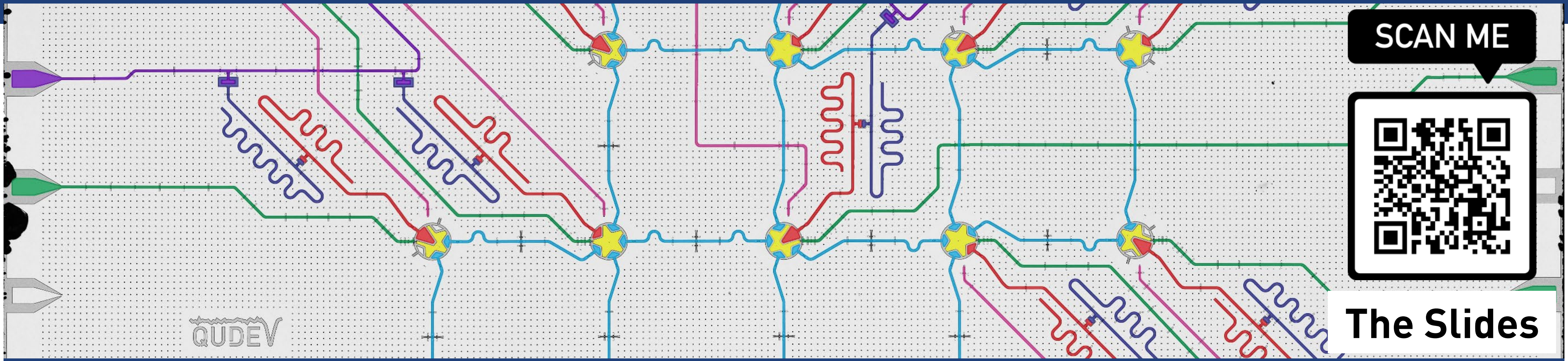

Quantum Error Correction with Superconducting Circuits (Lecture 1)

Sci. Team: E. Al-Tavil, L. Beltran, I. Besedin, J.-C. Besse, D. Colao Zanuz, Xi Dai, K. Dalton, J. Ekert, S. Frasca, A. Grigorev, D. Hagmann, C. Hellings, A. Hernandez-Anton, I. Hesner, L. Hofele, M. Kerschbaum, S. Krinner, A. Kulikov, N. Lacroix, M. Pechal, K. Reuer, A. Rosario, C. Scarato, J. Schaer, Y. Song, F. Swiadek, F. Wagner, A. Wallraff *(ETH Zurich)*
Eng. & Tech. Team: A. Akin, M. Bahrani, A. Flasby, A. Fauquex, R. Keller, N. Kohli, R. Siegbert, M. Werner *(ETH Zurich)*

IARPA BE THE FUTURE
Schweizerischer Nationalfonds
Innovation project supported by
Schweizerische Eidgenossenschaft
Confédération suisse
Confederazione Svizzera
Confederaziun svizra
Swiss Confederation
Innosuisse – Swiss Innovation Agency

Past Group Members & Current Collaboration Partners

www.qudev.ethz.ch

Former group members now
Faculty/PostDoc/PhD/Industry

A. Abdumalikov (Gorba AG)
M. Allan (LMU Munich)
C. K. Andersen (TU Delft)
M. Baur (ABB)
J. Basset (U. Paris Sud)
S. Berger (AWK Group)
R. Bianchetti (ABB)
D. Bozyigit (Scandit)
R. D. Buijs (ASML)
M. Collodo (Zurich Instruments)
A. Copetudo (NU Singapore)
C. Eichler (FAU Erlangen)
A. Fedorov (UQ Brisbane)
Q. Ficheux (CNRS Grenoble)
S. Filipp (WMI & TU Munich)
J. Fink (IST Austria)
A. Fragner (Kappa)
T. Frey (Bosch)
M. Gabureac (PSI)
S. Garcia (College de France)
S. Gasparinetti (Chalmers)
M. Goppl (Sensirion)
J. Govenius (VTT)
J. Heinsoo (IQM)
J. Herrmann (QuantrolOx)
L. Huthmacher (Stellbrink & Prtnr)
D.-D. Jarausch (Leica)
K. Juliusson (IQM)
P. Kurpiers (Rohde & Schwarz)
J. Krause (U. Of Cologne)
S. Krinner (Zurich Instruments)
C. Lang (Radionor)
S. Lazar (Zurich Instruments)
P. Leek (Oxford)
S. M. Llima (BSC-CNS)
J. Luetolf (D-PHYS, ETH Zurich)
P. Magnard (Alice and Bob)
P. Maurer (Chicago)
J. Mlynek (Siemens)
M. Mondal (IACS Kolkata)
G. Norris (AWS)
M. Oppliger
J. O'Sullivan (CEA Saclay)
A. Potocnik (imec)
G. Puebla (QZabre)
A. Remm (Atlantic Quantum)
A. Safavi-Naeini (Stanford)
Y. Salathe (Zurich Instruments)
P. Scarlino (EPF Lausanne)
M. Stammeier (Huba Control)
L. Steffen (AWK Group)
A. Stockklauser (Rigetti)
T. Thiele (Zurich Instruments)
I. Tsitsilin (TUM)
J. Ungerer (Harvard)
A. van Loo (RIKEN)
D. van Woerkom (Microsoft)
J. Waissman (HUJI)
T. Walter (deceased)
L. Wernli (Sensirion)
A. Wulff
S. Zeytinoğlu (Harvard)

Collaborations (last 5 years) with groups of

C. Abellan (Quside)
P. Bertet (CEA Saclay)
A. Blais (Sherbrooke)
J. Bylander (Chalmers)
H. J. Carmichael (Auckland)
A. Chin (Cambridge)
I. Cirac (MPQ)
K. Ensslin (ETH Zurich)
M. Hartmann (FAU Erlangen)
T. Ihn (ETH Zurich)
A. Imamoğlu (ETH Zurich)
F. Marquardt (MPL Erlangen)
F. Merkt (ETH Zurich)
A. Messmer (Zurich Instruments)
M. W. Mitchell (ICFO)
M. Müller (RWTH Aachen, FZJ)
M. A. Martin-Delgado (Madrid)
M. Poggio (Basel)
B. Royer (Sherbrooke)
N. Sangouard (CEA Saclay)
H. Tureci (Princeton)
W. Wegscheider (ETH Zurich)

ETH Eidgenössische Technische Hochschule Zürich
Swiss Federal Institute of Technology Zurich
FNSNF Swiss National Science Foundation
QSIT Quantum Science and Technology — National Centre of Competence in Research
QED Circuit and Cavity Quantum Electrodynamics
erc
Seventh Framework Programme
GEOMDISS
QuSurf
SOLID
aqute
scaleQIT

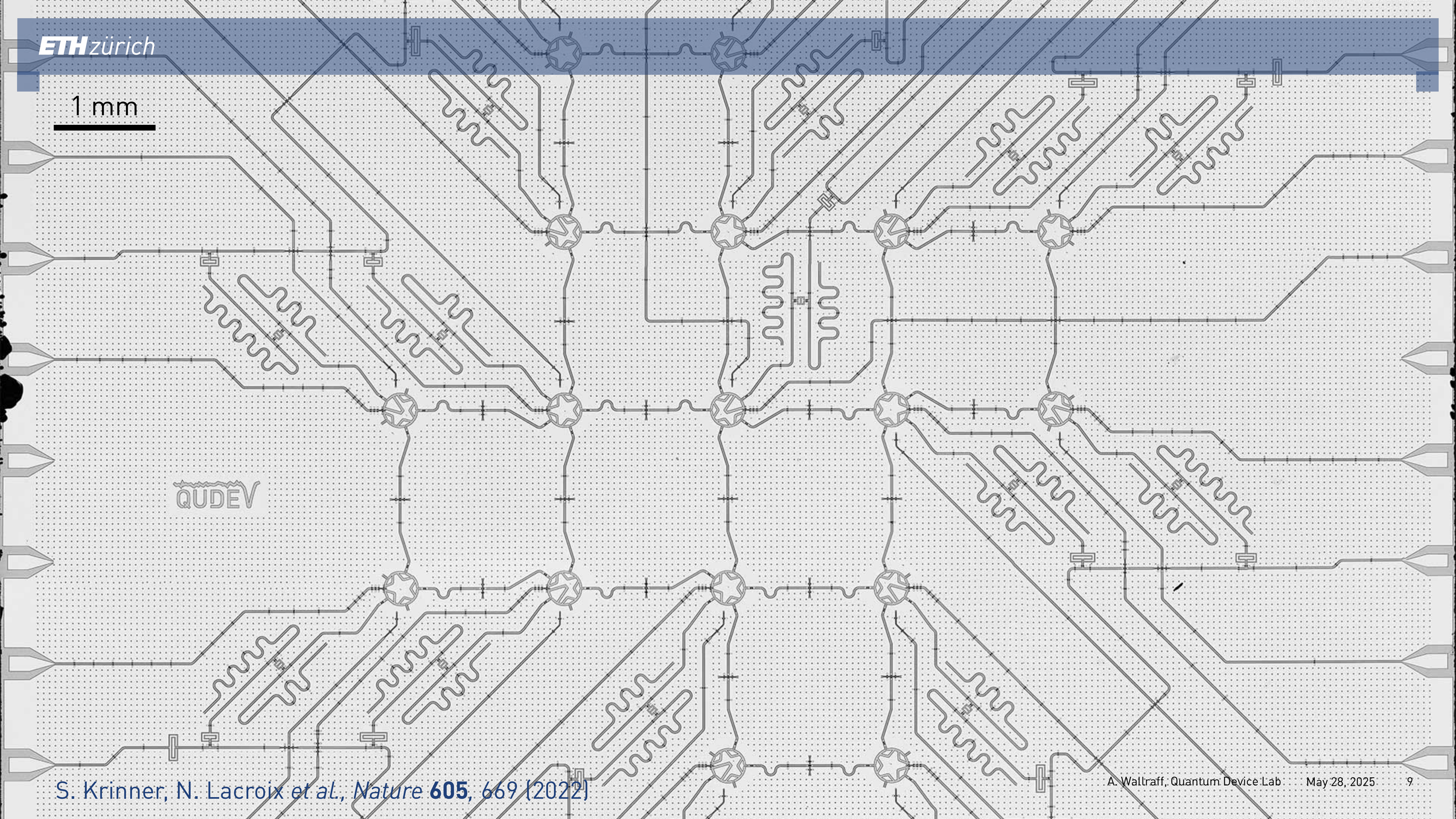

S. Krinner, N. Lacroix *et al.*, *Nature* **605**, 669 (2022)

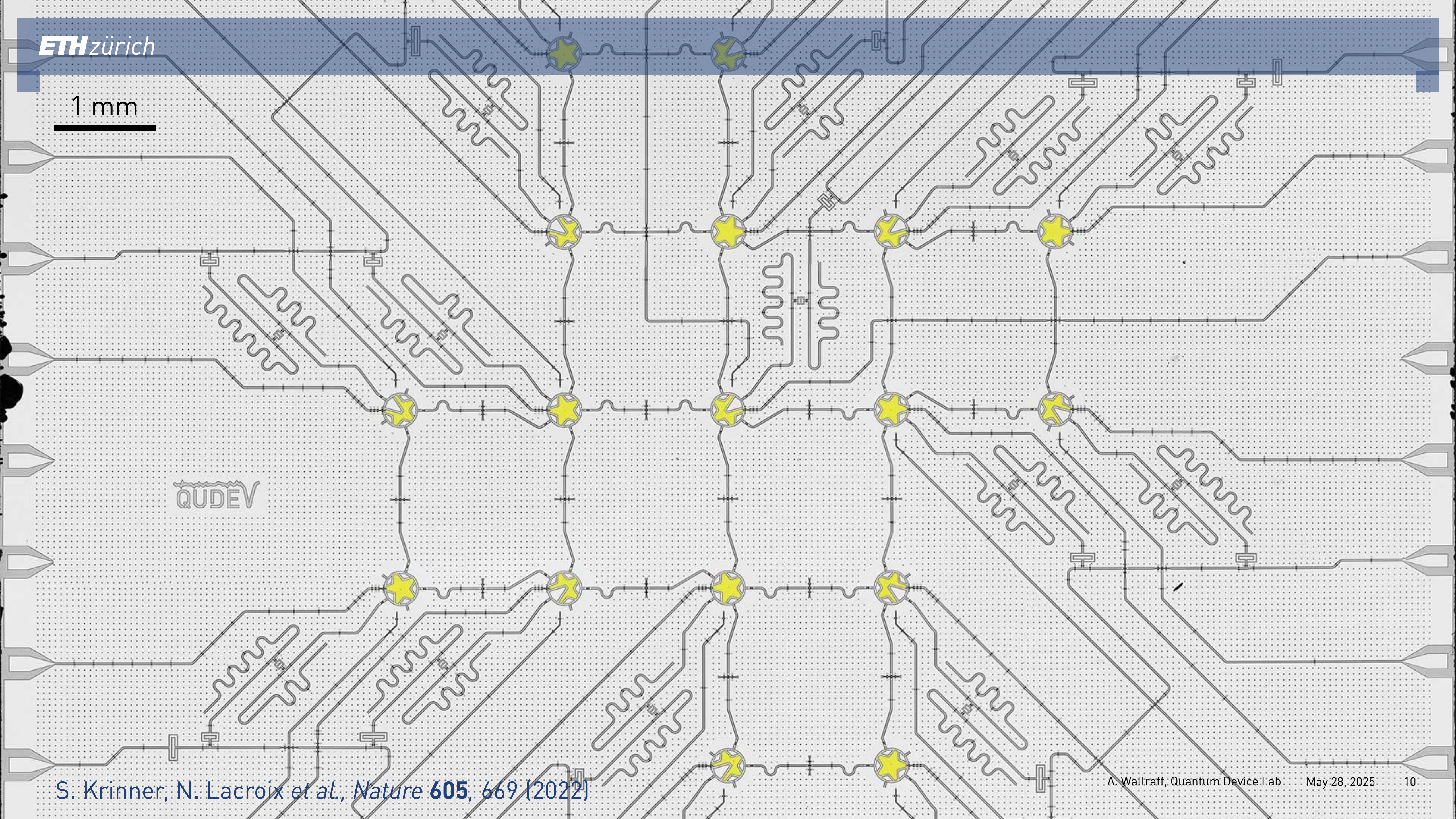

S. Krinner, N. Lacroix *et al.*, *Nature* **605**, 669 (2022)

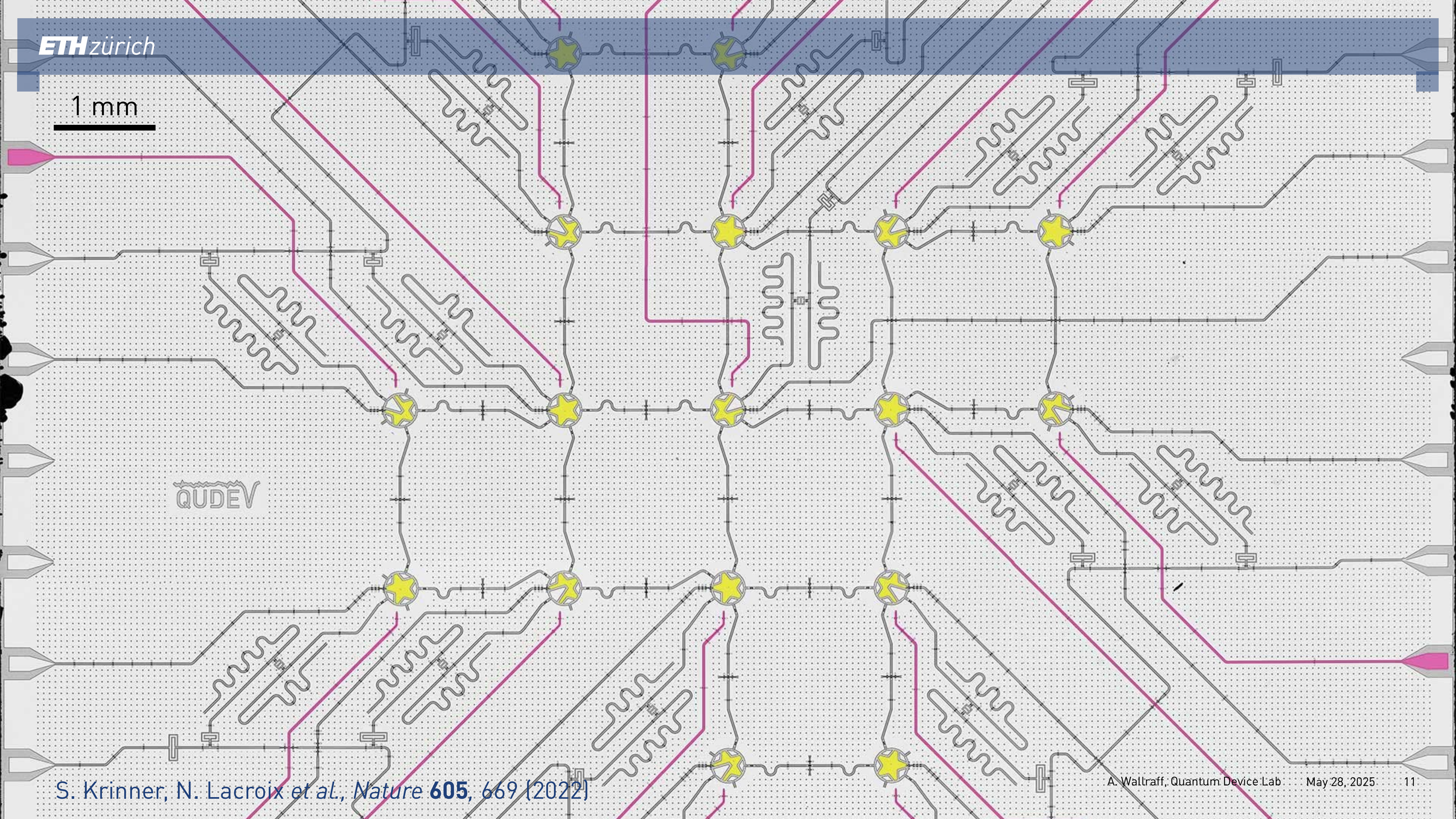

S. Krinner, N. Lacroix *et al.*, *Nature* **605**, 669 (2022)

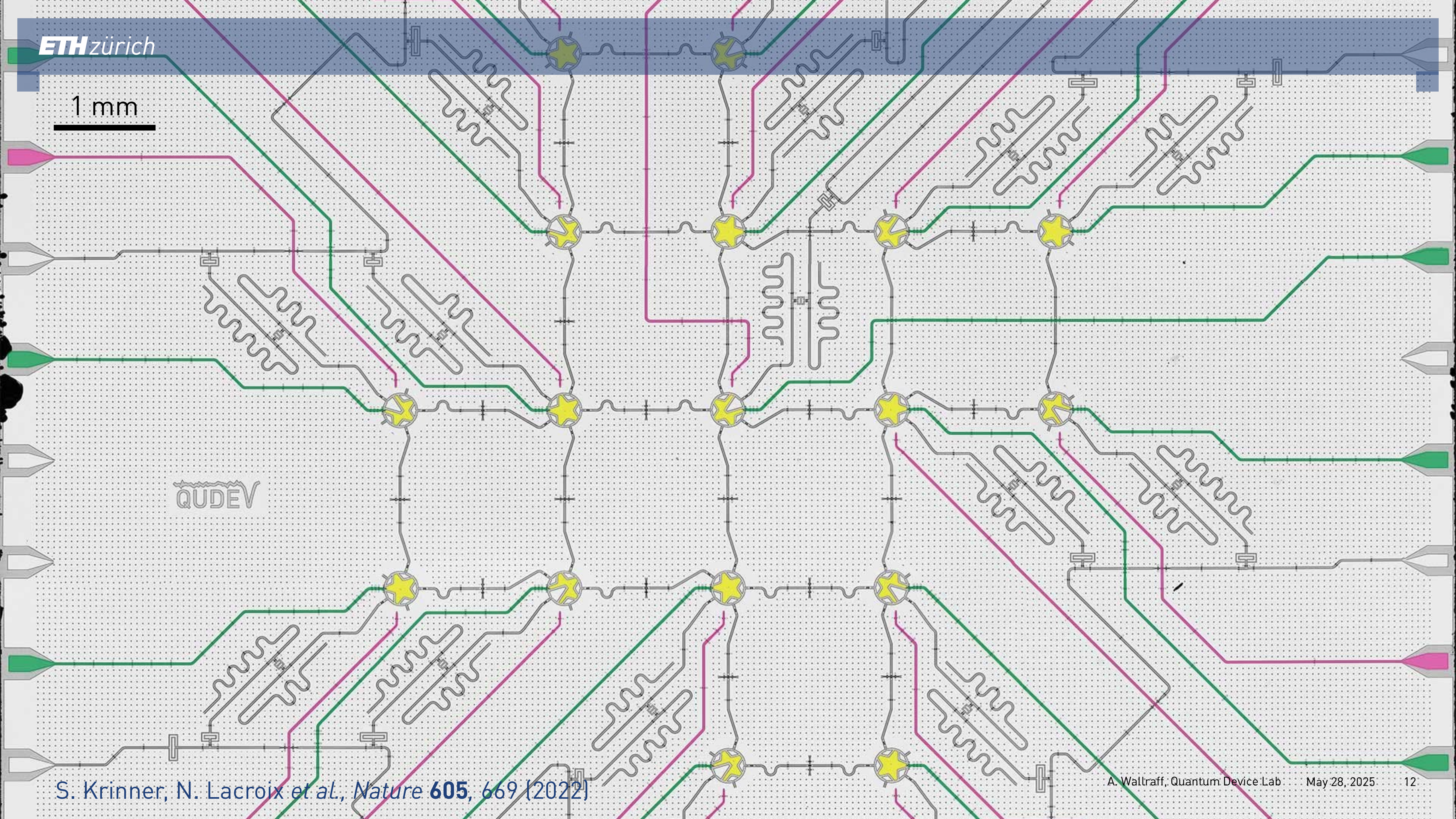

S. Krinner, N. Lacroix *et al.*, *Nature* **605**, 669 (2022)

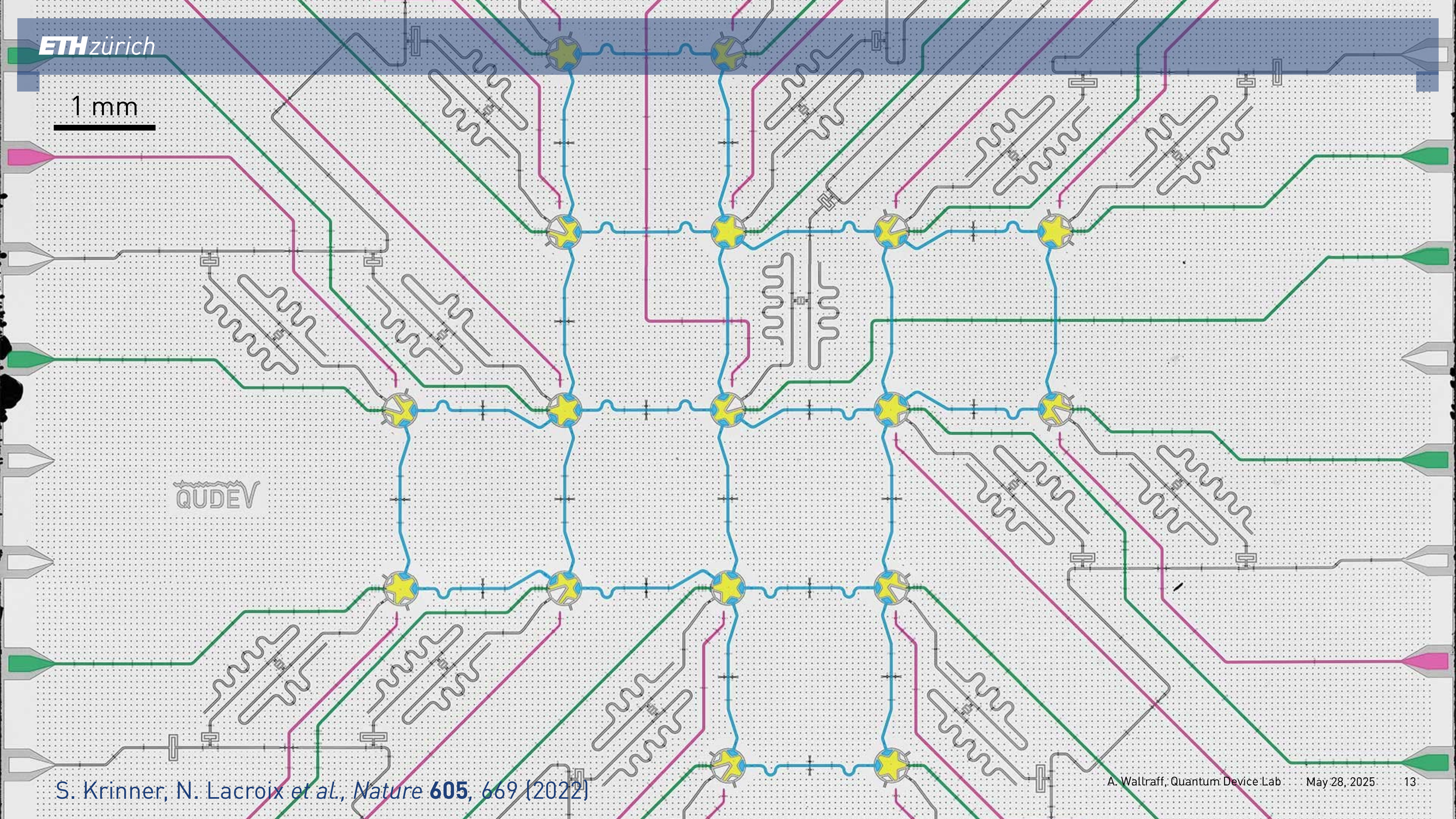

S. Krinner, N. Lacroix *et al.*, *Nature* **605**, 669 (2022)

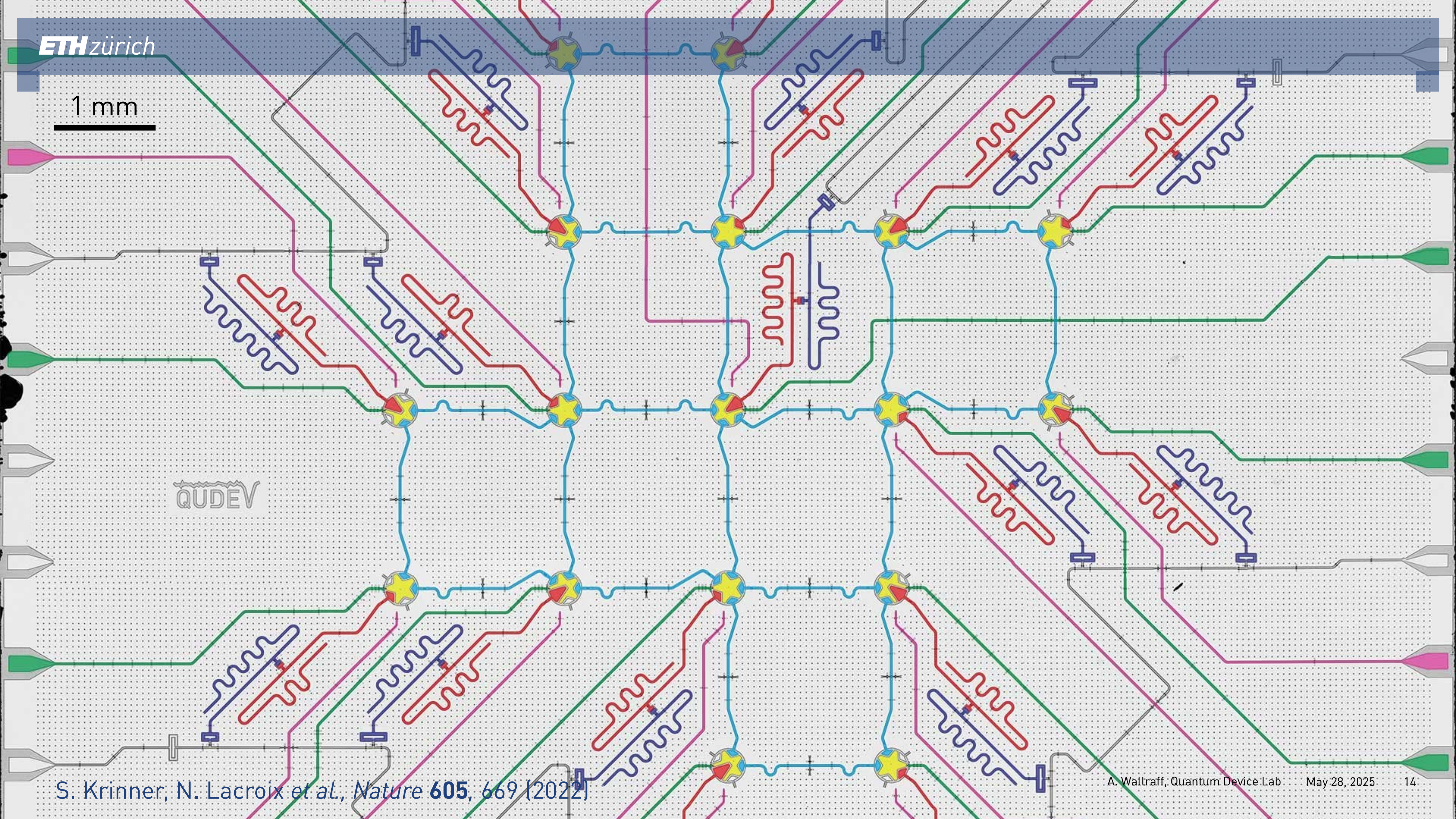

S. Krinner, N. Lacroix *et al.*, *Nature* **605**, 669 (2022)

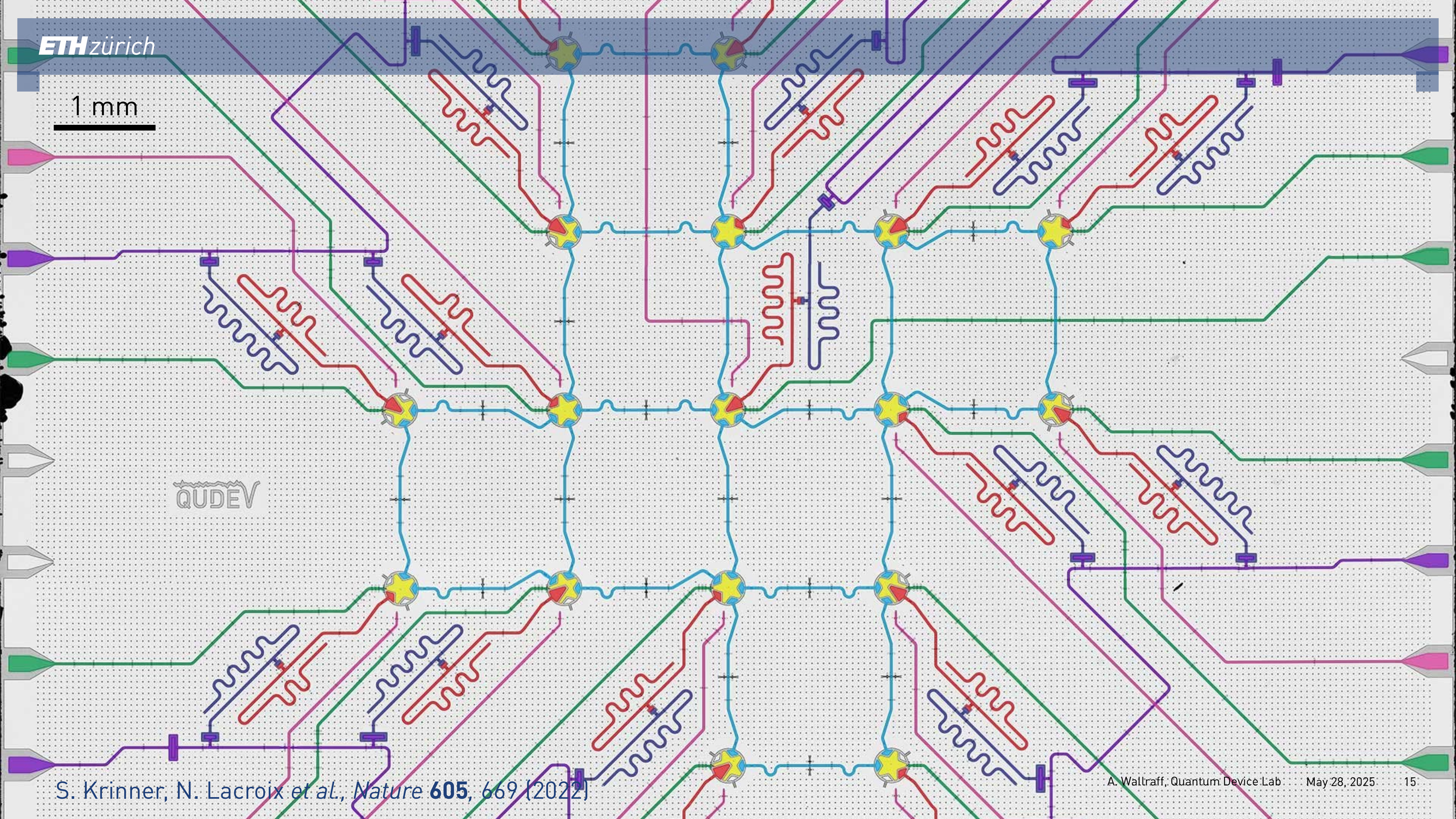

S. Krinner, N. Lacroix *et al.*, *Nature* **605**, 669 (2022)

Close-up of a Superconducting Qubit (Transmon-Style)

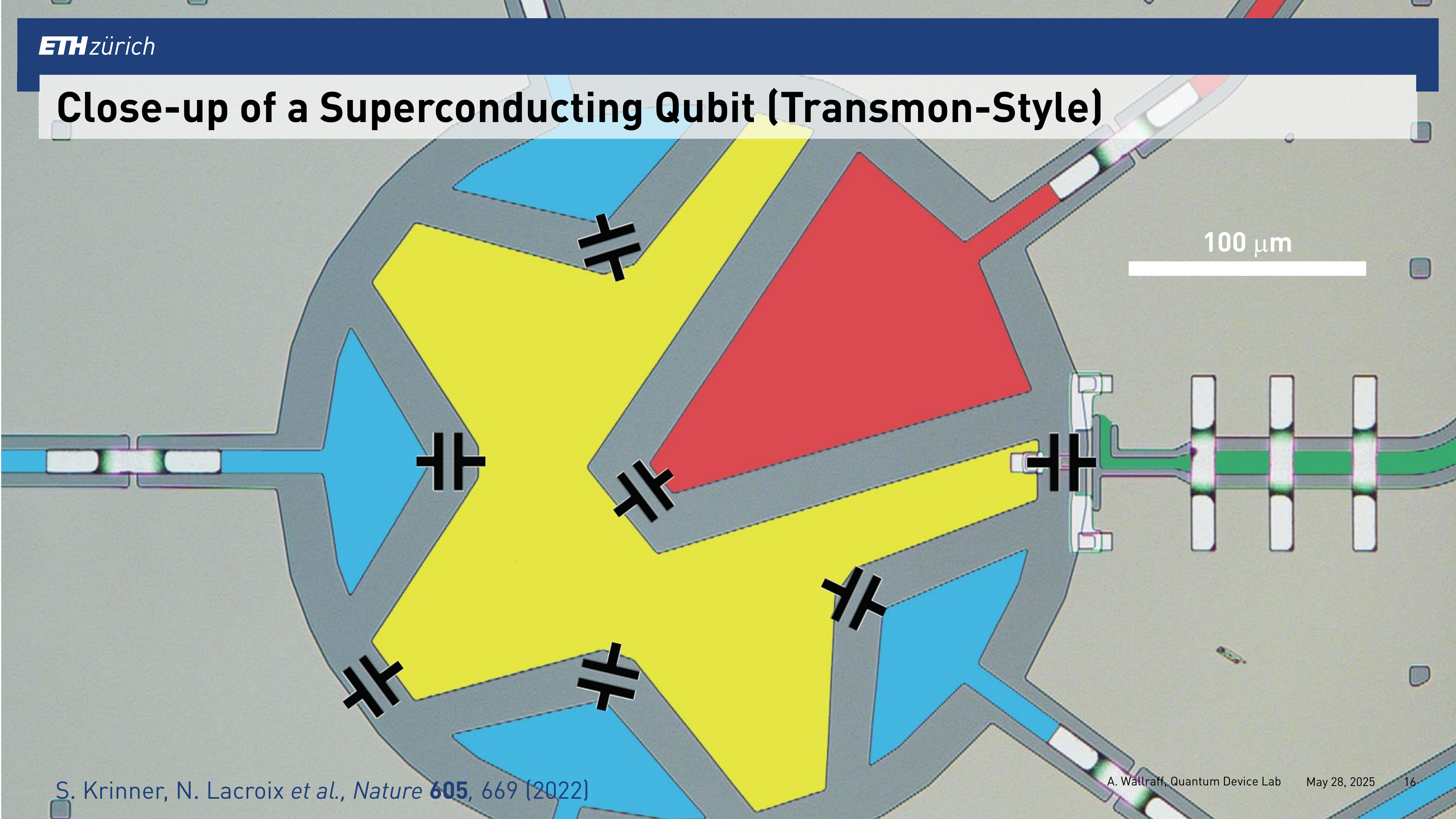

S. Krinner, N. Lacroix *et al.*, *Nature* **605**, 669 (2022)

Tunnel Junctions, SQUID, and Fluxline

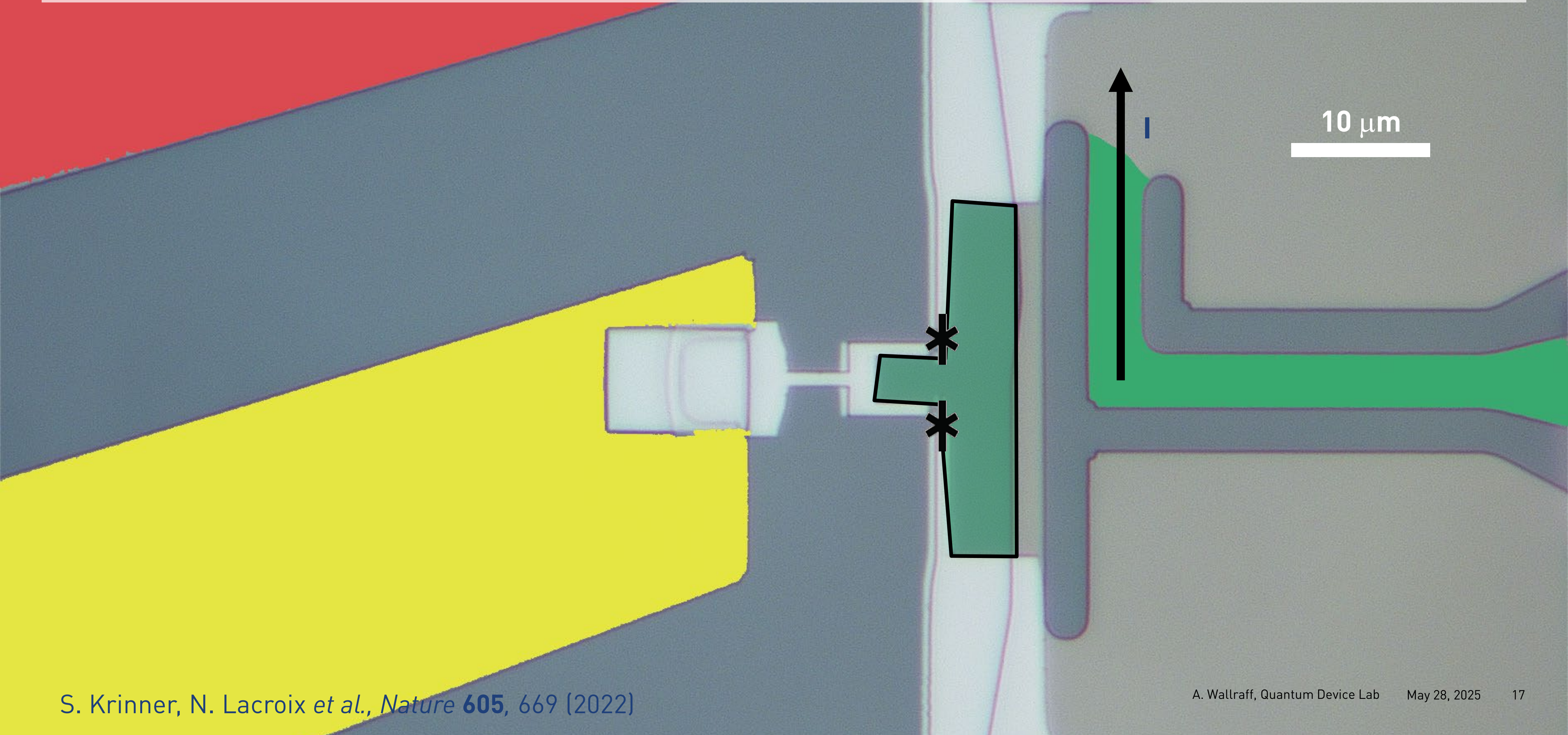

S. Krinner, N. Lacroix *et al.*, *Nature* **605**, 669 (2022)

Two of the Major Goals in Quantum Information Processing ...

... with superconducting circuits

Noisy Intermediate Scale Quantum (NISQ) algorithms displaying a quantum advantage

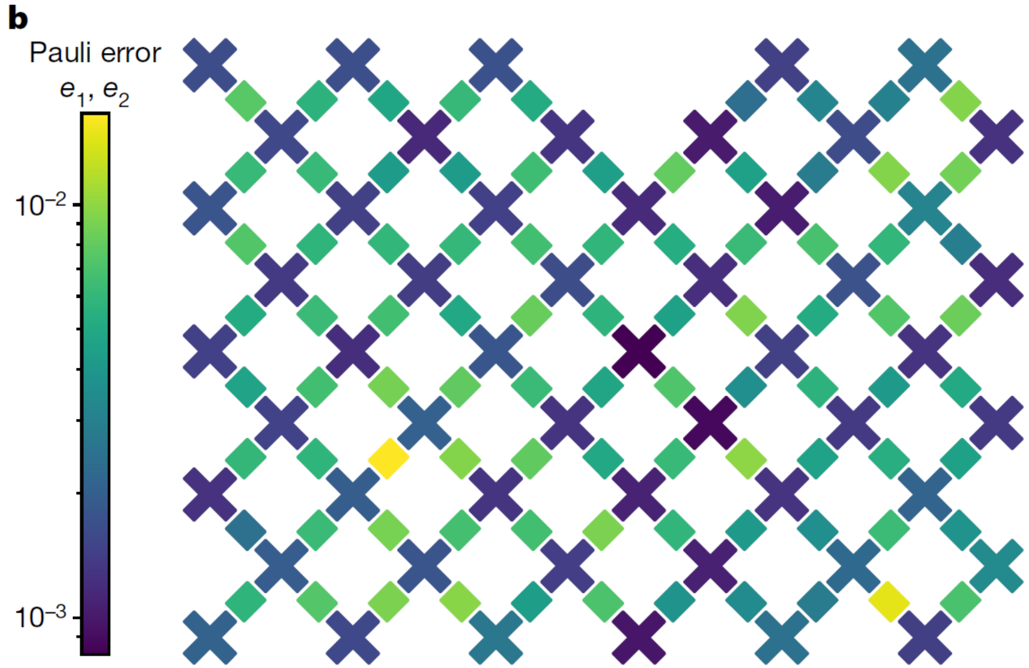

F. Arute, ..., J. M. Martinis *et al.*, *Nature* **574**, 505 (2019)

Fault-tolerant, error-corrected, universal quantum information processor

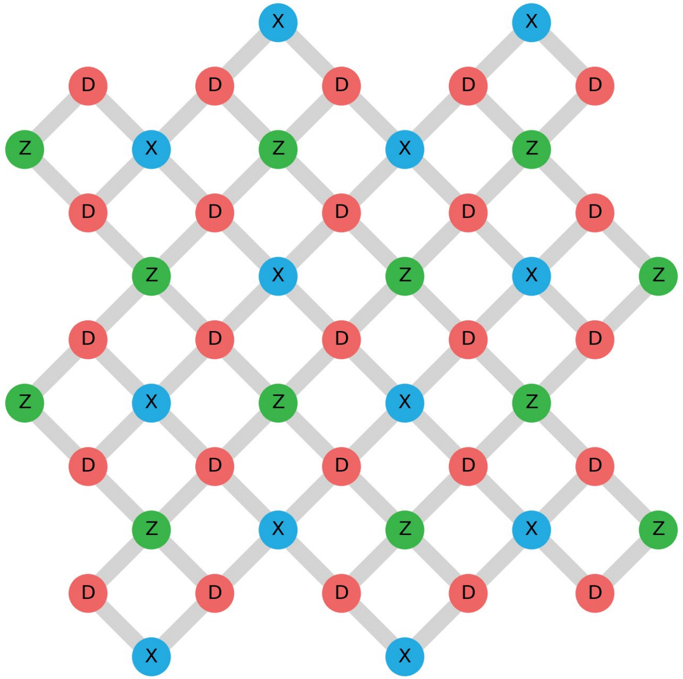

Fowler *et al.*, *Phys. Rev. A* **86**, 032324 (2012)

Quantum Error Correction with Superconducting Circuits

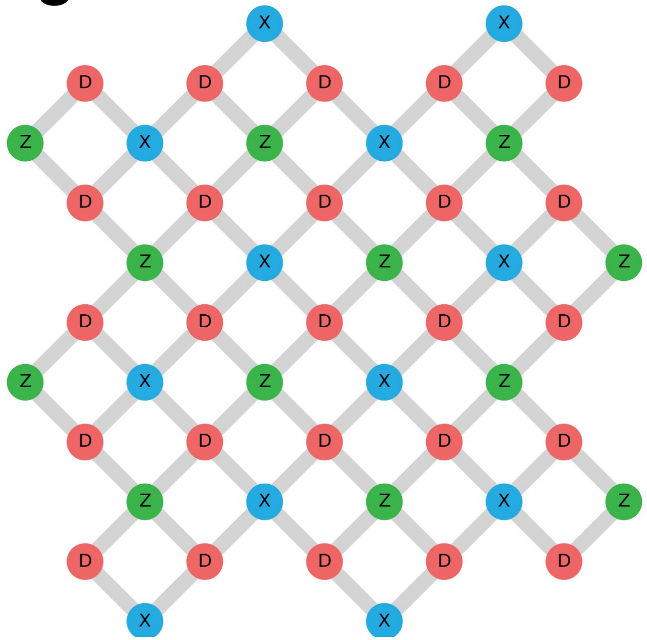

Approaches:

- Digital, qubit-based encodings: e.g. surface code, color code

- Continuous variable encodings in harmonic oscillator states: e.g. cat states, GKP states

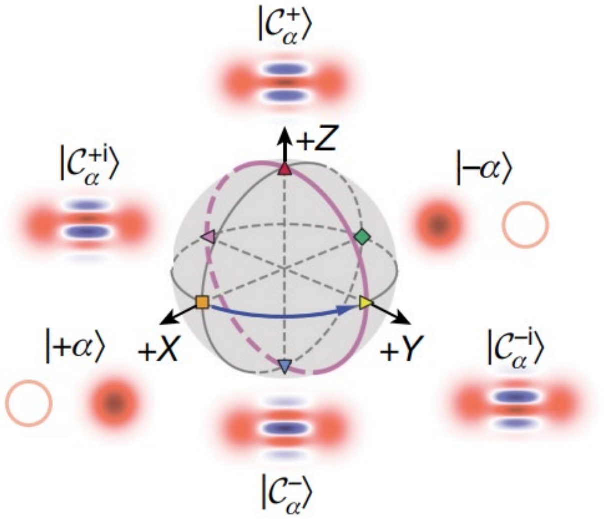

Preskill, *Quantum* **2**, 79 (2020)

Review: Terhal, *Rev. Mod. Phys*. **87**, 307 (2015)

picture from Grimm et al., *Nature* **584**, 205 (2020)

Bosonic Quantum Error Correction Experiments

Continuous QEC

- Dissipative-cat codes
  Leghtas, et. al. Science 347, 853 (2015)
  Lescanne, et. al. Nature Physics 16, 509 (2020)
  Gertler et. al. Nature 590, 243 (2021)
- Kerr-cat codes
  Grimm, et. al. Nature 584, 205 (2020)

Discrete QEC

- Binomial bosonic codes
  Ni, Z. et al., Nature 616, 56 (2023).
  Hu et al., Nature Physics 15, 503 (2019).
- Cat-Codes
  Ofek et. al., Nature 536, 441 (2016)

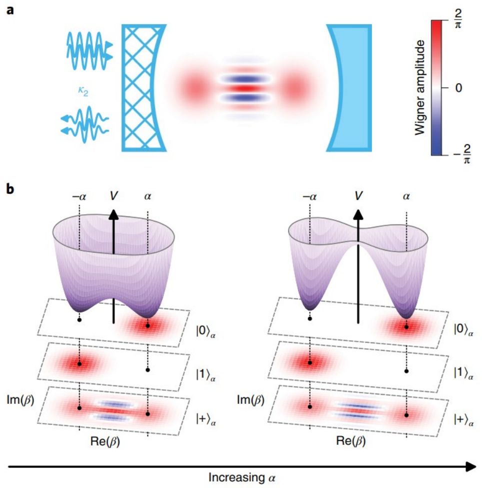

Lescanne et. al. Nat. Phys. 16, 509 (2020)

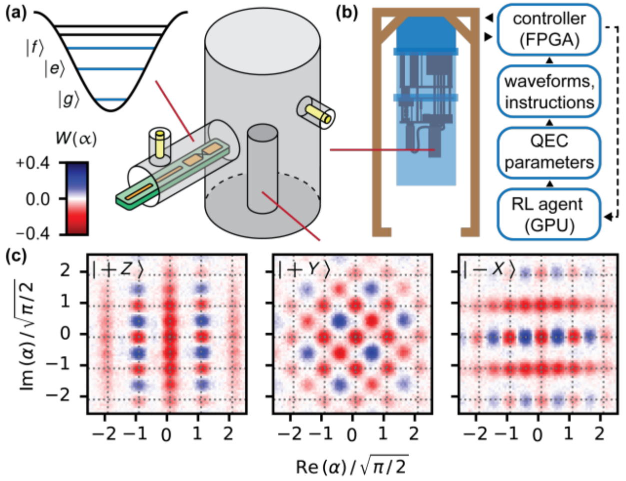

Sivak et. al. arXiv:2211.09116 (2022)

GKP codes

- Trapped ions
  Flühmann et. al., Nature 566, 513 (2019)
  de Neeve et. al., Nature Physics 18, 296 (2022)
- Superconducting circuits
  Campagne-Ibarcq et. al., Nature 584, 368 (2020)
  Sivak et al., Nature 616, 50 (2023).

Why is Error Correction Needed?

- Computational basis states are eigenstates of the Pauli Z operator

$$\hat{Z} = \begin{pmatrix} 1 & 0 \\ 0 & -1 \end{pmatrix}$$

$$\hat{Z}|0\rangle = +1\,|0\rangle$$
$$\hat{Z}|1\rangle = -1\,|1\rangle$$

- Every excited quantum system undergoes spontaneous emission

$$|1\rangle \rightarrow |0\rangle$$

- **Bit flip errors** also occur due to
  - Thermal excitation
  - Control inaccuracies
- The expectation value of $\hat{Z}$ characterizes the decay of the excited state on average

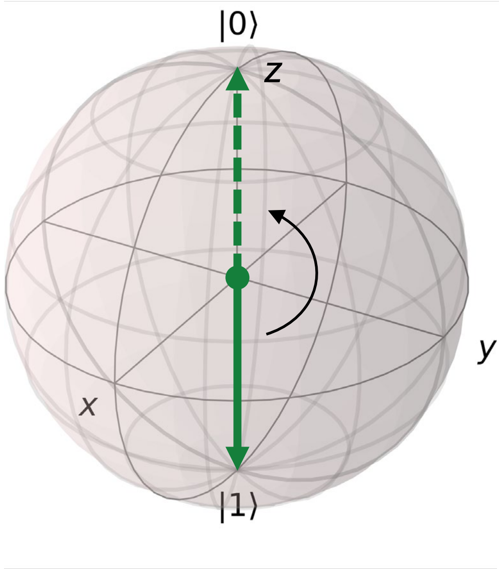

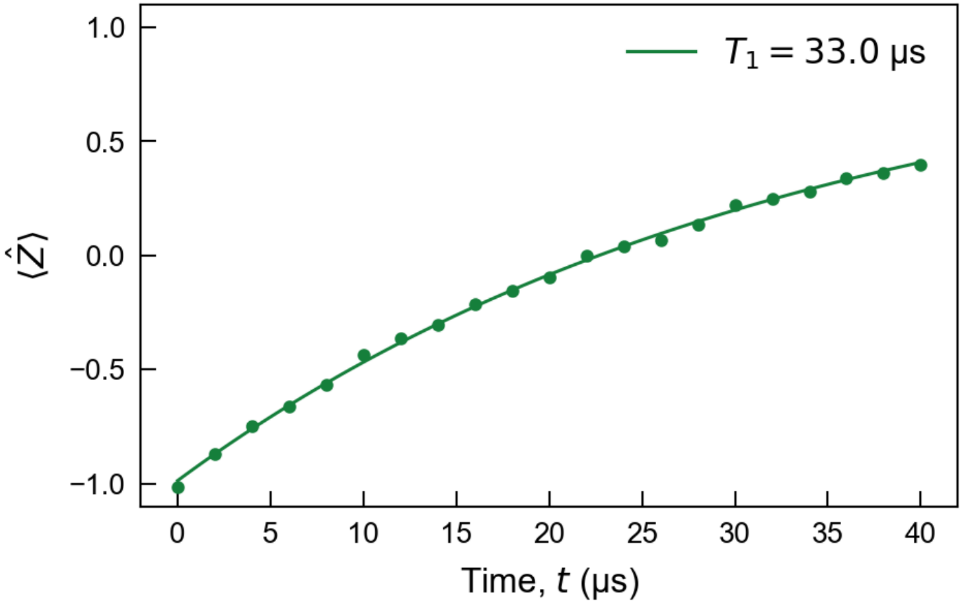

A Second Type of Error: Phase Flips

- Quantum computers make use of superposition states $|\pm\rangle = \frac{1}{\sqrt{2}}(|0\rangle \pm |1\rangle)$
- Eigenstates of

$$\hat{X} = \begin{pmatrix} 0 & 1 \\ 1 & 0 \end{pmatrix}$$

$$\hat{X}|+\rangle = +1\,|+\rangle$$
$$\hat{X}|-\rangle = -1\,|-\rangle$$

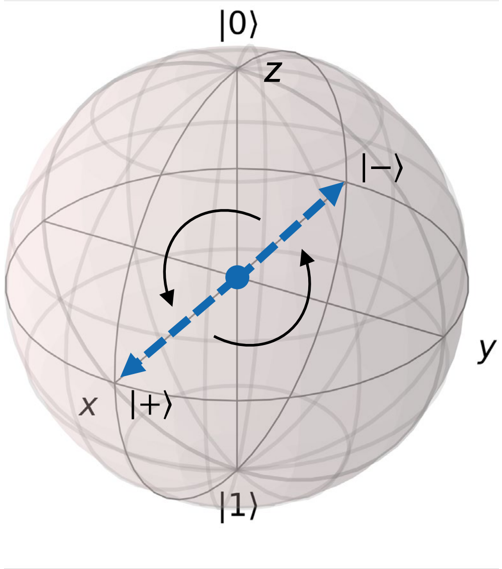

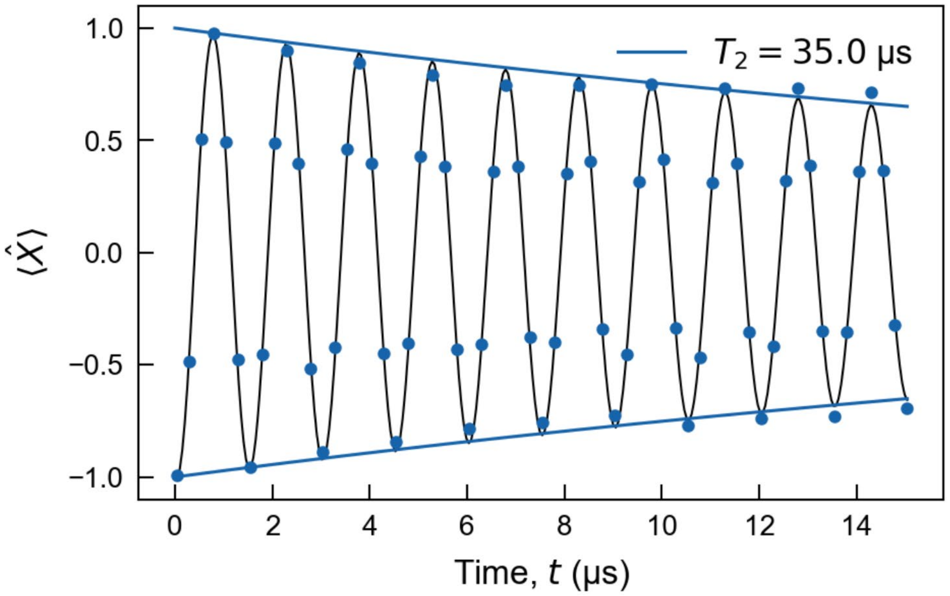

- **Phase flip errors** occur due to
  - Environmental field fluctuations
  - Control inaccuracies
  - Energy relaxation
- Expectation value of $\hat{X}$ characterizes the decay of the quantum phase on average

The Challenge of Quantum Error Correction

Detect and correct two types of errors:

- Bit flips
- Phase flips

Preserve stored quantum states while detecting and correcting errors:

- Measurements collapse quantum (superposition) states

Solution: Use encoding

- Store **logical qubit** state $|\psi\rangle$ in a system of many **physical qubits**
- Make use of **symmetry properties (parity)** of logical qubit states
  - revealing errors …
  - … but not the encoded quantum state

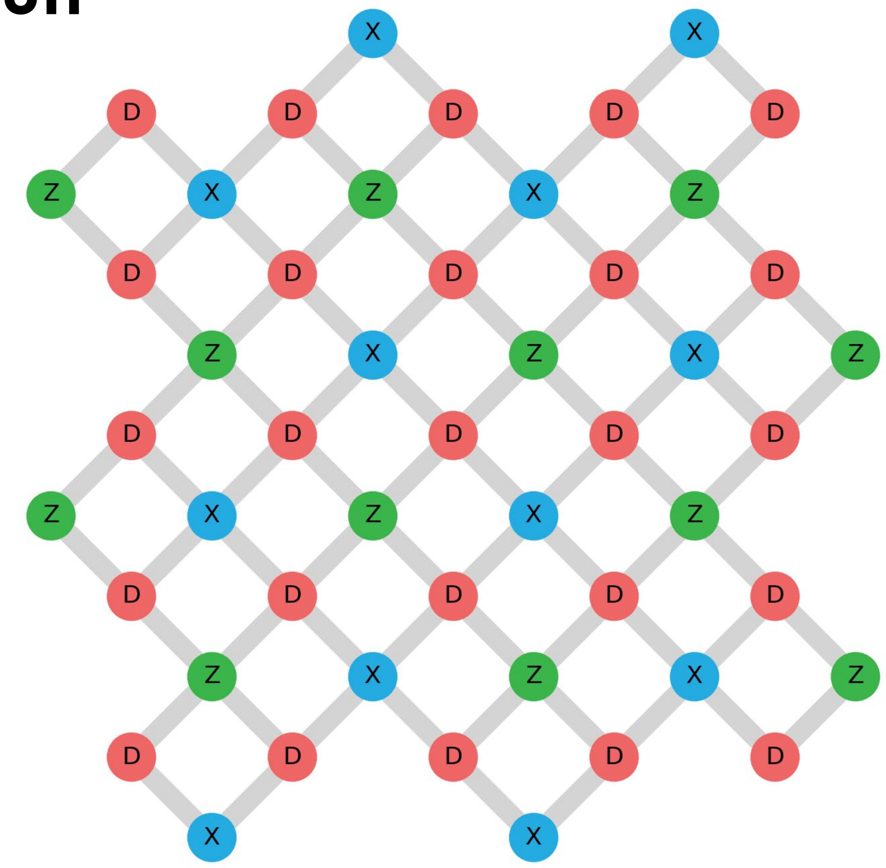

Kitaev, *Annals of Physics* **303**, 2 (2003),
Dennis et al., *Journ. of Math. Physics* **43**, 4452 (2002)
Raussendorff, Harrington, *Phys. Rev. Lett.* **98**, 190504 (2007)
Fowler *et al., Phys. Rev. A* **86**, 032324 (2012)

The Surface Code – Main Features

Large error threshold $\epsilon_{\text{th}} \sim 1\,\%$

- Logical error rate $\epsilon_{\text{L}} \propto \left(\epsilon_{\text{phys}}/\epsilon_{\text{th}}\right)^{(d+1)/2}$

  ϵ_{phys}: Physical error rate per step

  ϵ_{th}: Threshold error rate

  d: Distance of the code

Two-dimensional architecture

- All operations realizable on a planar qubit lattice
- Topological code: only local operations needed for error correction process

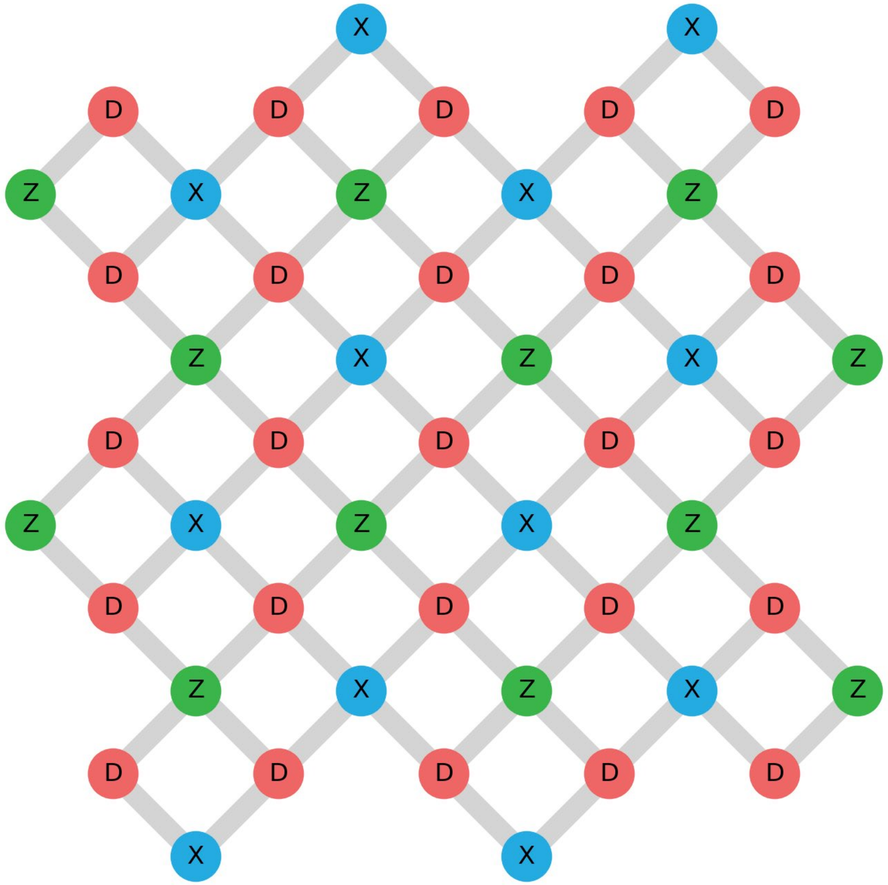

Kitaev, *Annals of Physics* **303**, 2 (2003),
Dennis et al., *Journ. of Math. Physics* **43**, 4452 (2002)
Raussendorff, Harrington, *Phys. Rev. Lett.* **98**, 190504 (2007)
Fowler *et al., Phys. Rev. A* **86**, 032324 (2012)

Elements of the Surface Code

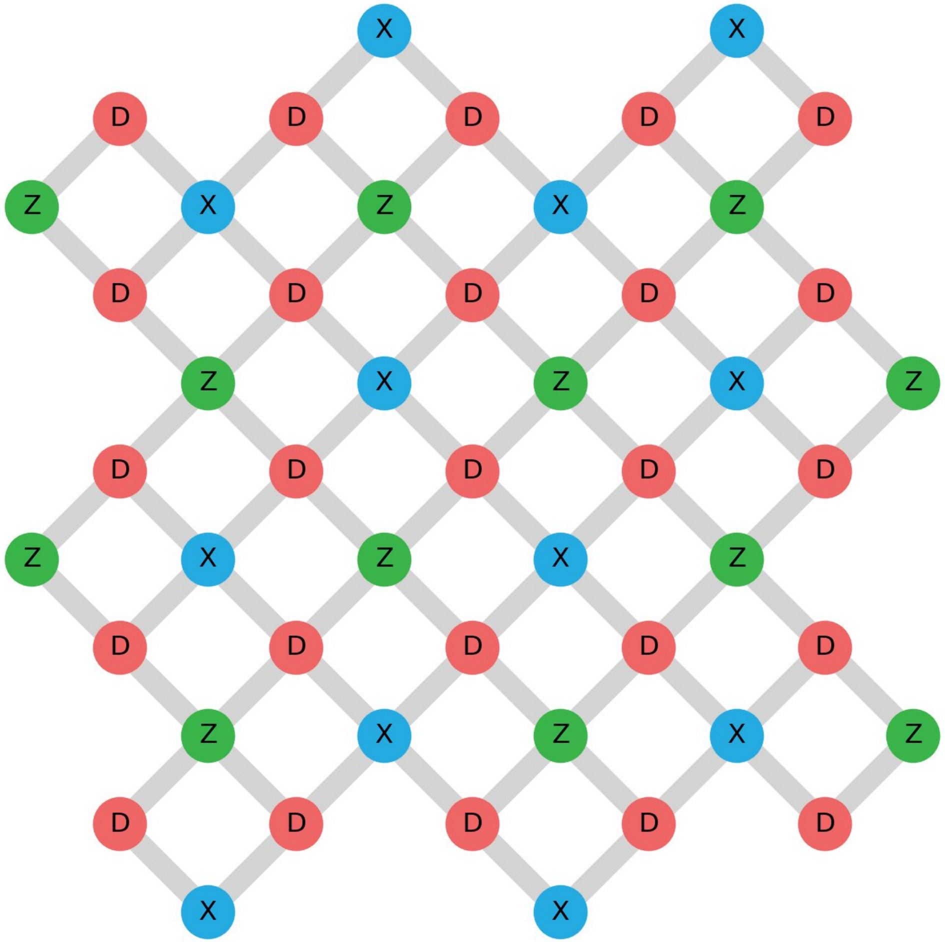

Features:
- Two-dimensional $(d \times d)$ grid of data qubits
- X-type and Z-type auxiliary qubits
- Auxiliary-qubit-assisted stabilizer measurement
  - $Z_1Z_2Z_3Z_4$ (or Z_1Z_2 at the edges)
  - $X_1X_2X_3X_4$ (or X_1X_2 at the edges)

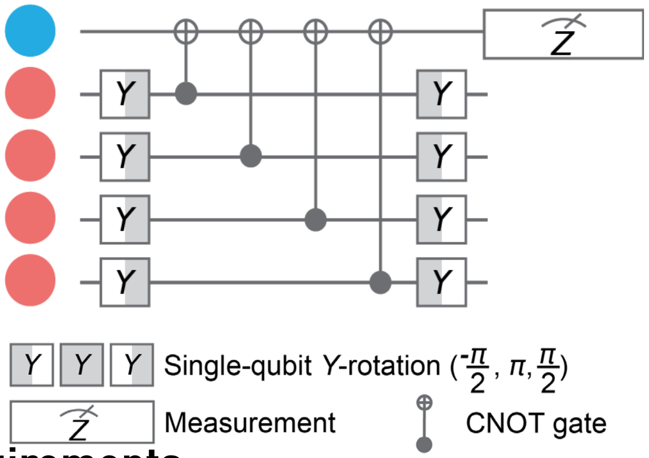

Requirements:
- High-fidelity entangling gates between data and ancilla qubits
- Fast high-fidelity measurements of the ancilla qubits
- Low readout crosstalk between ancilla and data qubits
- Ability to do repeated gates and mid-cycle measurements

Fowler *et al.*, *Phys. Rev. A* **86**, 032324 (2012)
Versluis *et al.*, *Phys. Rev. Applied* **8**, 034021 (2017)

Distance-Two Surface Code for Error Detection

- Distance-two code: detect 1 error, correct 0 errors
- Stabilizers for parity measurement:

$$\underbrace{\hat{X}_1\hat{X}_2\hat{X}_4\hat{X}_5, \quad \hat{Z}_1\hat{Z}_4, \quad \hat{Z}_2\hat{Z}_5}_{\text{Stabilizers commute, common eigenstates}}$$

- Logical eigenstates and their equal superpositions:

$$|0\rangle_L = \frac{1}{\sqrt{2}}(|0000\rangle + |1111\rangle)$$

$$|1\rangle_L = \frac{1}{\sqrt{2}}(|0101\rangle + |1010\rangle)$$

$$|+\rangle_L = \frac{1}{2}(|0000\rangle + |1111\rangle + |0101\rangle + |1010\rangle)$$

$$|-\rangle_L = \frac{1}{2}(|0000\rangle + |1111\rangle - |0101\rangle - |1010\rangle)$$

- Logical operators:
  - $\hat{X}_L = \hat{X}_1\hat{X}_4$ or $\hat{X}_L = \hat{X}_2\hat{X}_5$
  - $\hat{Z}_L = \hat{Z}_1\hat{Z}_2$ or $\hat{Z}_L = \hat{Z}_4\hat{Z}_5$

  Anti-commute with each other and commute with stabilizers (as needed for logical operators in a stabilizer code)

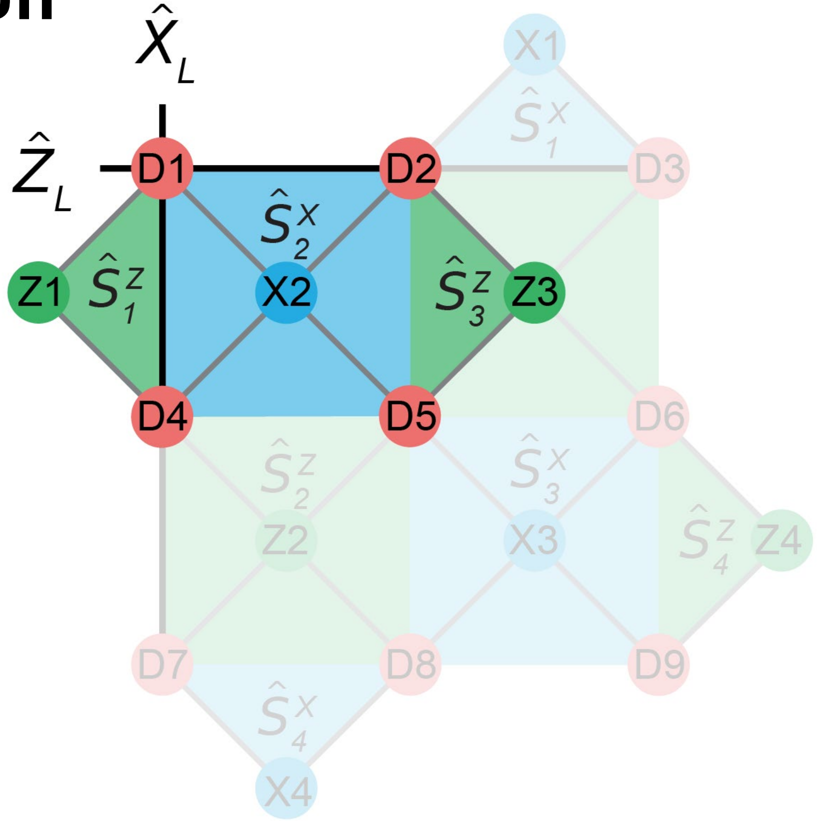

Andersen *et al.*, *Nat. Phys.* **16**, 875 (2020)
Chen *et al.*, *Nature* **595**, 7867 (2021)
Marques *et al.*, *Nat. Phys.* **18**, 80 (2022)

Distance-Three Surface Code for Error Correction

Two-dimensional square lattice of qubits

- $d^2 = 9$ Data qubits: encode single (logical) qubit
  - Logical operators: $\hat{Z}_L = \hat{Z}_1\hat{Z}_2\hat{Z}_3$ $\hat{X}_L = \hat{X}_1\hat{X}_4\hat{X}_7$
  - Distance d: min. number of Pauli operators in $\hat{Z}_L, \hat{X}_L$
  - Number of correctable errors: $\lfloor (d-1)/2 \rfloor = 1$
- $d^2 - 1 = 8$ Auxiliary qubits: for parity measurements

Parity/Stabilizer measurements

- Detect errors without collapsing data-qubit state (Stabilizer operators commute with $\hat{Z}_L, \hat{X}_L$)
- 4 Z-type Stabilizers $\hat{S}^{Zi}$ to detect bit-flip errors
- 4 X-type Stabilizers $\hat{S}^{Xi}$ to detect phase-flip errors

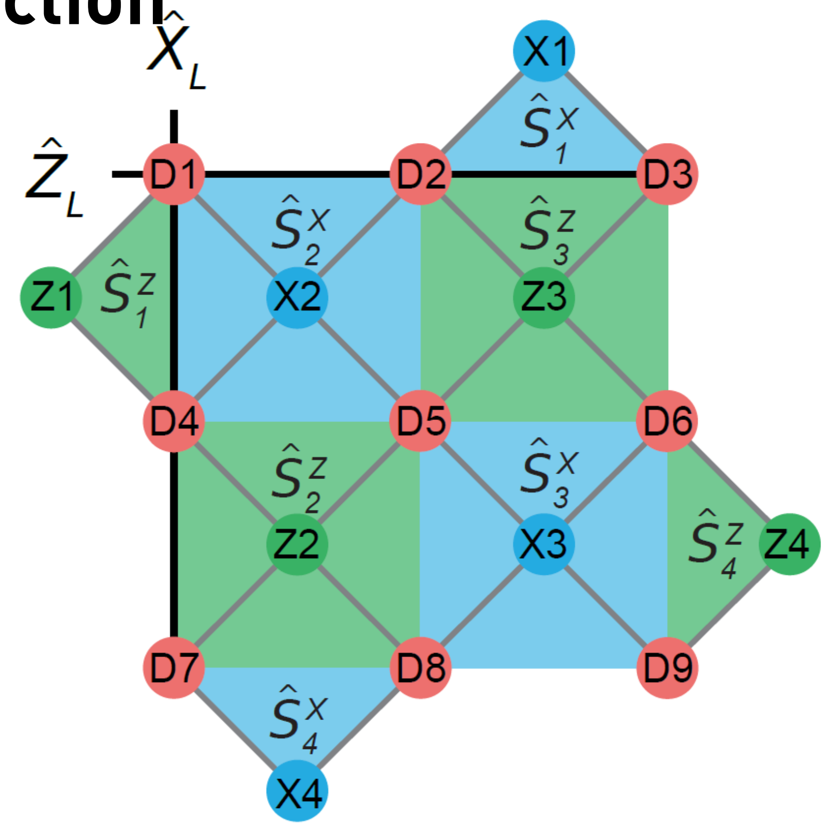

$\hat{S}^{Z1}$	$\hat{Z}_1\hat{Z}_4$
$\hat{S}^{Z2}$	$\hat{Z}_4\hat{Z}_5\hat{Z}_7\hat{Z}_8$
$\hat{S}^{Z3}$	$\hat{Z}_2\hat{Z}_3\hat{Z}_5\hat{Z}_6$
$\hat{S}^{Z4}$	$\hat{Z}_6\hat{Z}_9$

$\hat{S}^{X1}$	$\hat{X}_2\hat{X}_3$
$\hat{S}^{X2}$	$\hat{X}_1\hat{X}_2\hat{X}_4\hat{X}_5$
$\hat{S}^{X3}$	$\hat{X}_5\hat{X}_6\hat{X}_8\hat{X}_9$
$\hat{S}^{X4}$	$\hat{X}_7\hat{X}_8$

Bombin, Delgado, *Phys. Rev. A* **76**, 012305 (2007)
Tomita, Svore, *Phys. Rev. A* **90**, 062320 (2014)

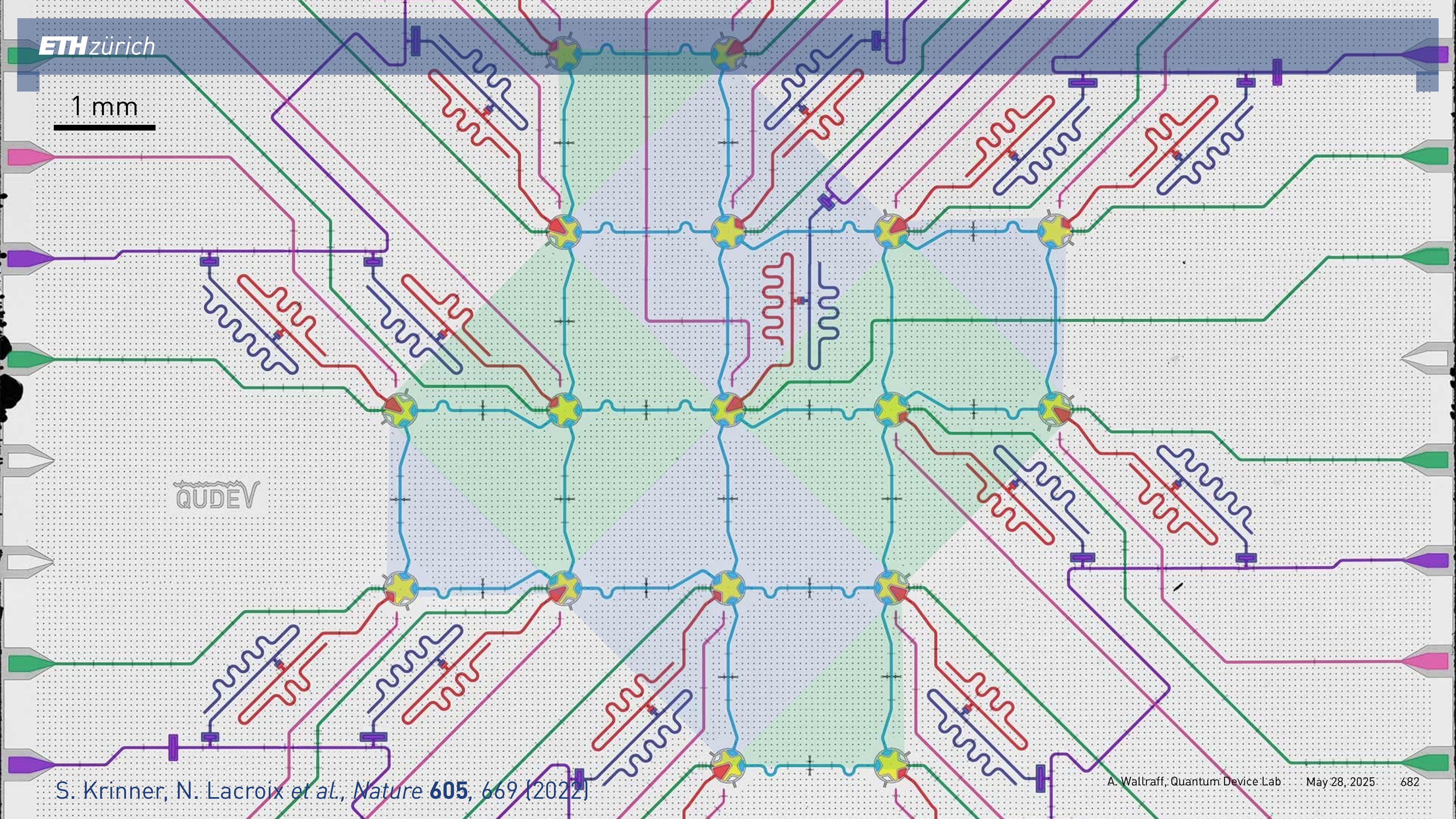

S. Krinner, N. Lacroix *et al.*, *Nature* **605**, 669 (2022)

Device Architecture

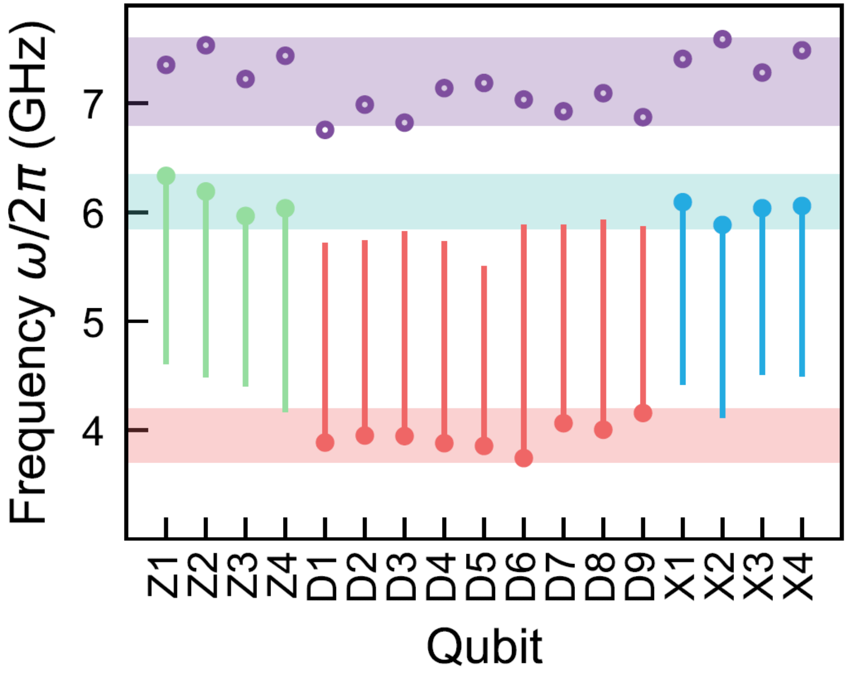

Frequency tunable qubits in two bands

- Data qubits at ~ 4 GHz
- Auxiliary qubits at ~ 6 GHz

Features

- Small residual-ZZ couplings ($\leq$ 8 kHz)
- Improved coherence using asymmetric SQUIDs creating upper and lower-frequency sweet spots
- Two-qubit CZ gates initiated by tuning both qubits
- Tuning range indicated by vertical bars
- Only auxiliary qubits evolve through $|2\rangle$ during a two-qubit gate

Readout resonators

- Single frequency band ~ 7 GHz

S. Krinner, N. Lacroix *et al.*, *Nature* **605**, 669 (2022)

Device Performance

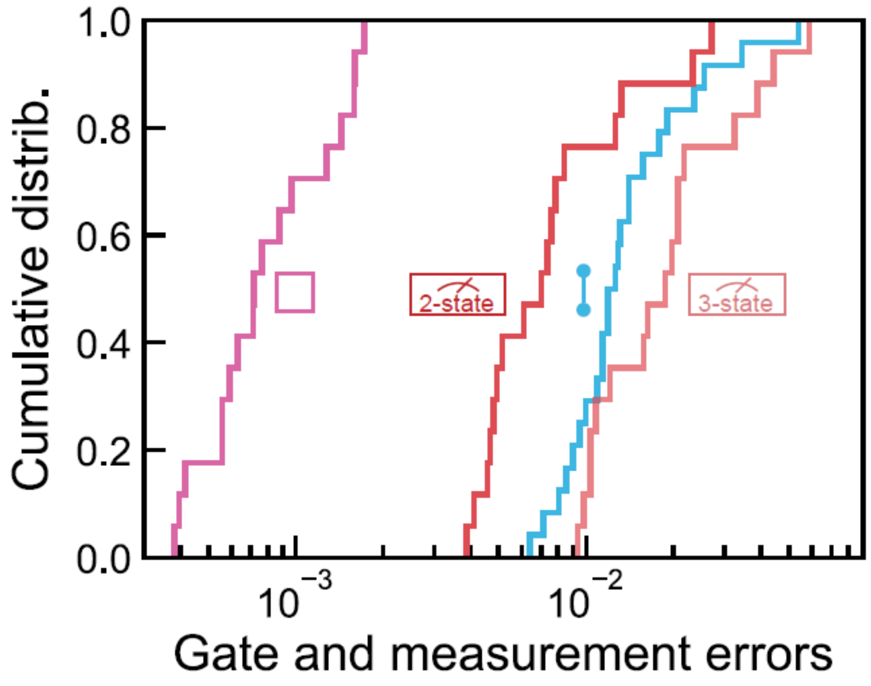

Averaged qubit coherence

- Energy relaxation time $T_1 \sim 33$ μs
- Ramsey decay time $T_2^* \sim 38$ μs

Single-qubit gates

- Mean gate error of 0.9(4) 10^{-3}
- Duration of 40 ns

Two-qubit gates

- Mean gate error of 15(10) 10^{-3}
- Mean duration of 98(7) ns (including buffers)

Readout:

- Mean two-state assignment error: 9(7) 10^{-3} and three-state assignment error: 22(14) 10^{-3}
- Duration: 300 ns (aux.) to 400 ns (data)

S. Krinner, N. Lacroix *et al.*, *Nature* **605**, 669 (2022)

Controlling Single Qubits (Y Rotation)

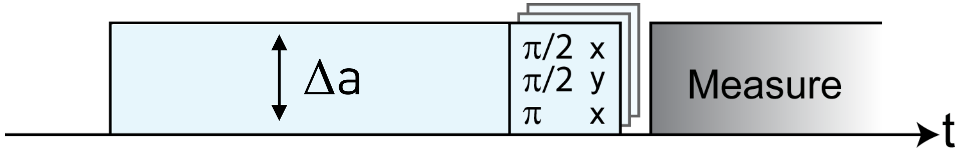

- apply microwave pulse
- followed by read-out pulse
- both with controlled length, amplitude and phase
- Characterize gates by randomized benchmarking
- F > 99 %

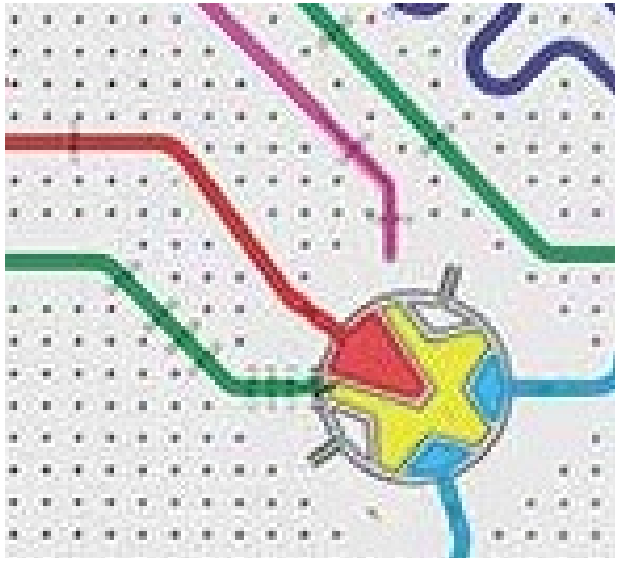

experimental density matrix and Pauli set:

Controlling Single Qubits (X Rotation)

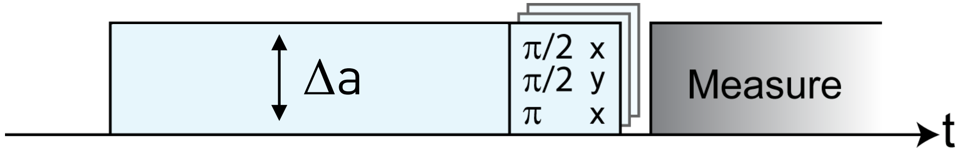

- apply microwave pulse
- followed by read-out pulse
- both with controlled length, amplitude and phase
- Characterize gates by randomized benchmarking
- F > 99 %

experimental density matrix and Pauli set:

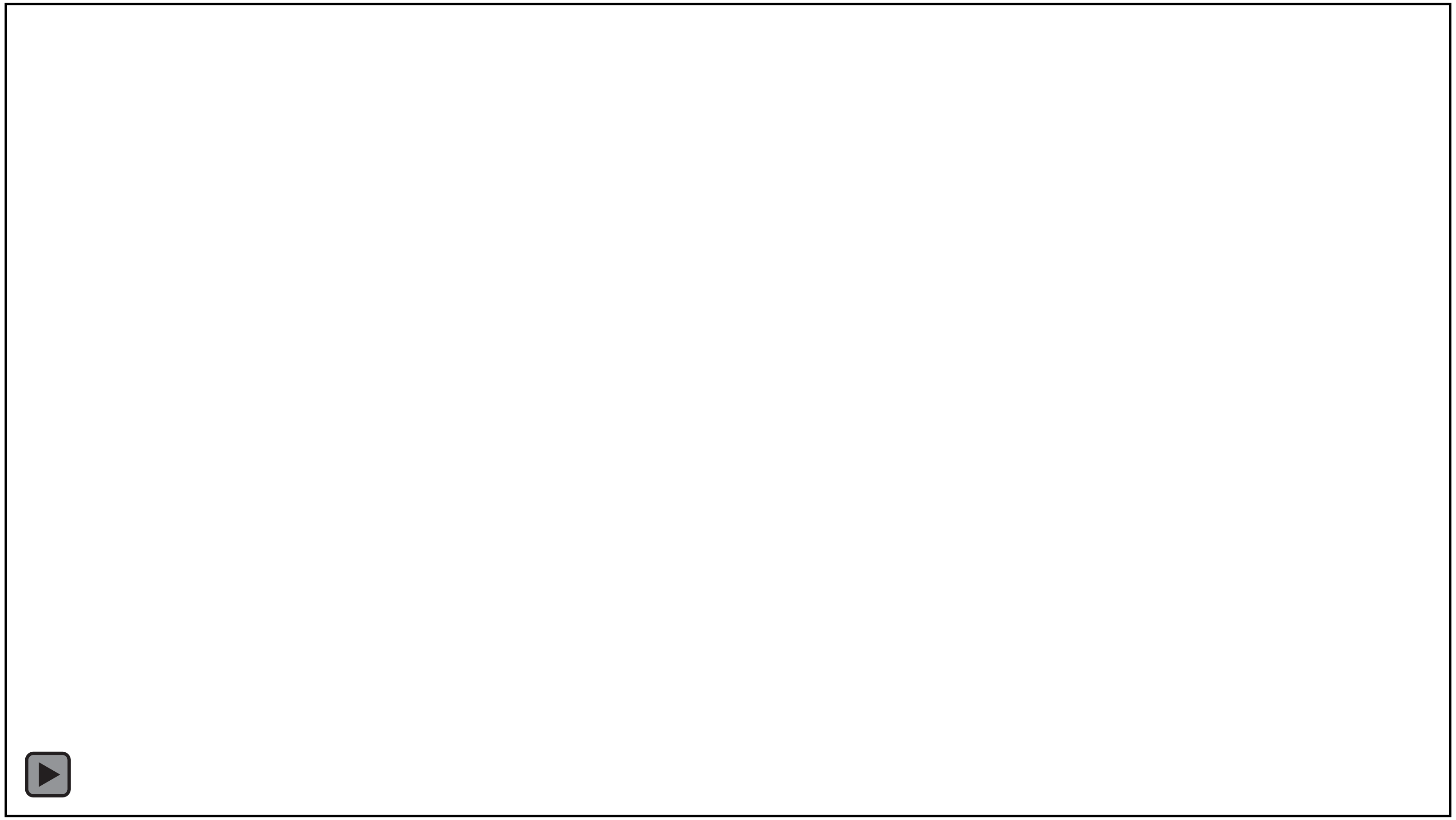

Universal Two-Qubit Controlled Phase Gate

Make use of qubit states beyond 0, 1

$|\text{qubit } A, \text{qubit } B\rangle$

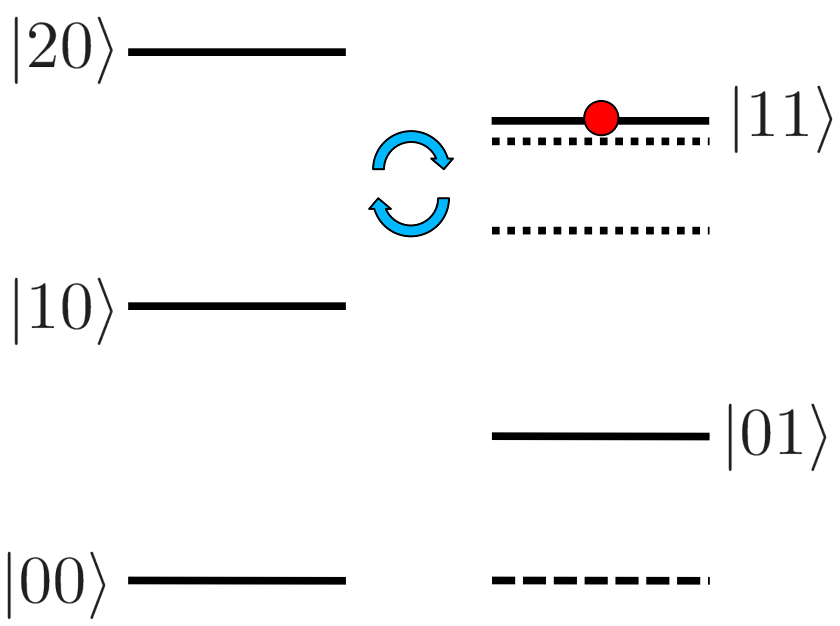

$$|11\rangle \longrightarrow i|20\rangle \longrightarrow -|11\rangle$$

Interaction mediated
by virtual photon exchange
through resonator

Full 2π rotation induces
phase factor -1

Tune levels into
resonance using
magnetic field

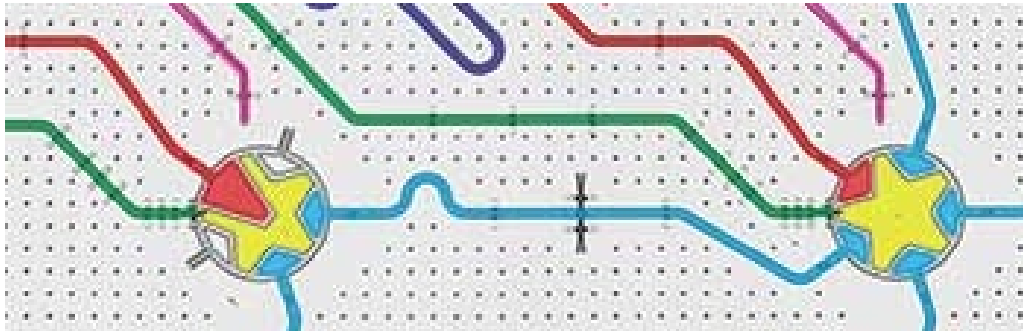

proposal: F. W. Strauch *et al., Phys. Rev. Lett.* **91**, 167005 (2003).
first implementation: L. DiCarlo *et al., Nature* **460**, 240 (2010).

Universal Two-Qubit Controlled Phase Gate

Make use of qubit states beyond 0, 1

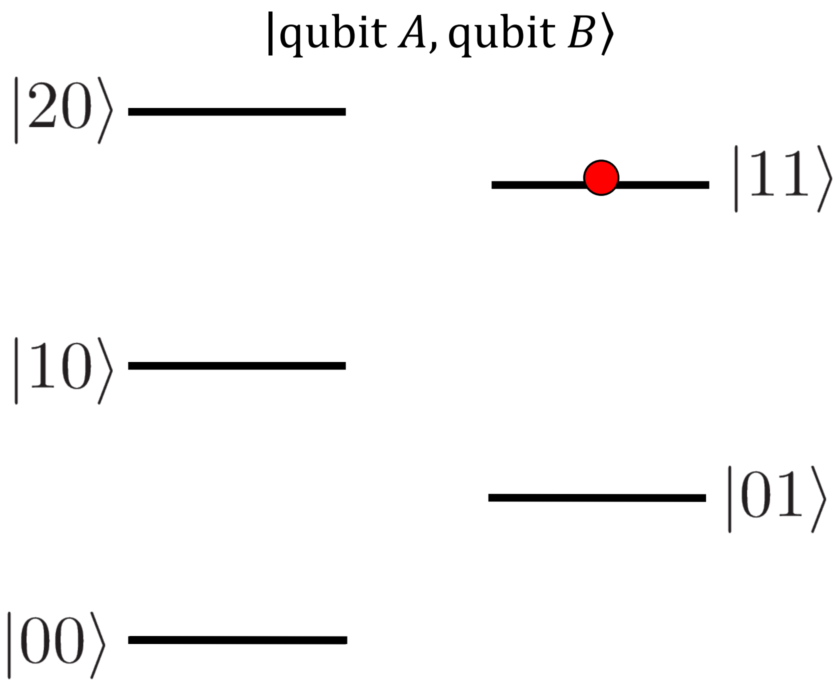

Qubits in states 01, 10 and 00 do not interact and thus acquire no phase shift

$$|11\rangle \longrightarrow i|20\rangle \longrightarrow -|11\rangle$$

$$|01\rangle \longrightarrow |01\rangle$$

$$|10\rangle \longrightarrow |10\rangle$$

$$|00\rangle \longrightarrow |00\rangle$$

C-Phase gate:

$$\begin{pmatrix} 1 & 0 & 0 & 0 \\ 0 & 1 & 0 & 0 \\ 0 & 0 & 1 & 0 \\ 0 & 0 & 0 & -1 \end{pmatrix}$$

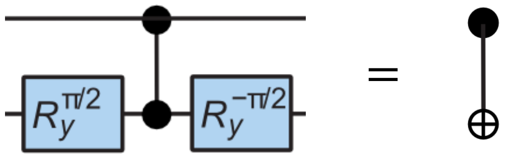

CNOT gate

Universal two-qubit gate.

Test performance with process tomography or randomized benchmarking.

proposal: F. W. Strauch *et al., Phys. Rev. Lett.* **91**, 167005 (2003).

first implementation: L. DiCarlo *et al., Nature* **460**, 240 (2010).

Qubit Readout

Circuit design
- $\lambda/4$ readout resonator & $\lambda/4$ Purcell filter

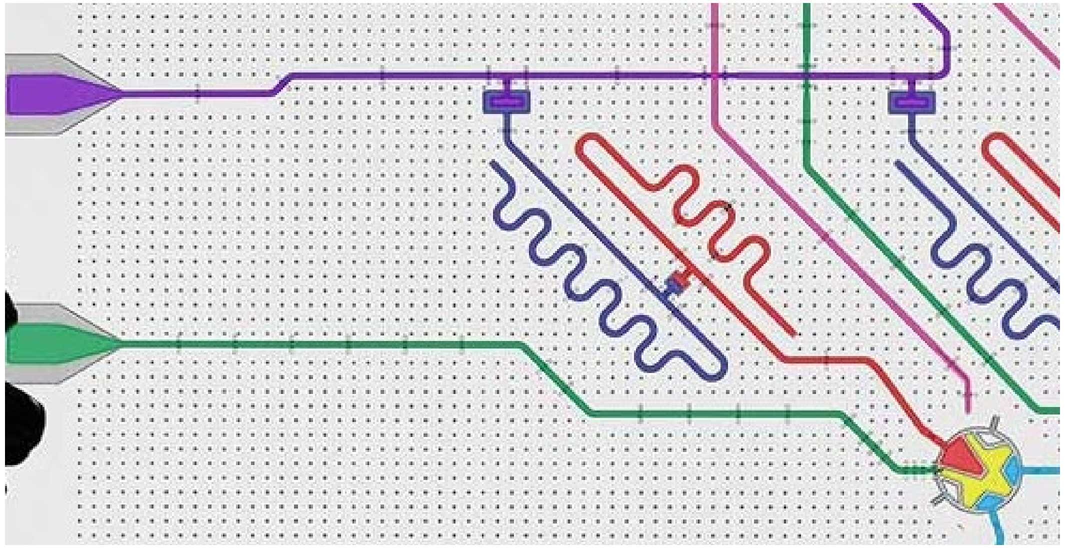

Performance
- F ~ 99.2 % at 88 ns integration time
- Optimized sample design
- Low-noise phase-sensitive JP-Amplifier

Transmission amplitude of readout circuit for qubit prepared in ground (g) or excited (e) state :

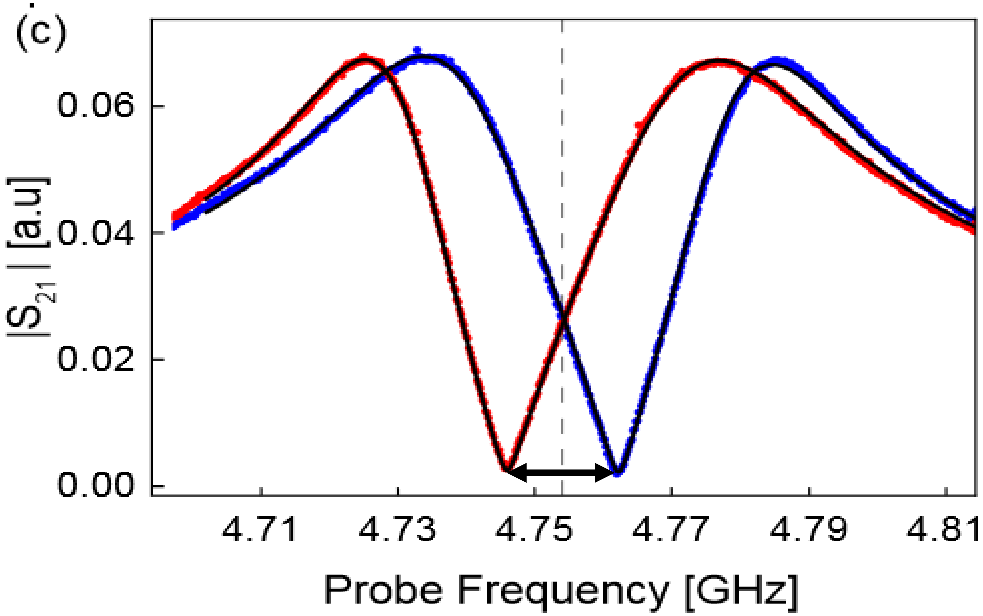

Features:
- large dispersive shift χ
- large resonator BW κ
- Purcell protection
- Low cross-talk when multiplexed

T. Walter, P. Kurpiers *et al., Phys. Rev. Applied* **7**, 054020 (2017)

Leakage Detection and Rejection

- Leakage errors are detrimental for quantum error correction
- Device designed to minimize leakage on data qubits: $< 2\ 10^{-3}$ per qubit and per cycle
- Detect residual leakage using three-state readout
  - Auxiliary qubits: in each cycle
  - Data qubits: after final cycle
- Rejected fraction per qubit per cycle
  - Auxiliary qubits: 9.4(4) 10^{-3}
  - Data qubits: 1.7(2) 10^{-3}
- Some contribution from false positives

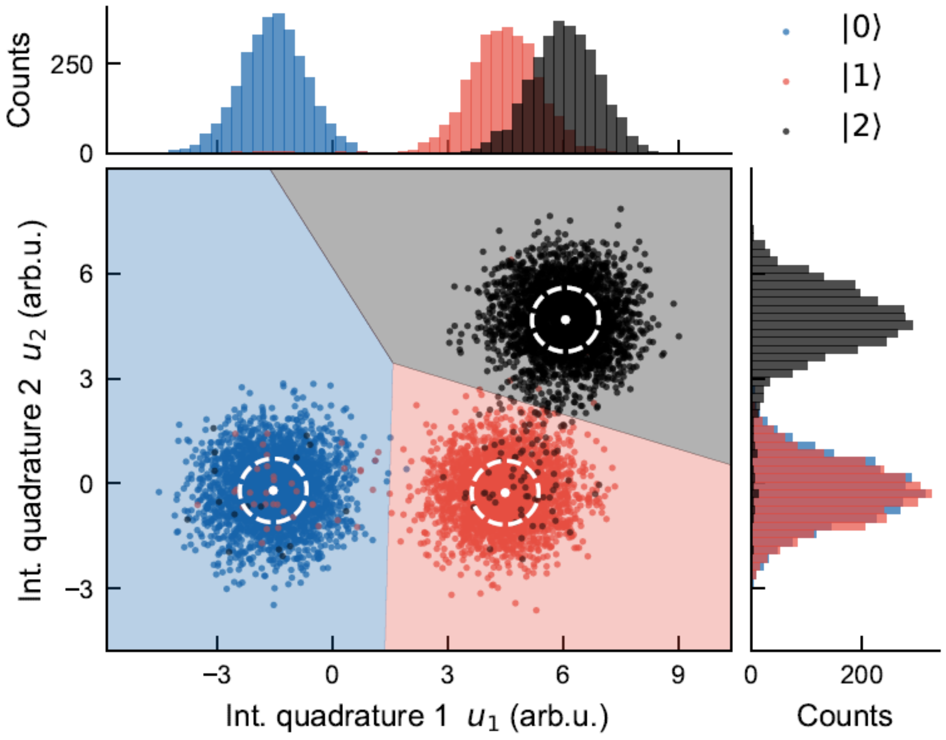

S. Krinner, N. Lacroix *et al.*, *Nature* **605**, 669 (2022)

Alferis, Terhal, *Quant. Info. Comp.* **7**, 139 (2007)
Fowler, *PRA* **88**, 042308 (2013)
Bultink *et al.*, *Science Advances* **6**, eaay3050 (2020)
Varbanov *et al.*, *npj Quantum Information* **15**, 997 (2020)

Distance-Three Surface-Code Device Mounted in Sample Holder

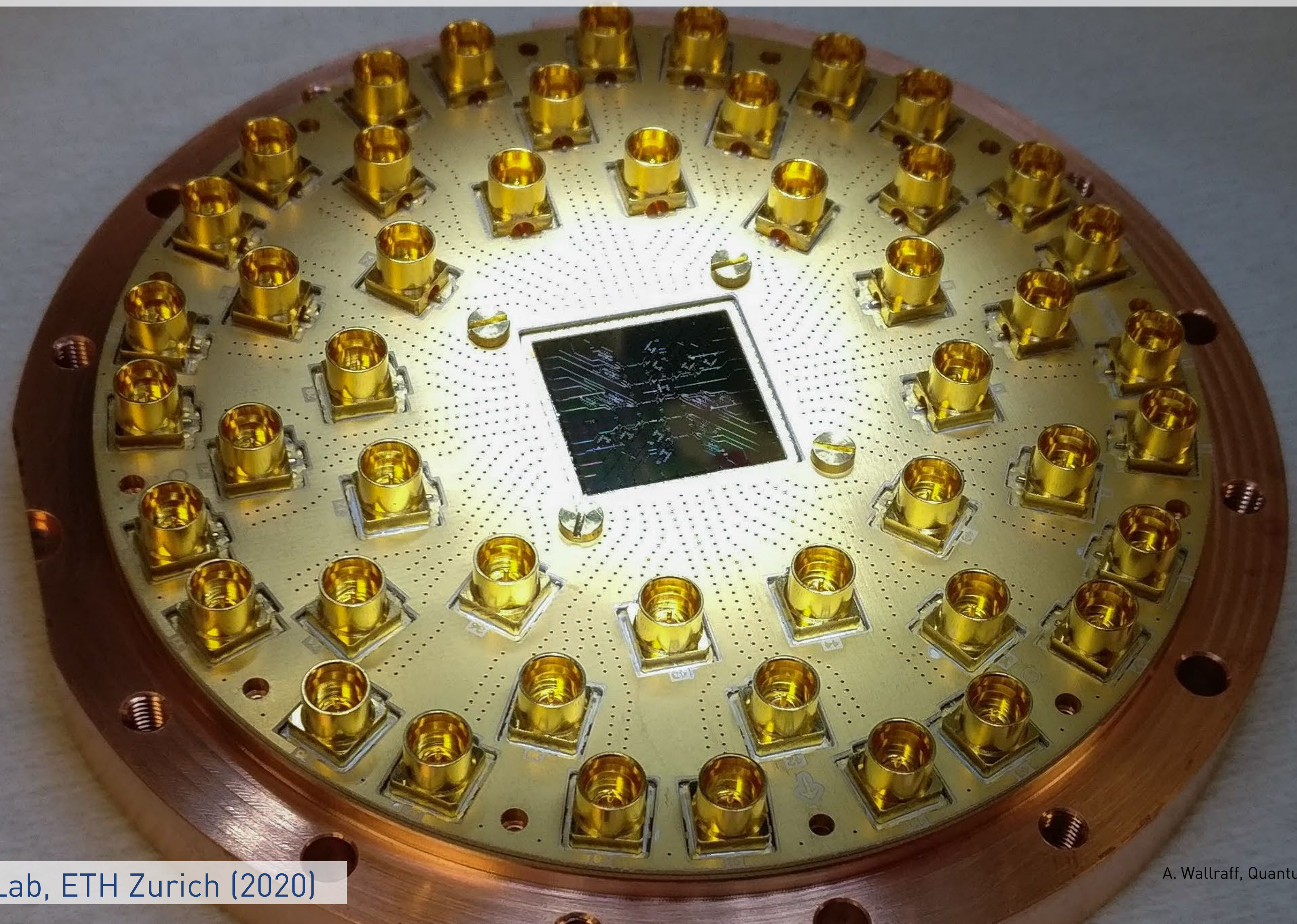

Quantum Device Lab, ETH Zurich (2020)

48-Port Sample Package (17-Qubit Device)

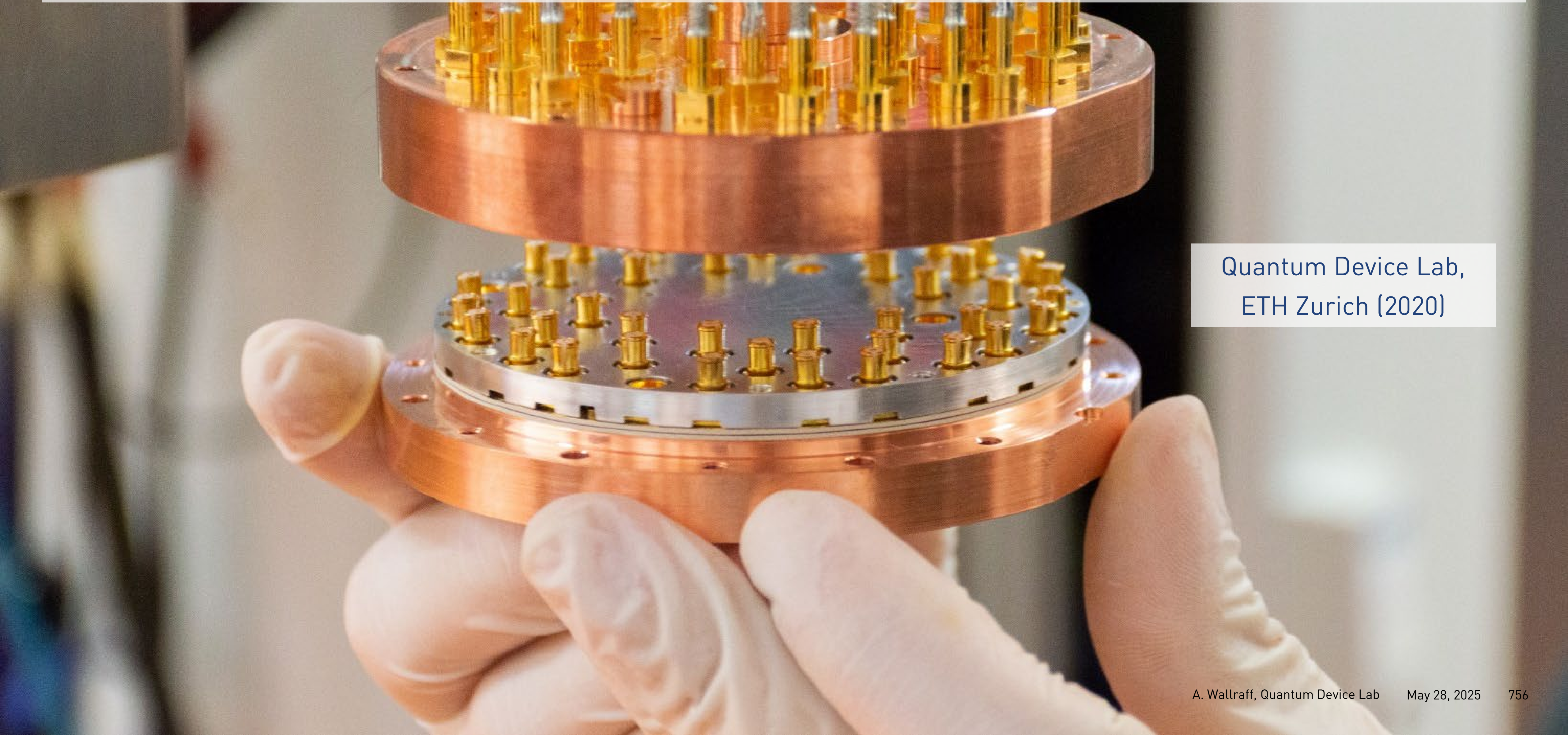

Quantum Device Lab,
ETH Zurich (2020)

Quantum Device Lab, ETH Zurich (2021)

Quantum Device Lab, ETH Zurich (2021)

Room-Temperature Electronics

- Close collaboration with Zurich Instruments

Qubit control (7x HDAWG)

- Flux drives (17x)
- Baseband RF drives (17x)

Qubit Readout (4x UHFQA)

- FPGA Baseband signal generation & analysis

Up- and down-conversion electronics for qubit drive and readout

Synchronization using PQSC

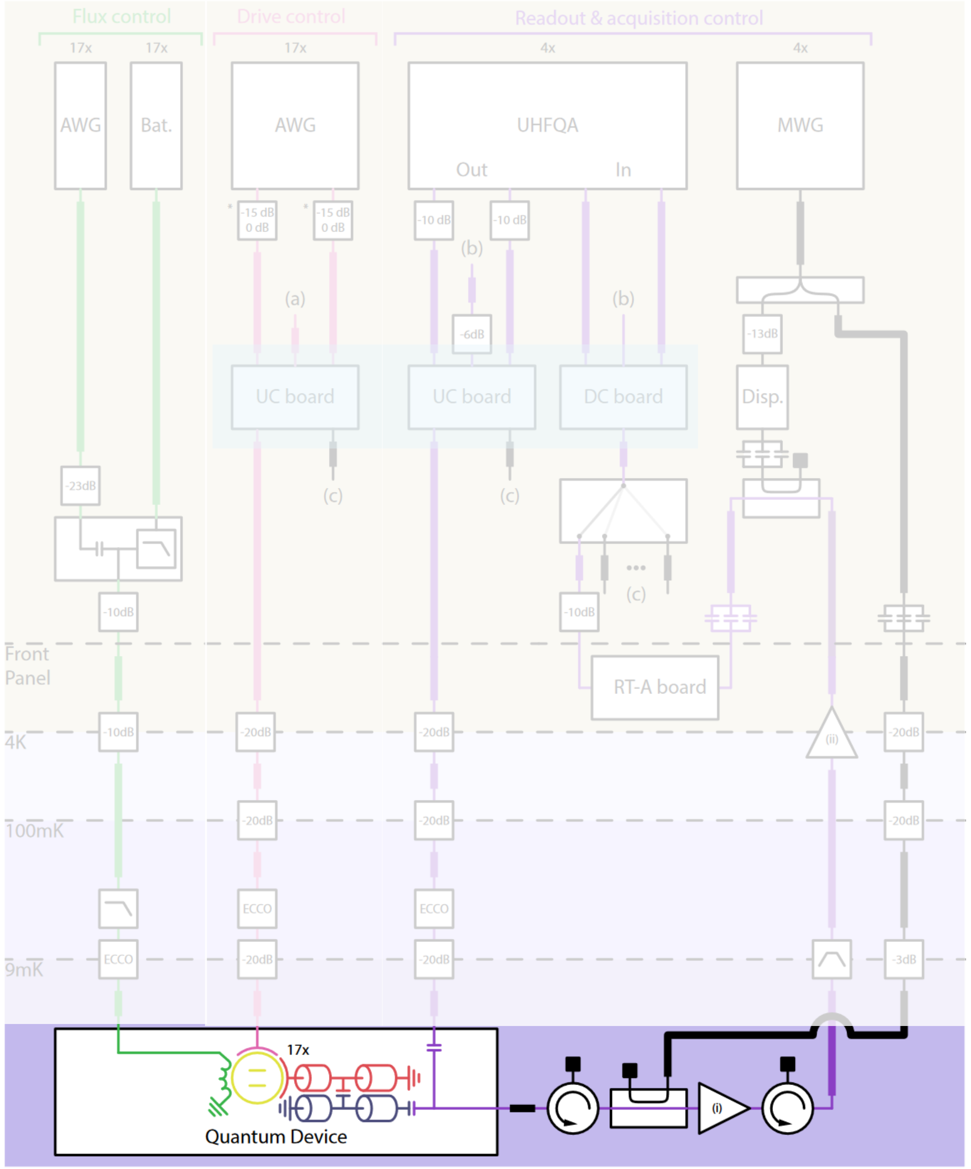

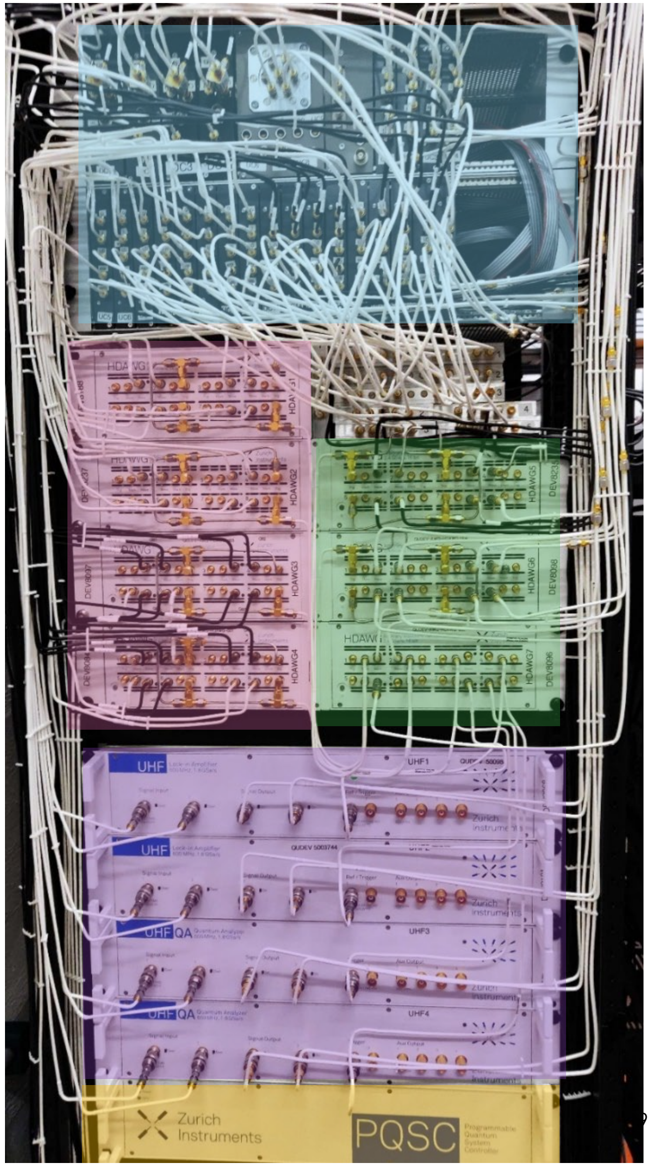

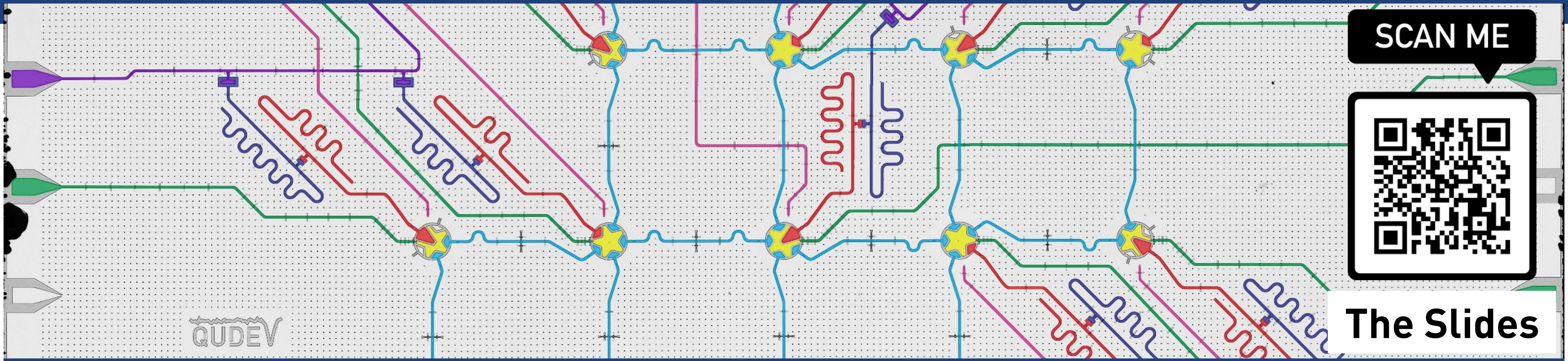

Quantum Error Correction with Superconducting Circuits (Lecture 2)

Sci. Team: E. Al-Tavil, L. Beltran, I. Besedin, J.-C. Besse, D. Colao Zanuz, Xi Dai, K. Dalton, J. Ekert, S. Frasca, A. Grigorev, D. Hagmann, C. Hellings, A. Hernandez-Anton, I. Hesner, L. Hofele, M. Kerschbaum, S. Krinner, A. Kulikov, N. Lacroix, M. Pechal, K. Reuer, A. Rosario, C. Scarato, J. Schaer, Y. Song, F. Swiadek, F. Wagner, A. Wallraff *(ETH Zurich)*

Eng. & Tech. Team: A. Akin, M. Bahrani, A. Flasby, A. Fauquex, R. Keller, N. Kohli, R. Siegbert, M. Werner *(ETH Zurich)*

I A R P A
BE THE FUTURE

Schweizerischer Nationalfonds

Innovation project supported by

Schweizerische Eidgenossenschaft
Confédération suisse
Confederazione Svizzera
Confederaziun svizra

Swiss Confederation

Innosuisse – Swiss Innovation Agency

Qubit-Encoded Quantum Error Correction Experiments

Bit or phase-flip codes (only X or Z errors):

- NMR [Cory et al. Phys. Rev. Lett. 81, 2152 (1998)]
- Ions [Chiaverini et al. Nature 432, 602 (2004), Schindler et al. Science 322, 1059 (2011)]
- NV-Centers [Cramer et al. Nature Comm. 7, 11526 (2016)]
- Superconducting qubits [Riste et.al. Nature Comm. 6, 6983 (2015), Kelly et al. Nature 519, 66 (2015), Chen et al., Nature 595, 7867 (2021)]

Quantum codes, single-cycle experiments:

- Five-qubit code [Knill et al., PRL 86, 5811 (2001), Abobeih et al., arXiv:2108.01646 (2021)]
- Bacon-Shor code [Egan et al., Nature 598, 281 (2021)]

Repeated error detection in the surface code

- Andersen et al., Nat. Phys. 16, 875 (2020)
- Chen et al., Nature 595, 7867 (2021)
- Marques et al., Nat. Phys. **18**, 80 (2022)

Trapped ions

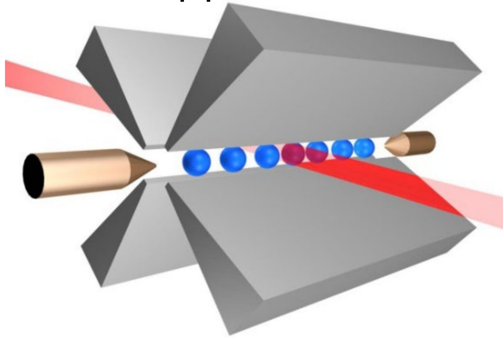

e.g. Blatt & Roos, Nat. Phys. 8, 277 (2012)

Supercond. circuits

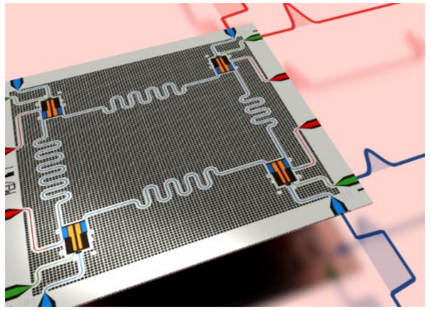

Picture: Y. Salathé
Review: e.g. Krantz et al., Appl. Phys. Rev. 6, 021318 (2019)

Repeated quantum error correction

- Color code (trapped ions)
  Ryan-Anderson et al., PRX 11, 041058 (2021)
- Distance-3 surface code (s.c.)
  Krinner, Lacroix *et al.*, *Nature* **605**, 669 (2022)
  Zhao et al., *PRL* **129**, 030501 (2022)
- Distance-3 heavy-hexagon code (s.c.)
  Sundaresan et al., *Nat. Commun.* **14**, 2852 (2023)
- Distance-3 to 5 scaling of the surface code (s.c.)
  Google AI, *Nature* **614**, 676 (2023)

Stabilizer Measurements

Quantum circuit

- Ramsey measurement on auxiliary qubit Ai

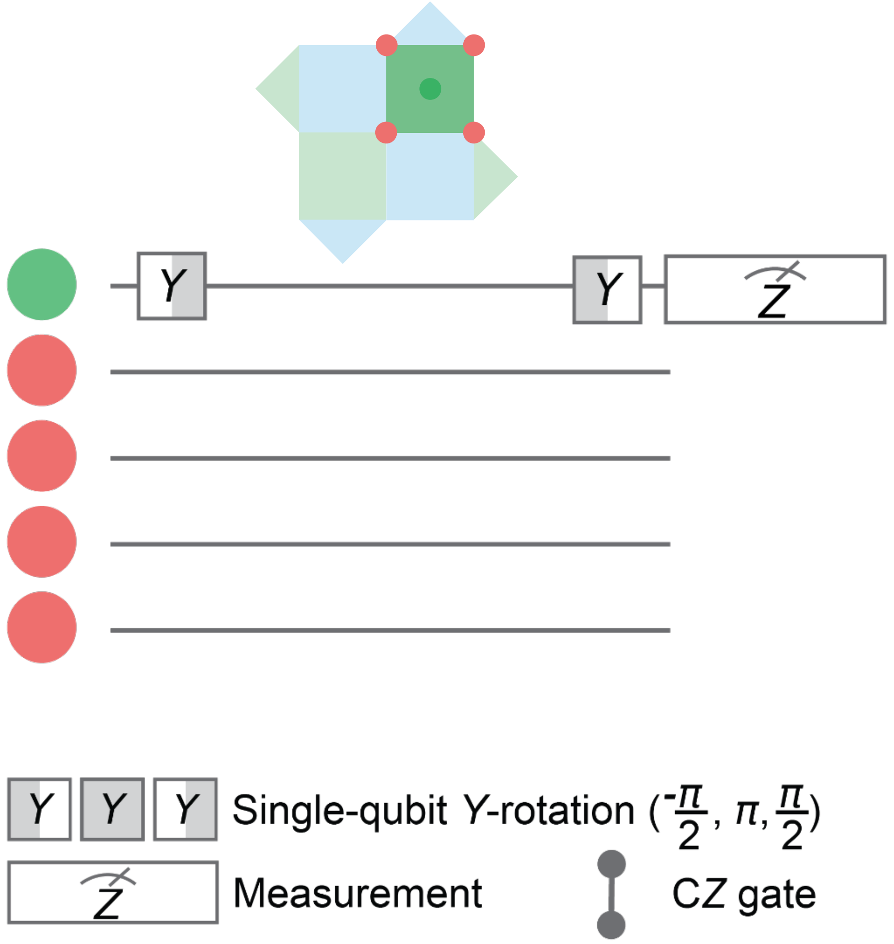

Stabilizer Measurements

Quantum circuit

- Ramsey measurement on auxiliary qubit Ai
- Controlled-phase (CZ) gates between Ai and four data qubits $\mathrm{D}j$
  - If $\mathrm{D}j$ in $|1\rangle$: phase of Ai changes by π
  - ➢ Resulting mapping:

Number of $\mathrm{D}j$ in $|1\rangle$:	Final phase of Ai	Final state of Ai	Stabilizer value s^{Ai}
Even	0	Unchanged	+1
Odd	π	Changed	-1

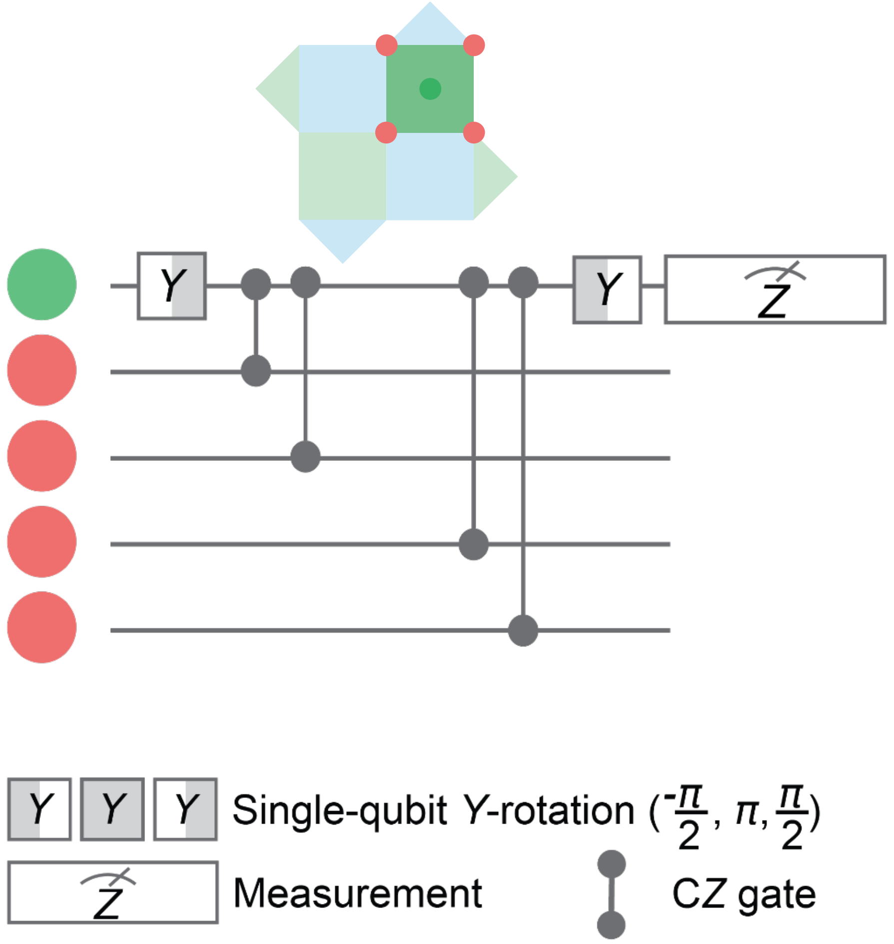

S. Krinner, N. Lacroix *et al.*, *Nature* **605**, 669 (2022)

Stabilizer Measurements

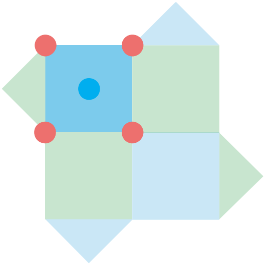

Quantum circuit

- Ramsey measurement on auxiliary qubit Ai
- Controlled-phase (CZ) gates between Ai and four data qubits $\mathrm{D}j$
  - If $\mathrm{D}j$ in $|1\rangle$: phase of Ai changes by π
  - ➢ Resulting mapping:

Number of $\mathrm{D}j$ in $\vert 1\rangle$:	Final phase of Ai	Final state of Ai	Stabilizer value s^{Ai}
Even	0	Unchanged	+1
Odd	π	Changed	-1

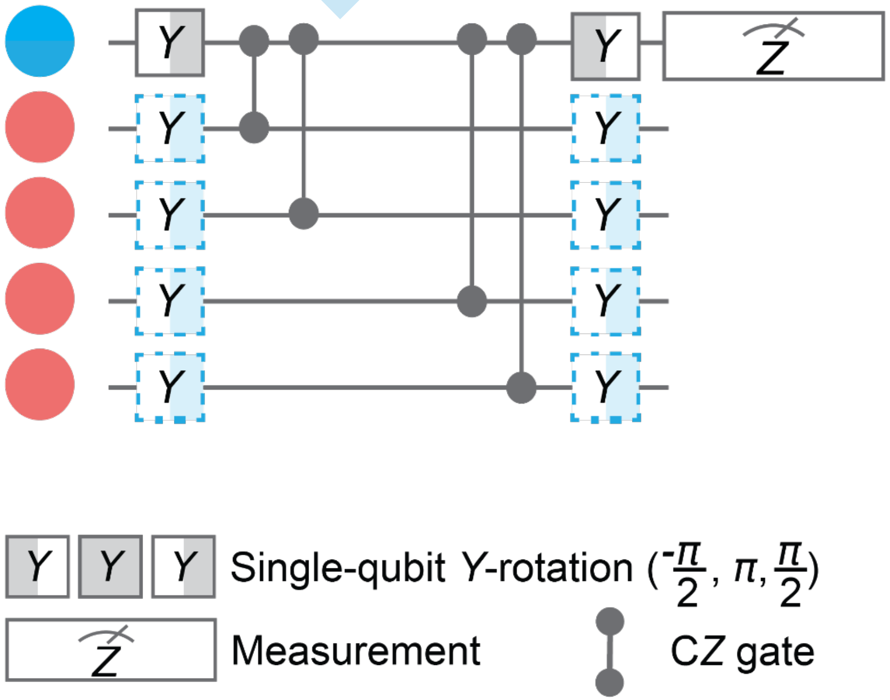

- X-type stabilizer with basis change on data qubits

S. Krinner, N. Lacroix *et al.*, *Nature* **605**, 669 (2022)

Stabilizer Measurements

Quantum circuit

- Ramsey measurement on auxiliary qubit Ai
- Controlled-phase (CZ) gates between Ai and four data qubits $\mathrm{D}j$
  - If $\mathrm{D}j$ in $|1\rangle$: phase of Ai changes by π
  - ➢ Resulting mapping:

Number of $\mathrm{D}j$ in $\|1\rangle$:	Final phase of Ai	Final state of Ai	Stabilizer value s^{Ai}
Even	0	Unchanged	+1
Odd	π	Changed	-1

- X-type stabilizer with basis change on data qubits
- Echo pulses on data qubits to reduce both
  - Dephasing
  - Residual coherent coupling to spectator qubits

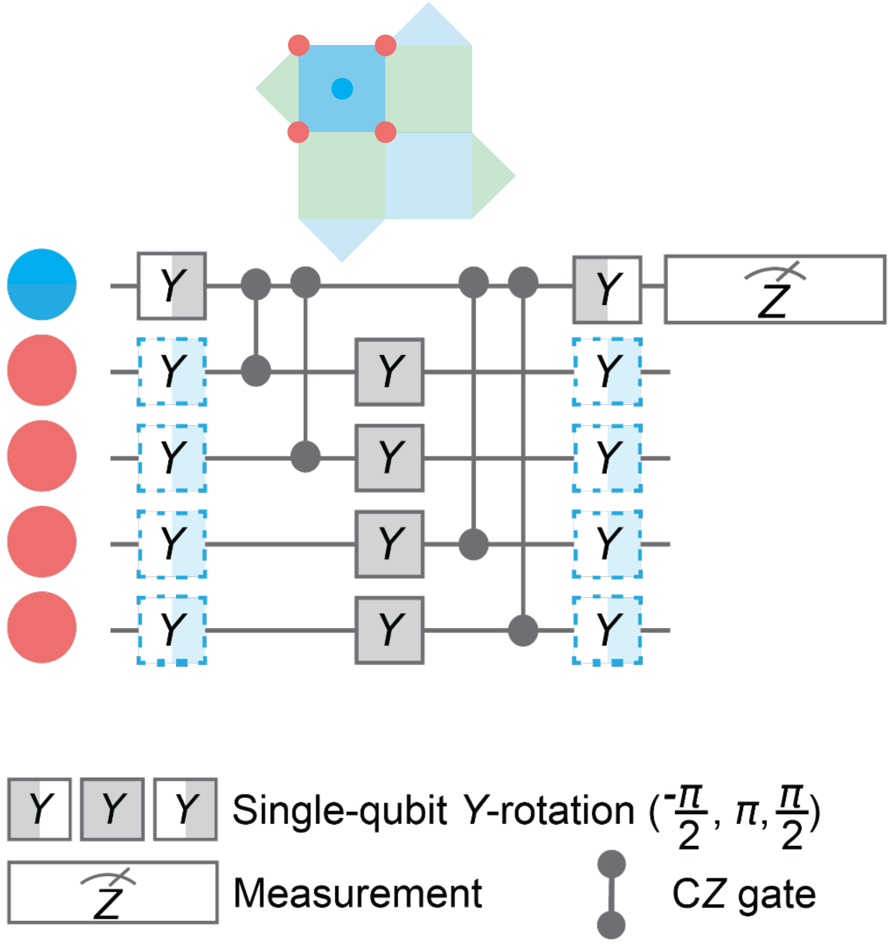

Krinner et al., *Phys. Rev. Applied* **14**, 024042 (2020)

Stabilizer Characterization

Individual characterization

- Prepare data qubits of plaquette in all 4 (weight-2) or 16 (weight-4) basis states
- Stabilizer execution yields $s^{Ai} = \pm 1$
- Average over $\sim 4 \times 10^4$ measurements to obtain $\bar{s}^{Ai}$
- Measured and calculated error

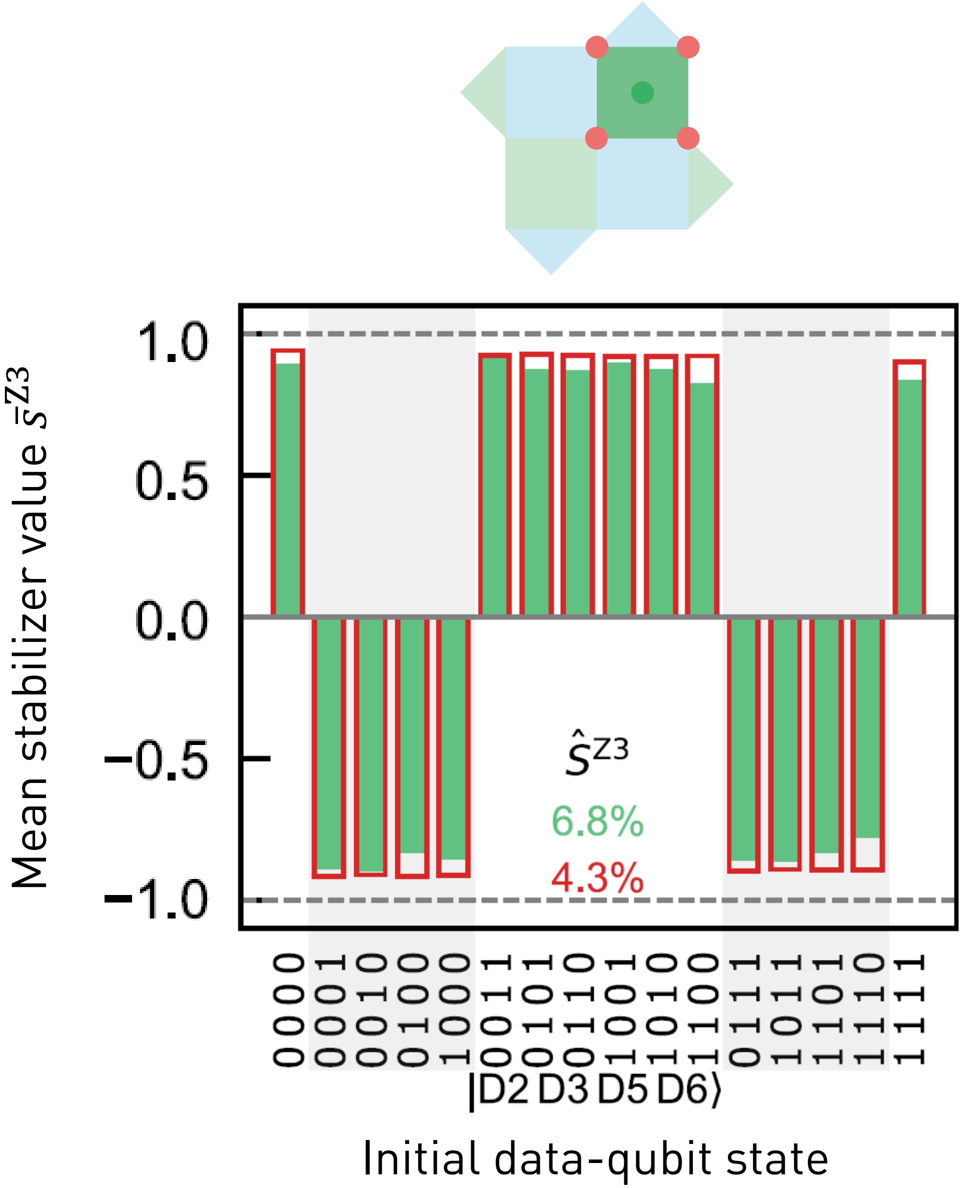

S. Krinner, N. Lacroix *et al.*, *Nature* **605**, 669 (2022)

Stabilizer Characterization

Individual characterization

- Prepare data qubits of plaquette in all 4 (weight-2) or 16 (weight-4) basis states
- Stabilizer execution yields $s^{Ai} = \pm 1$
- Average over $\sim 4 \times 10^4$ measurements to obtain $\bar{s}^{Ai}$
- Measured and calculated error

Average parity error

- Weight-2 stabilizers: 3.9(1.3) %
- Weight-4 stabilizers: 8.2(2.2) %

Qualitative agreement with master-equation simulations

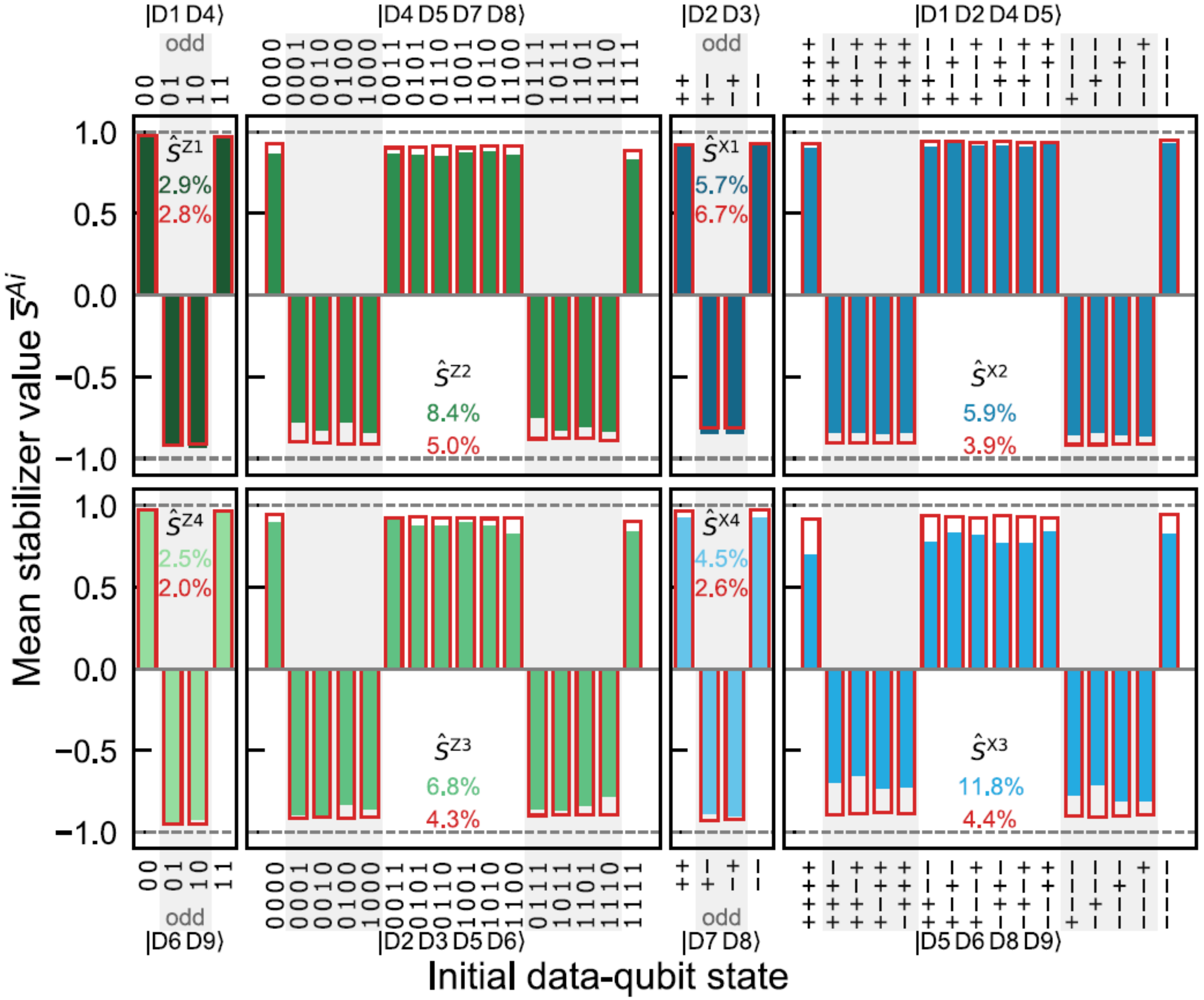

S. Krinner, N. Lacroix *et al.*, *Nature* **605**, 669 (2022)

The Surface Code Cycle

- All four $\hat{S}^{Zi}$ measured in parallel
- All four $\hat{S}^{Xi}$ measured in parallel
- Pipelining: Read out one stabilizer type while running gates of the other.
- Logical state preparation: $|0\rangle_L, |1\rangle_L$ and $|\pm\rangle_L = (|0\rangle_L \pm |1\rangle_L)/\sqrt{2}$ in single cycle.
- State preservation over n cycles
  - Cycle duration: 1.1 μs
  - Leakage detection and rejection executed in every cycle
  - circuits with ~ 800 single-qubit gates and ~ 400 two-qubit gates

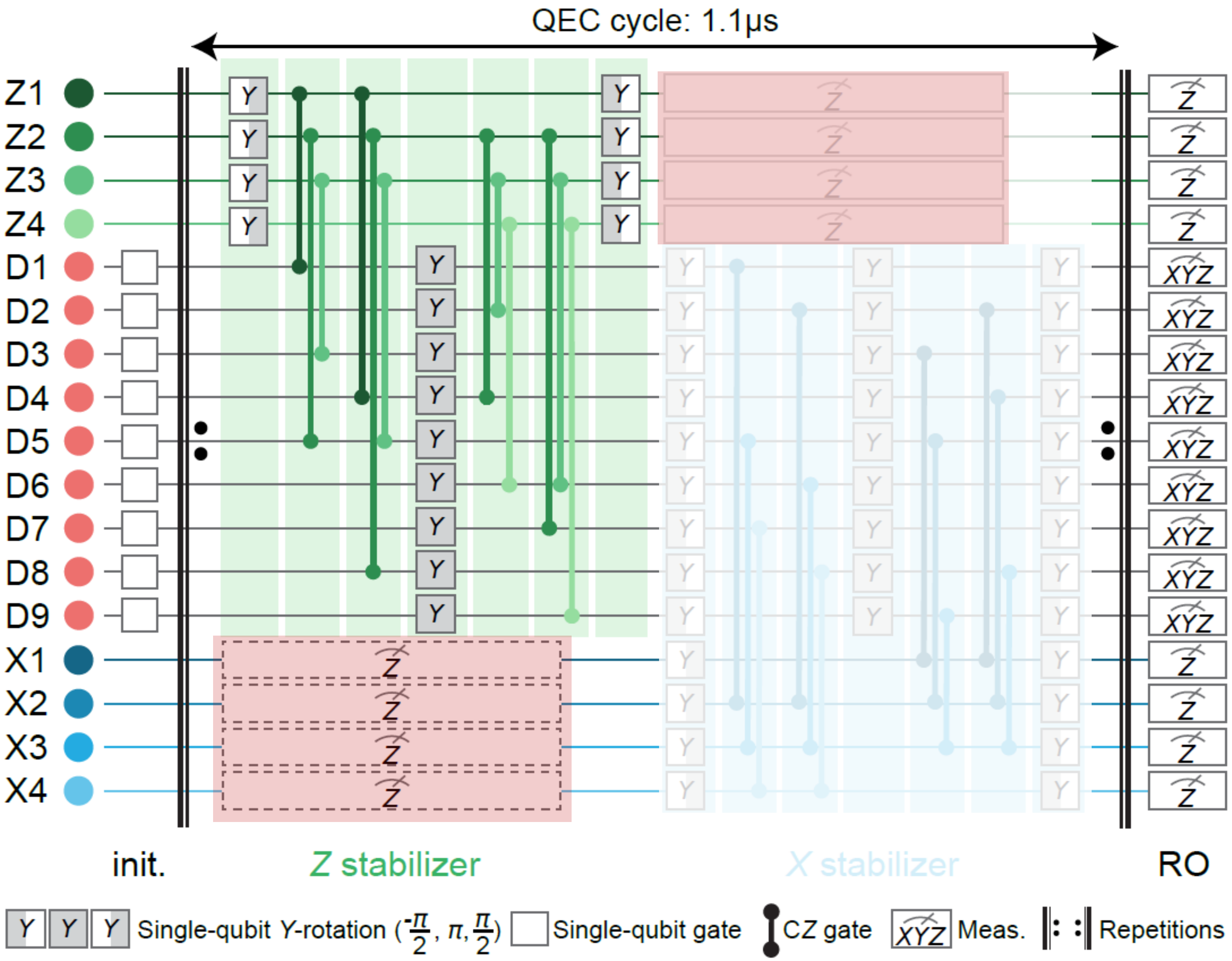

Versluis et al., *PR Applied* **8**, 034021 (2017)
S. Krinner, N. Lacroix *et al.*, *Nature* **605**, 669 (2022)

Syndrome Measurements

- Average σ_m^{Ai} over experimental repetitions: $\bar{\sigma}_m^{Ai}$
- Average over Ai and m: $\bar{\sigma} = 0.14 \ll 1$

- For $m \geq 2$: $\bar{\sigma}_m^{Ai}$ approximately constant
- Finite remaining slope due to increasing excited state population of auxiliary qubits

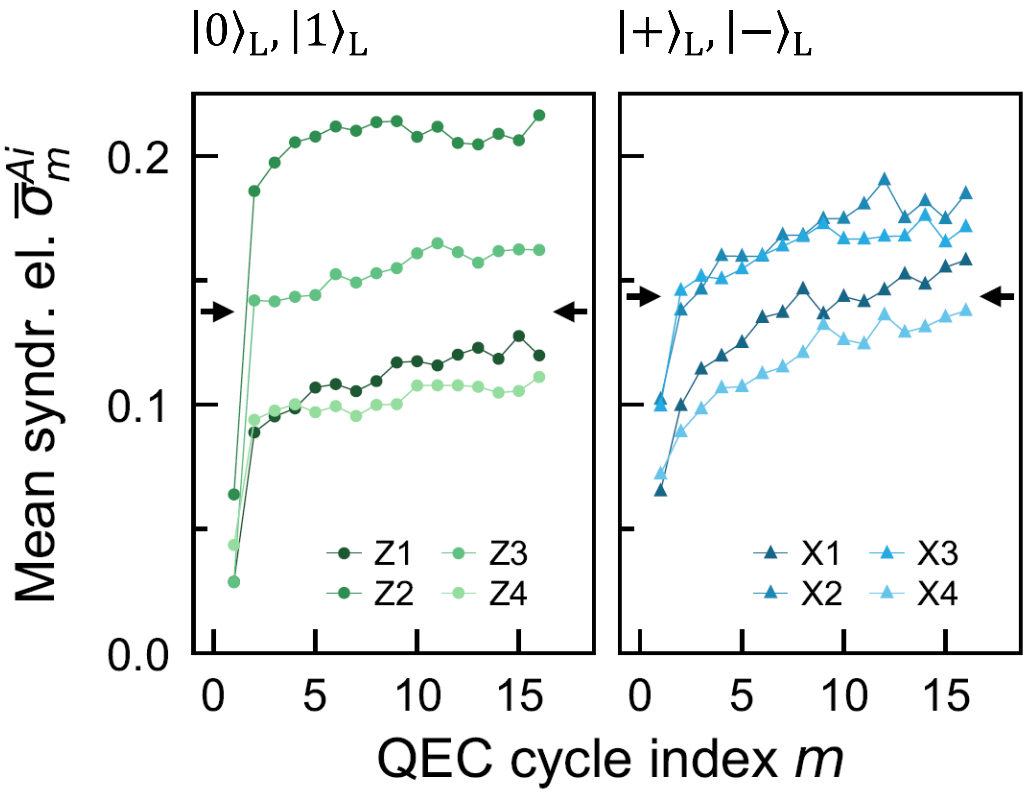

S. Krinner, N. Lacroix *et al.*, *Nature* **605**, 669 (2022)

Syndrome Measurements

- Average σ_m^{Ai} over experimental repetitions: $\bar{\sigma}_m^{Ai}$
- Average over Ai and m: $\bar{\sigma} = 0.14 \ll 1$

- For $m \geq 2$: $\bar{\sigma}_m^{Ai}$ approximately constant
- Finite remaining slope due to increasing excited state population of auxiliary qubits

- Qualitative agreement with simulations

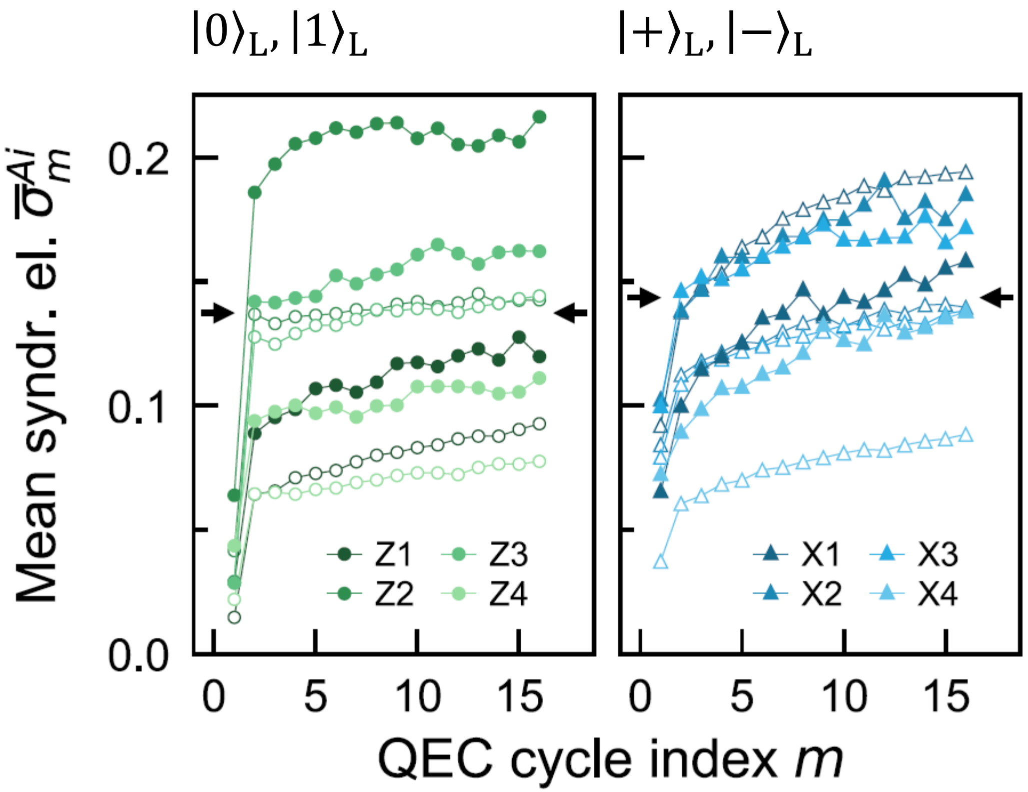

S. Krinner, N. Lacroix *et al.*, *Nature* **605**, 669 (2022)

Decoding of Syndromes

Decoder:

- Determine most likely errors given observed sequence of syndromes
- Mapping to minimum-weight-perfect-matching algorithm
  - Syndrome graph
  - Weights determined in error-model-free approach

Spitz et al., *Adv. Quantum Techn.* **1**, 1800012 (2018)
Chen et al., *Nature* **595**, 383 (2021)
Remm et al., arXiv:2502.17722 (2025)

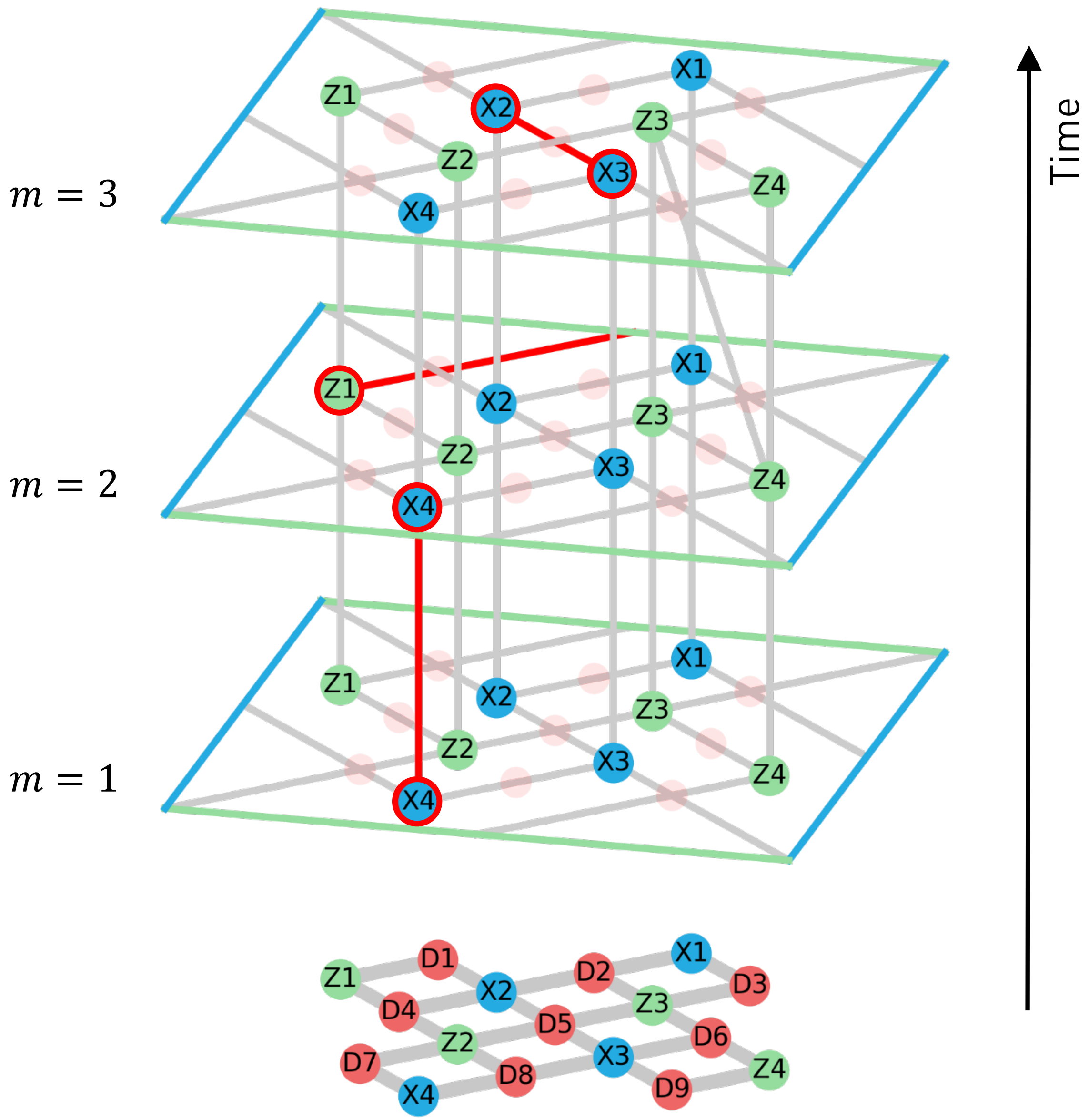

Repeated Quantum Error Correction

Measurement of Logical Z and Logical X Operators

- Initialization
  - $|0\rangle_L$: prepare data qubits in $|0\rangle^{\otimes 9}$
  - $|1\rangle_L$: prepare data qubits in $X_L|0\rangle^{\otimes 9}$
  - $|+\rangle_L$: prepare data qubits in $|+\rangle^{\otimes 9}$
  - $|-\rangle_L$: prepare data qubits in $Z_L|+\rangle^{\otimes 9}$
- Perform n QEC cyles
- Read out all data qubits in Z-basis (X-basis)

Analysis

- Determine logical operator $z_\mathrm{L} = z_1 z_2 z_3 = \pm 1$ ($x_\mathrm{L} = x_1 x_4 x_7 = \pm 1$) for each run with up to n repeated cycles
- Apply correction conditioned on decoded syndromes for each run
- Average over runs with n repeated cycles to compute $\bar{z}_\mathrm{L} = \langle \hat{Z}_\mathrm{L} \rangle$ ($\bar{x}_\mathrm{L} = \langle \hat{X}_\mathrm{L} \rangle$)

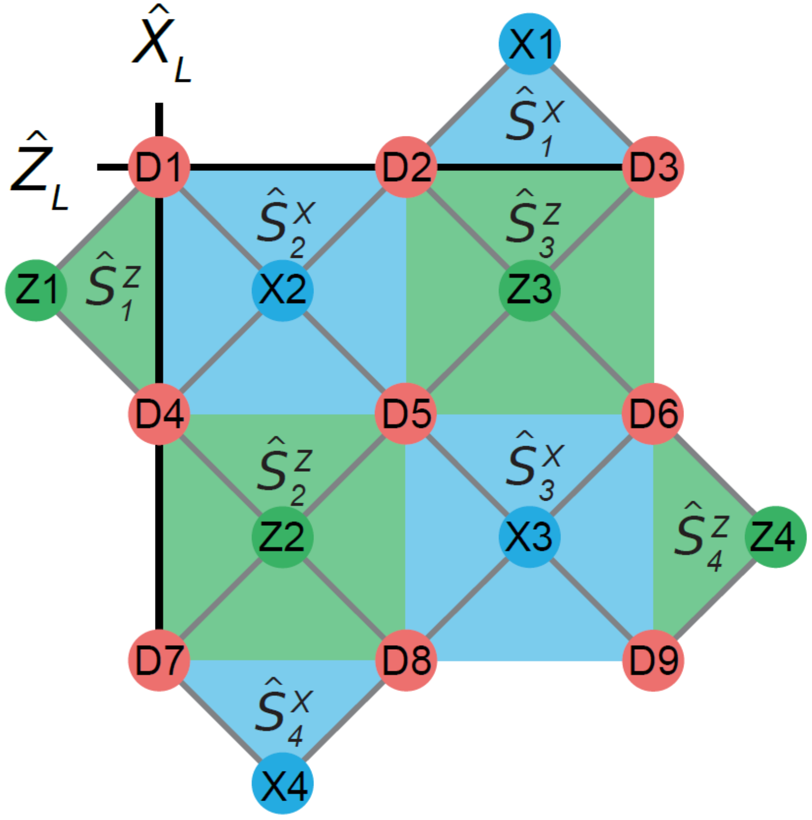

S. Krinner, N. Lacroix *et al.*, *Nature* **605**, 669 (2022)

Repeated Quantum Error Correction

Outcomes Logical Z and Logical X

- Exponential decay of logical expectation values
- Logical lifetime
  $T_{1,\mathrm{L}} = 16.4(8)\ \mu\mathrm{s} \gg t_c = 1.1\ \mu\mathrm{s}$
- Logical coherence time
  $T_{2,\mathrm{L}} = 18.2(5)\ \mu\mathrm{s} \gg t_c = 1.1\ \mu\mathrm{s}$
- Master equation simulation of logical lifetimes of ~ 26 μs provide upper bound for achievable lifetimes with our device performance

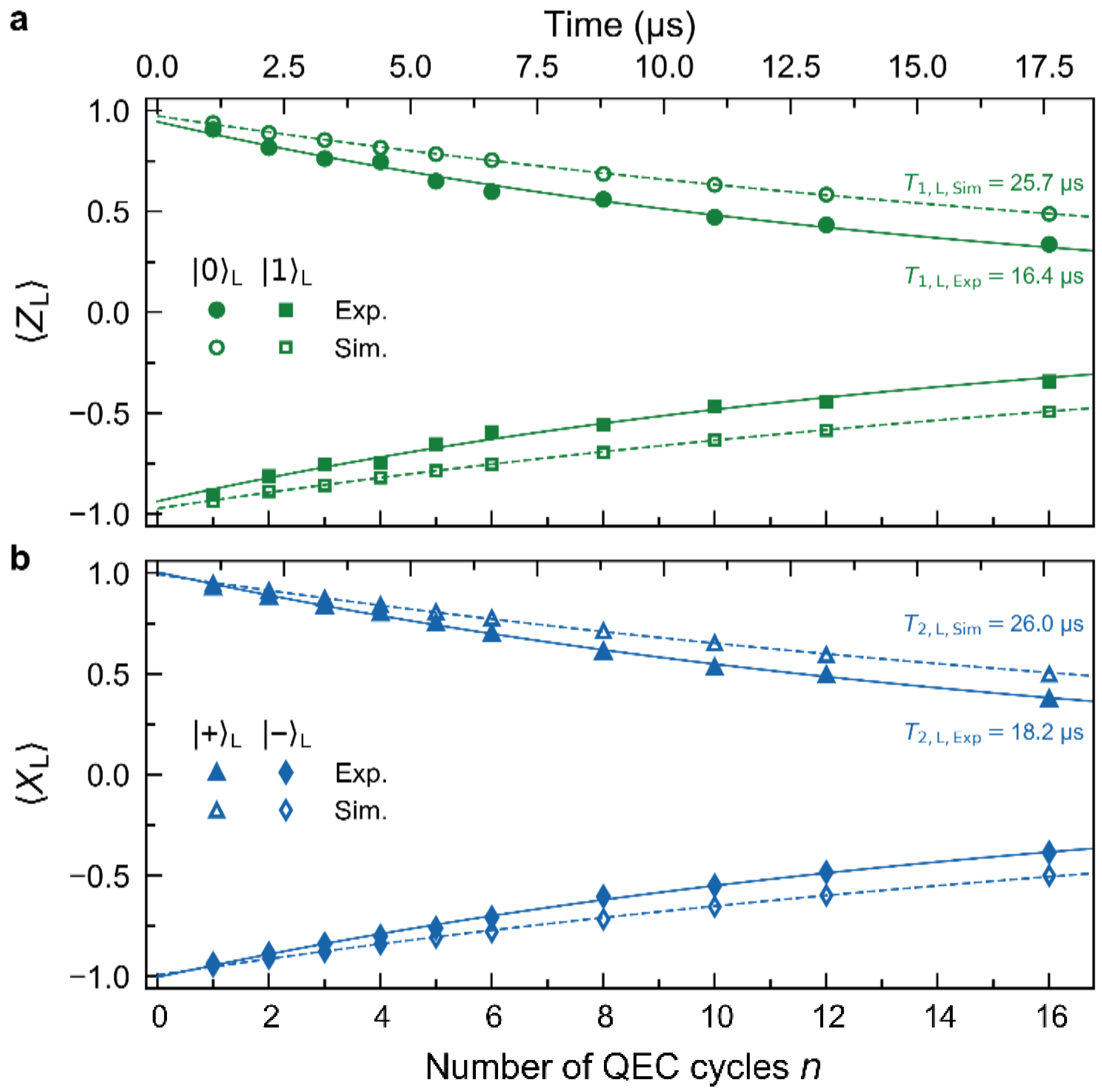

S. Krinner, N. Lacroix *et al.*, *Nature* **605**, 669 (2022)

Logical Error Probability and Logical Error per Cycle

Logical error probability:

- $E_\mathrm{L} = (1 - \langle \hat{Z}_\mathrm{L} \rangle)/2$ for eigenstates of $\hat{Z}_\mathrm{L}$
- $E_\mathrm{L} = (1 - \langle \hat{X}_\mathrm{L} \rangle)/2$ for eigenstates of $\hat{X}_\mathrm{L}$

Logical error per cycle:

- Extracted from fit to $E_\mathrm{L}(n)$ or from $T_{1/2,\mathrm{L}}$:

  $\epsilon_\mathrm{L} = \frac{1}{2}\left[1 - \exp(-t_\mathrm{c}/T_{1/2,\mathrm{L}})\right] \approx t_\mathrm{c}/2T_{1/2,\mathrm{L}}$
- $\epsilon_\mathrm{L} \sim 0.03$

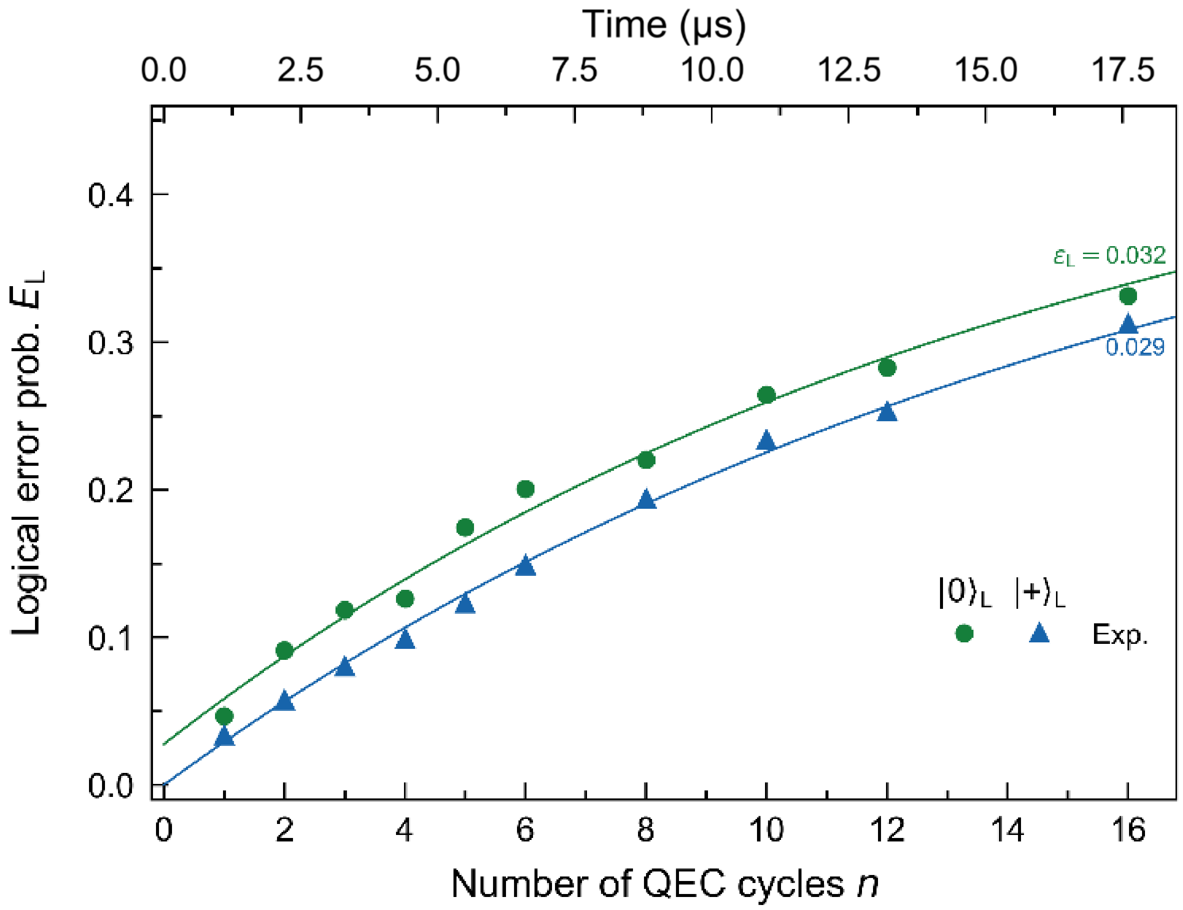

S. Krinner, N. Lacroix *et al.*, *Nature* **605**, 669 (2022)

Repeated Quantum Error Correction Experiments with d=3 or Larger

Published work:

- Honeywell: [1] Ryan-Anderson *et al.*, *Phys. Rev. X* **11**, 041058 (2021)
  ETHZ: [2] Krinner, Lacroix *et al. Nature* **605**, 669 (2022)
  USTC: [3] Zhao et al., *PRL* **129**, 030501 (2022)
  IBM: [4] Sundaresan *et al.*, *Nat. Commun.* **14**, *2852* (2023)
  Google: [5] Google Quantum AI, *Nature* **614**, 676 (2023)
  Google: [6] Google Quantum AI, *Nature* **638**, 920 (2025)
  Google: [7] Lacroix *et al.*, *arXiv:2412.14256* (2024)

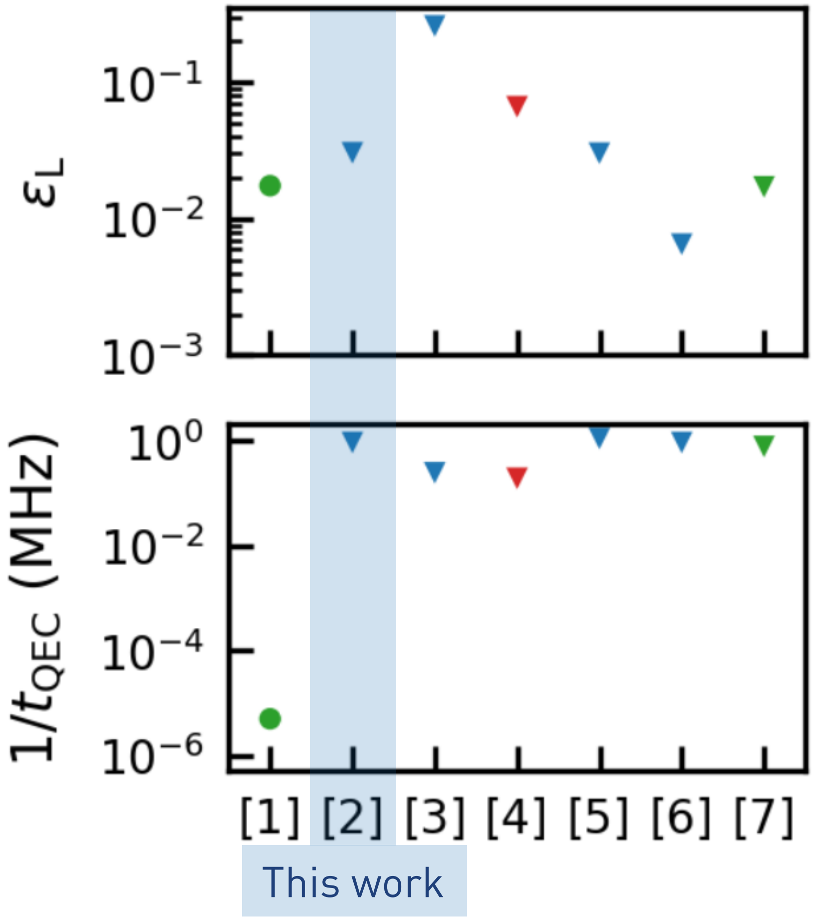

Implementations:

- superconducting-circuits (∇) and trapped-ions (O)
- Color code, surface code and heavy-hexagon code

Performance criteria

- Small logical error per cycle ε_L
- High QEC cycle rate $1/t_{QEC}$

Performance Assessment and Projection

Two-qubit-gate break-even

- Compare $\epsilon_{\mathrm{L}} = 0.03$ to dominant physical error
  - Two-qubit gate error $\epsilon_{2\mathrm{Q}} = 0.015$
  - Logical two-qubit gate error is expected to be dominated by ϵ_{L}
- Used simulations to project performance with physical error rates reduced by factor x
  - $\epsilon_{\mathrm{L}} \propto 1/x^2$
  - Break-even within reach

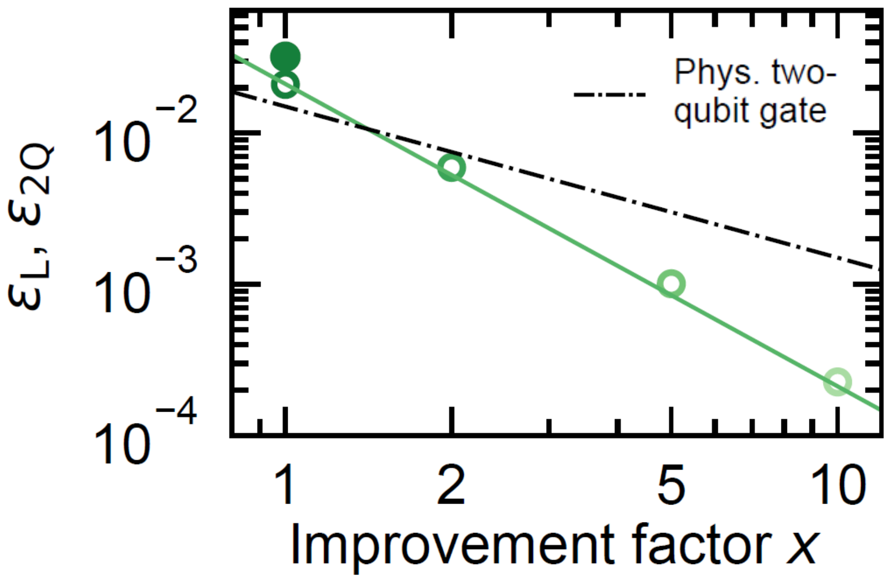

Error threshold

- $\epsilon_{\mathrm{L}} \sim 0.03$ comparable to predicted logical error per cycle at error threshold
  Fowler *et al.*, *Phys. Rev. A* **86**, 032324 (2012)
  Stephens, *Phys. Rev. A* **89**, 022321 (2014).

S. Krinner, N. Lacroix *et al.*, *Nature* **605**, 669 (2022)

Distance-Three, -Five and –Seven Surface Code Layout

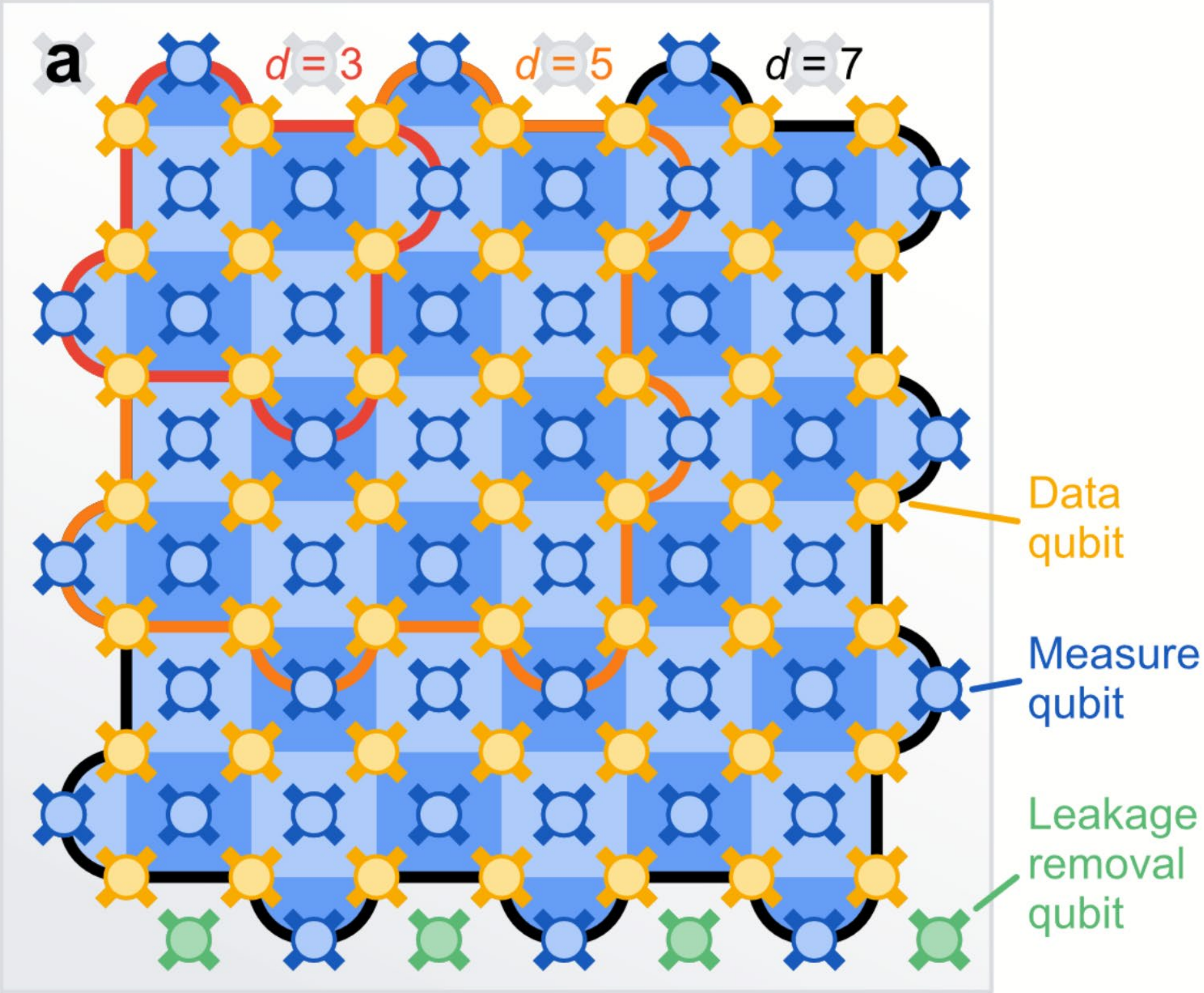

Google Quantum AI, *Nature* **638**, 920 (2025)

Distance Scaling and Logical Error Suppression

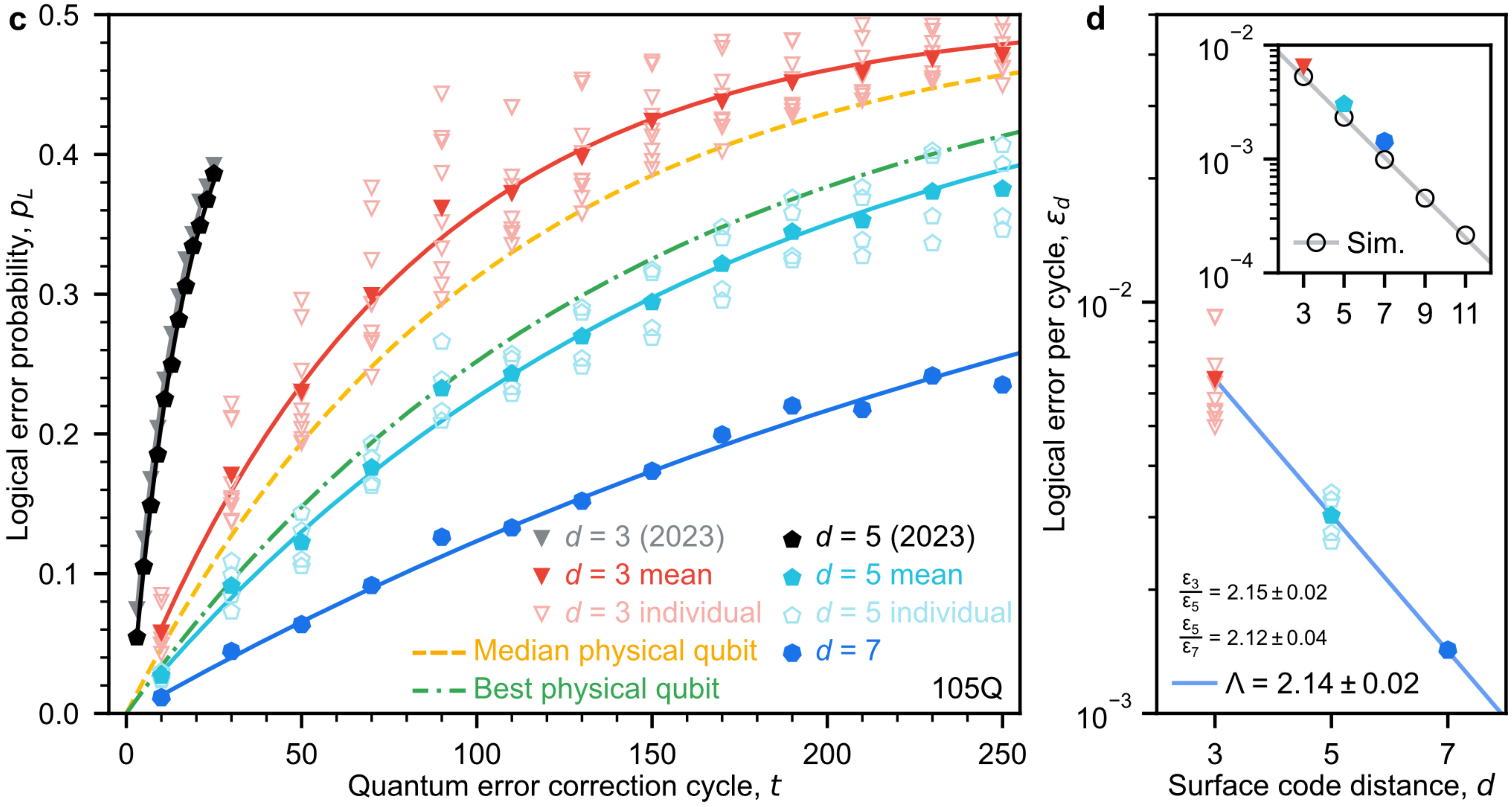

Google Quantum AI, *Nature* **638**, 920 (2025)

Surface Code and Lattice Surgery

- Surface code promising candidate for implementation of logical qubits in superconducting circuits
  - Kitaev, A. Ann. Phys. 303 1 (2003)
  - Fowler, A. et al. Phys. Rev. A 86, 032324 (2012)

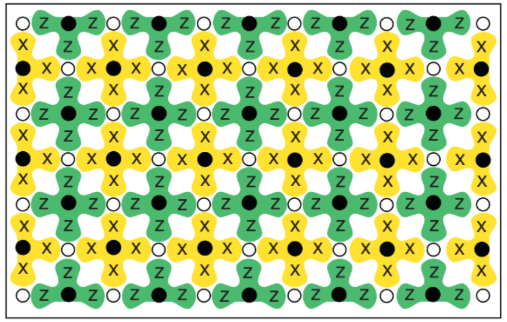

- Experimental realizations of logical state preservation close to the threshold
  - Krinner, S. et al. Nature 605, pages 669–674 (2022)
  - Google Quantum AI, Nature 614, pages 676–681 (2023)
  - Google Quantum AI and Collaborators, Nature (2024)

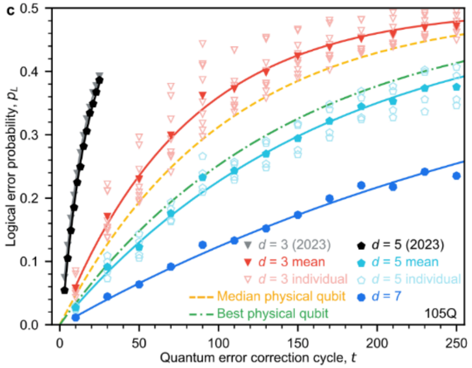

- Lattice surgery allows realization of non-transversal interactions between encoded qubits with low qubit-overhead
  - Horsman, D. et al. New J. Phys. 14 123011 (2012)

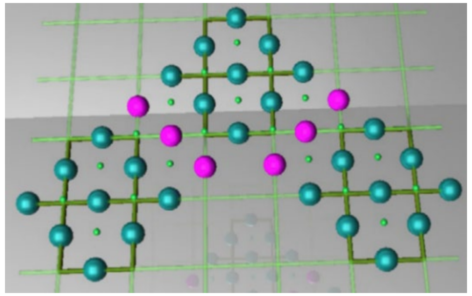

Experimental Work on Logical Qubit Operations

Logical operations on **encoded qubits**:

- Fault-tolerant subset of Clifford group on [4,2,2] code (s.c.)
  Harper, R. et al. Phys. Rev. Lett. **122**, 080504 (2019)
- Transversal CNOT on two [7,1,3] color codes (ions)
  Postler, L. et al. Nature **605**, 675 (2022)

Non-fault-tolerant **arbitrary state preparation**

- d = 3 Bacon-Shor code (ions)
  Egan, L. et al. Nature **598**, 281 (2021)
- d = 3 surface code (s.c.)
  Ye, Y. et al. Phys. Rev. Lett. **131**, 210603 (2023)

Lattice surgery ...

- ... on a d = 2 surface code (ions)
  Erhard, A. et al. Nature **589**, 220 (2021)
- ... on interleaved d = 3 3CX and Bacon-Shor code (s.c.)
  Hetenyi, B. et al. PRX Quantum **5**, 040334 (2024)
- ... on a d = 3 color code (s.c.)
  Lacroix, N. et al. arXiv:2412.14256v1 (2024)

Independent logical qubits during idling (modularity):

- transversal implementation of various QEC codes (ryd.)
  Bluvstein, D. et al. Nature **626**, 58 (2024)
- state teleportation on three d = 3 color codes (ions)
  Ryan-Anderson, C. et al. Science **385**, 1327 (2024)

Here: Modular lattice surgery on surface code with partial decoding from repeated syndrome extraction on superconducting qubits

Transversal Gates vs. Lattice Surgery

All-to-all connectivity (ions, Rydberg atoms)

- Allows for transversal logical two-qubit gates

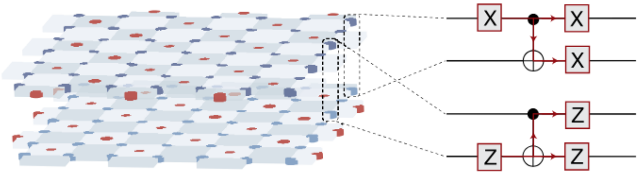

D. Bluvstein et al, Nature **626**, pages 58–65 (2024)

2D square lattice connectivity (s.c.)

- Requires lattice surgery

Lattice surgery operations:

- Merge
- Split
- Measurement of logical two-qubit observables $\hat{X}_{L1}\hat{X}_{L2}$ (or $\hat{Z}_{L1}\hat{Z}_{L2}$)

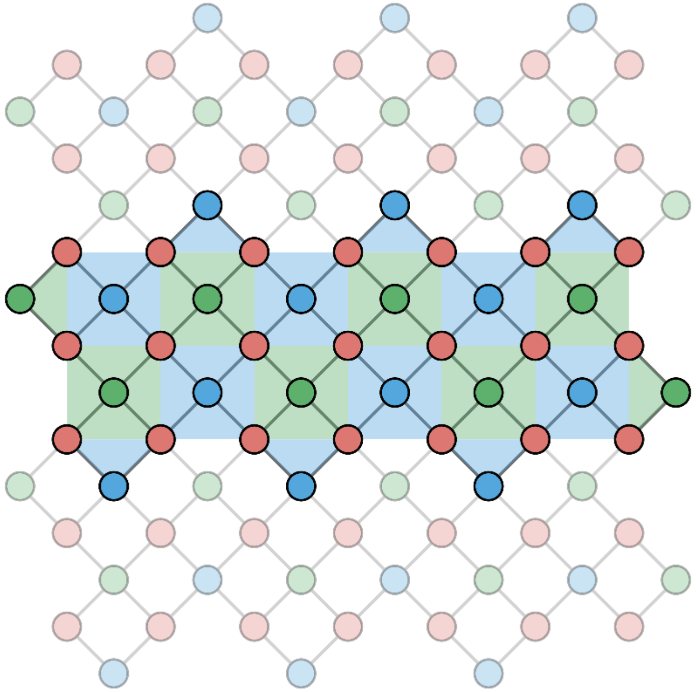

Z-type stabilizers

X-type stabilizers

Inactive aux qubits

Data qubit

Data qubit (inactive)

Horsman, D. et al. New J. Phys. **14** 123011 (2012)

Austin G. Fowler, Craig Gidney arXiv:1808.06709 (2018)

Logical Operators of the Surface and the Repetition Codes

- Distance-three surface code qubit:
  - 3×3 patch on the data qubit lattice,
  - single bit-flip and phase-flip errors correctable
  - Logical operator definitions
- Lattice split operation transforms the d = 3 surface code into two d = 3 bit-flip codes:
  - Stop measuring X-type stabilizers
  - Readout of middle column of data qubits in Z-basis
- Two d = 3 bit-flip repetition codes:
  - Two 1×3 patches
  - Single bit-flip error correctable
  - Logical operator definitions

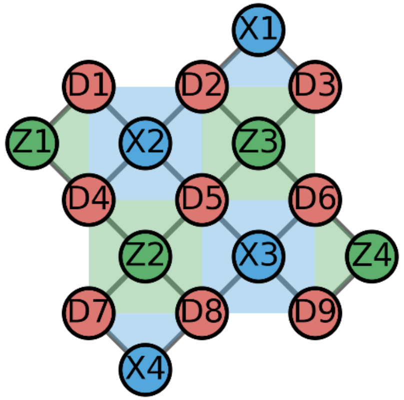

$$\hat{Z}_{L2} = \hat{Z}_{D6}$$
$$\hat{X}_{L2} = \hat{X}_{D3}\hat{X}_{D6}\hat{X}_{D9}$$
$$\hat{Y}_{L2} = \hat{X}_{D3}\hat{Y}_{D6}\hat{X}_{D9}$$

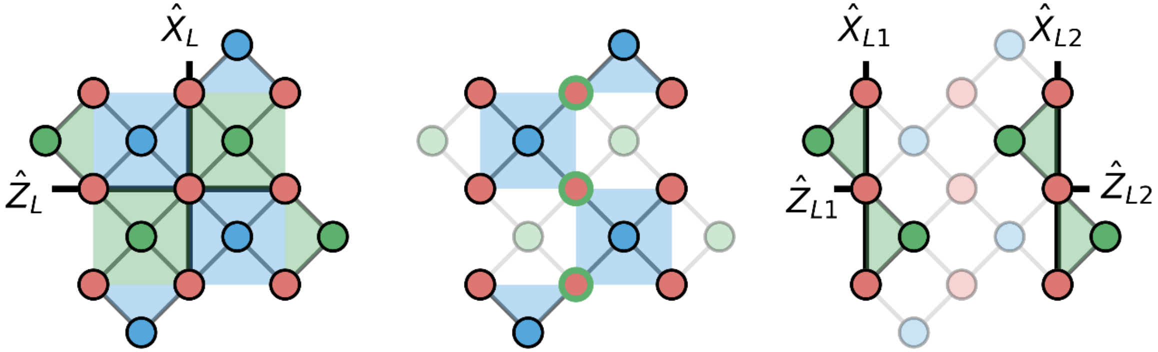

$$\hat{Z}_L = \hat{Z}_{D4}\hat{Z}_{D5}\hat{Z}_{D6}$$
$$\hat{X}_L = \hat{X}_{D2}\hat{X}_{D5}\hat{X}_{D8}$$
$$\hat{Y}_L = \hat{Z}_L\hat{X}_L = \hat{X}_{D2}\hat{Z}_{D4}\hat{Y}_{D5}\hat{Z}_{D6}\hat{X}_{D8}$$

$$\hat{Z}_{L1} = \hat{Z}_{D4}$$
$$\hat{X}_{L1} = \hat{X}_{D1}\hat{X}_{D4}\hat{X}_{D7}$$
$$\hat{Y}_{L1} = \hat{X}_{D1}\hat{Y}_{D4}\hat{X}_{D7}$$

Besedin, I., Kerschbaum M. *et al.*, arXiv: 2501.04612 (2025)

Pauli Frame Update

- Logical states after split depend on measurement outcomes
- Relation between repetition and surface code logical operators
  - Logical X-operators:
    $$\hat{X}_{L1} = \hat{X}_L \hat{S}^{X2} \hat{S}^{X4}$$
    $$\hat{X}_{L2} = \hat{X}_L \hat{S}^{X1} \hat{S}^{X3}$$
  - Logical Z-operators:
    $$\hat{Z}_L = \hat{Z}_{D4} \hat{Z}_{D5} \hat{Z}_{D6} = \hat{Z}_{L1} (\hat{Z}_{L2} \hat{Z}_{D5})$$
- Deterministic operation realized by feed-forward Pauli-Frame update:
  - $\hat{X}_L \rightarrow \hat{X}_{L1}, \hat{X}_{L2}$
  - $\hat{Z}_L \rightarrow \hat{Z}_{L1} \hat{Z}_{L2}$
  - performed in post-processing
- Weight-4 Z-type stabilizers become weight-2, value updated by data qubit readout outcome

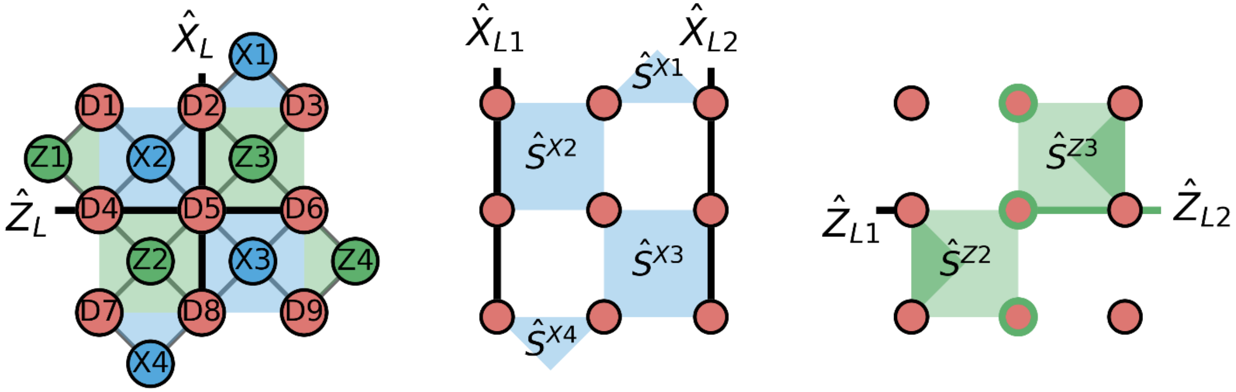

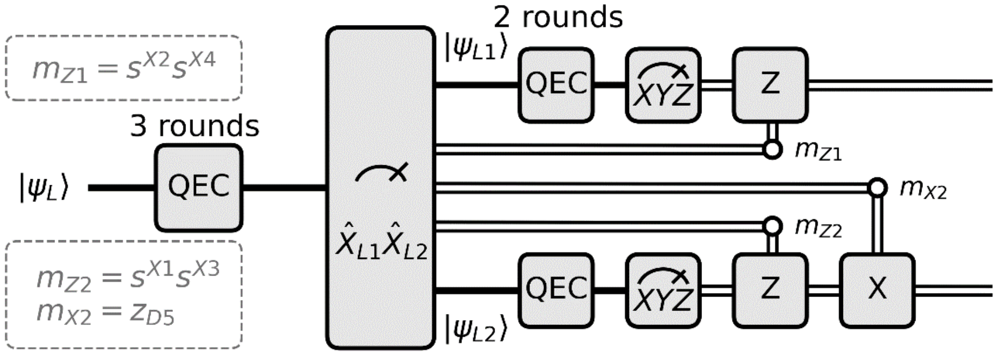

Besedin, I., Kerschbaum M. *et al.*, arXiv: 2501.04612 (2025)

Stabilizer Measurement and Syndrome Extraction

Auxiliary-qubit-based stabilizer measurement

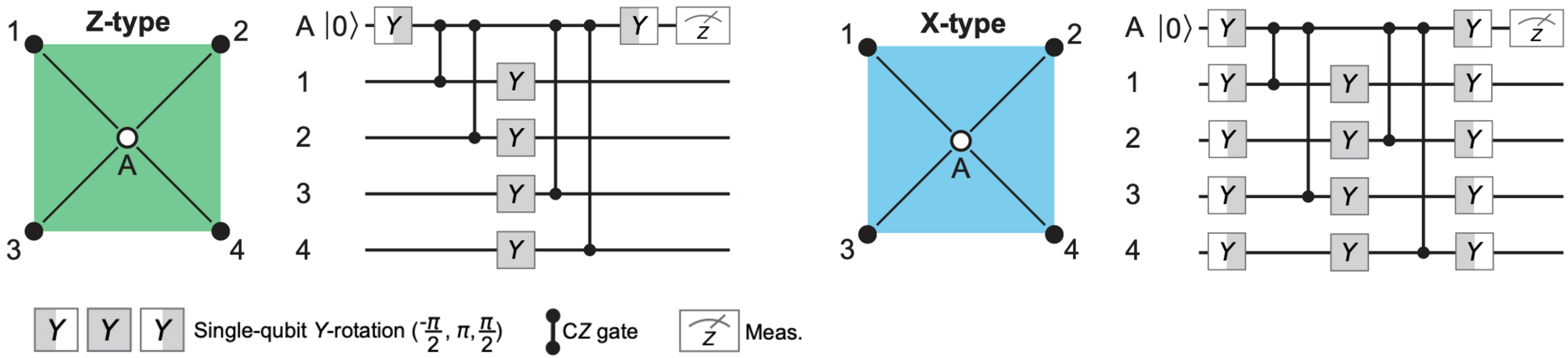

- Z- or X-parity measurement of data qubits on vertices of plaquette
- Bit-flip detected when Z-stabilizer s_N^Z switches from +1 to -1 in round N
- Phase-flip detected when X-stabilizer s_N^X switchies from +1 to -1 in round N
- syndrome element of round N for operator A_i:
  $$\sigma_N^{Ai} = (1 - s_N^{Ai} s_{N-1}^{Ai})/2$$

17-Qubit Device

- flux-tunable transmon qubits
- Readout resonators and Purcell filters coupled to joint feedline

Device performance metrics

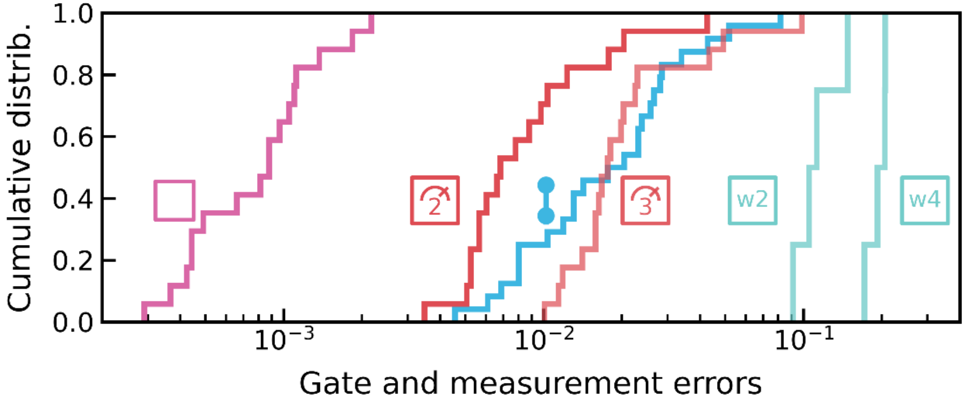

- Single-qubit gate error 0.1%
- Two-qubit gate error 2%
- Two-/three-state readout error 1.1% / 2.5%
- Weight-2/-4 syndrome element 11.6% / 18.5%

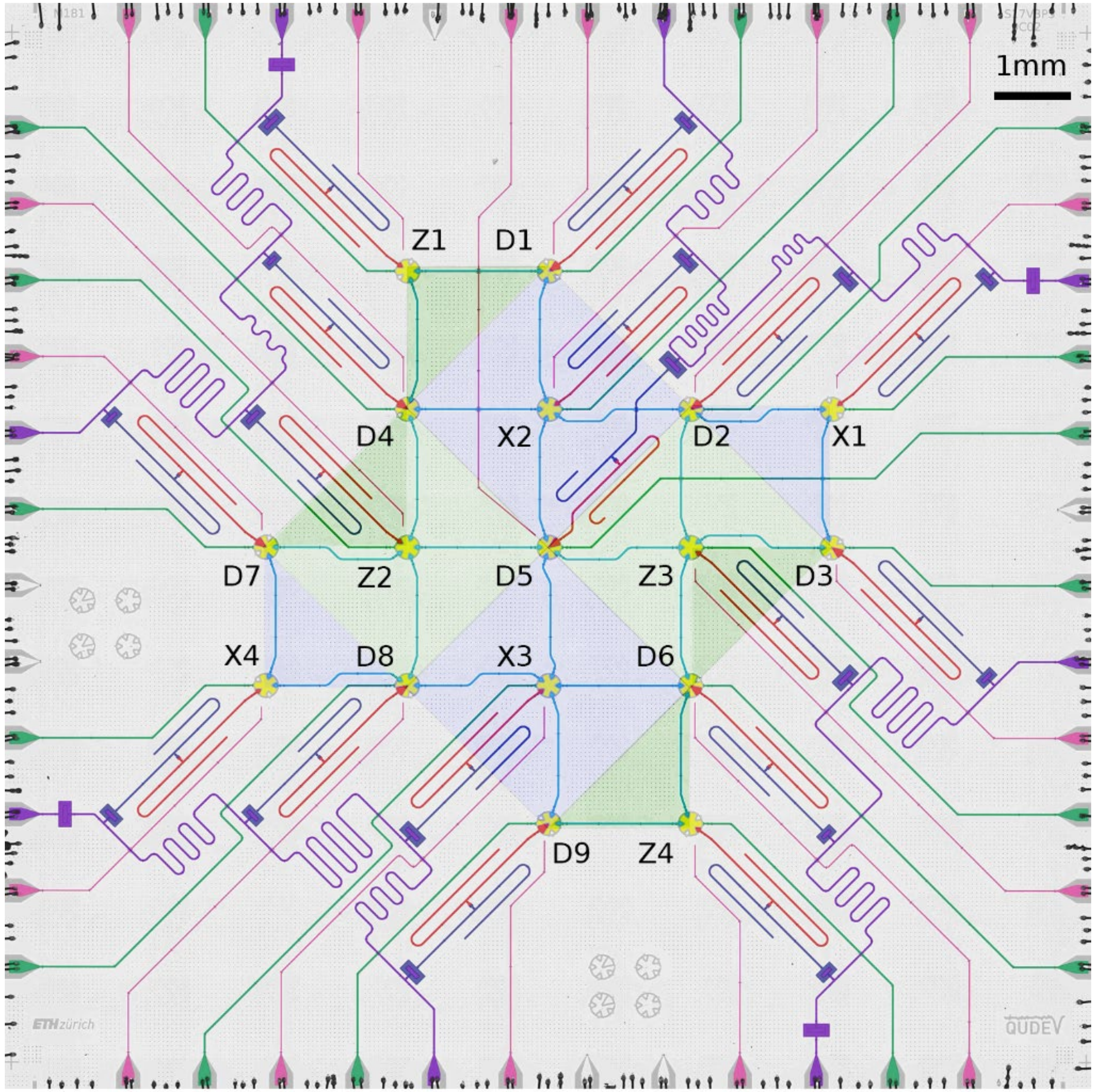

Besedin, I., Kerschbaum M. *et al.*, arXiv: 2501.04612 (2025)

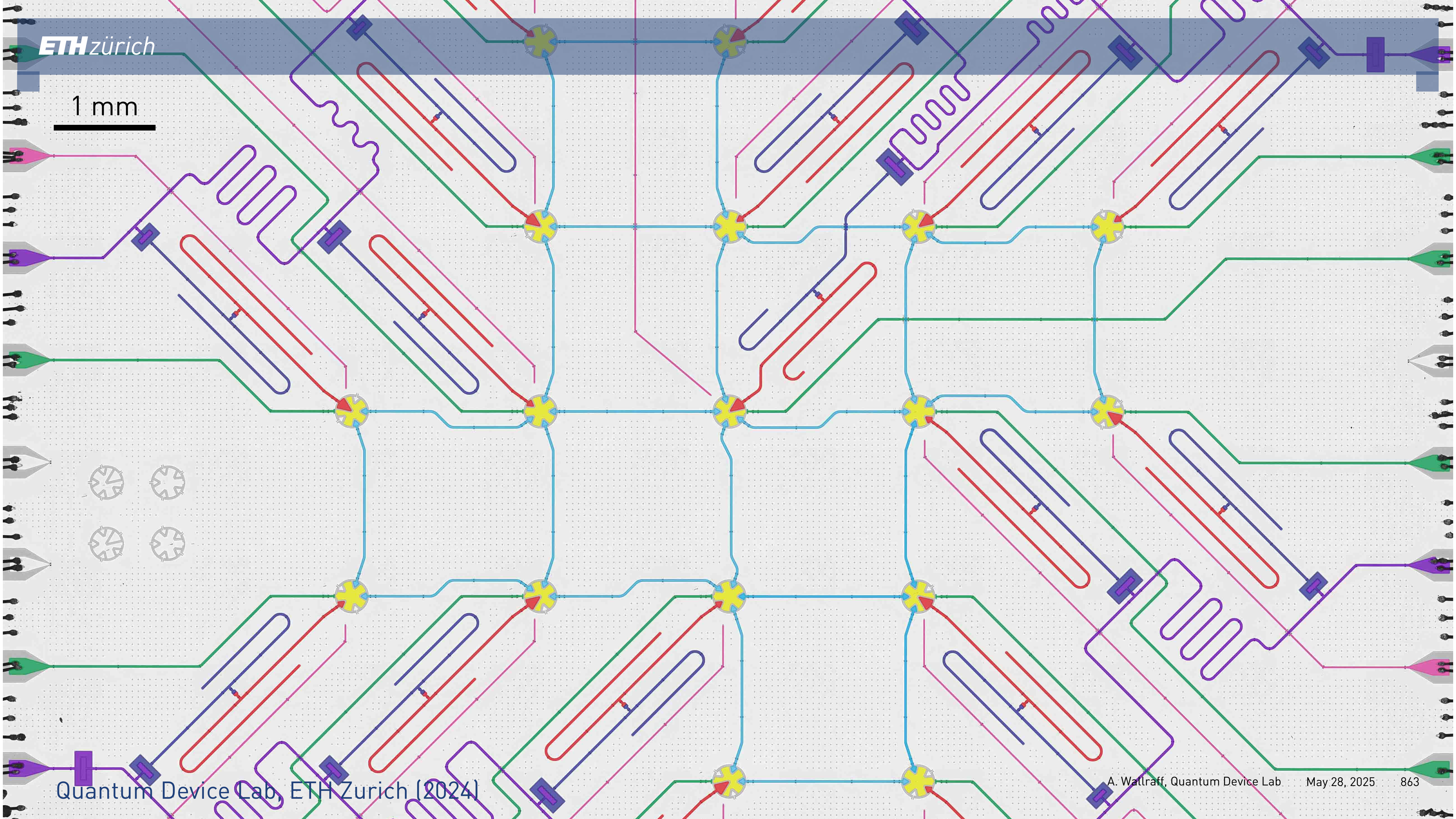

Quantum Device Lab, ETH Zurich (2024)

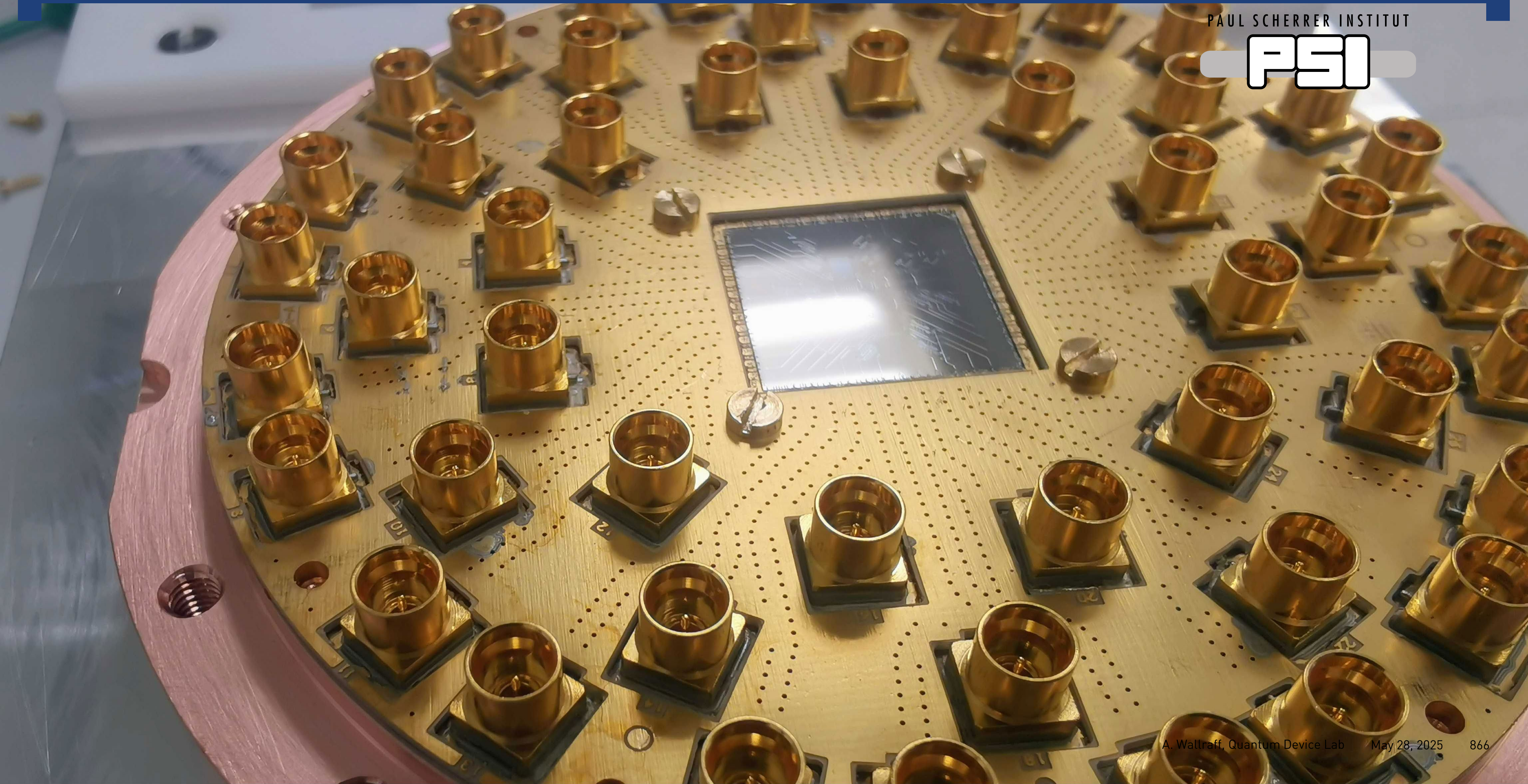


25


PAUL SCHERRER INSTITUT
PSI
BLUE FORS
SHFQC

Surface-Code State-Preservation Experiment

Surface code

- 20 rounds of X and Z stabilizer measurements for $|0\rangle_L, |1\rangle_L, |+\rangle_L, |-\rangle_L$ initial states

Fault-tolerant state preparation:

- preparing all data qubits in $\hat{Z}$ ($\hat{X}$) eigenstates yields well-defined S^{Zi} (S^{Xi}) and Z_L (X_L)
- 1 Preparation syndrome, 19 state preservation and 1 readout syndrome: $\sigma_N^{Ai} = (1 - s_N^{Ai} s_{N-1}^{Ai})/2$

Errors

- evaluate Z_L (X_L) from final data qubit readout
- use syndrome data with MWPM decoder to correct errors
- Error per cycle: $\epsilon_X = 11.1(4)\%, \epsilon_Z = 7.8(2)\%$

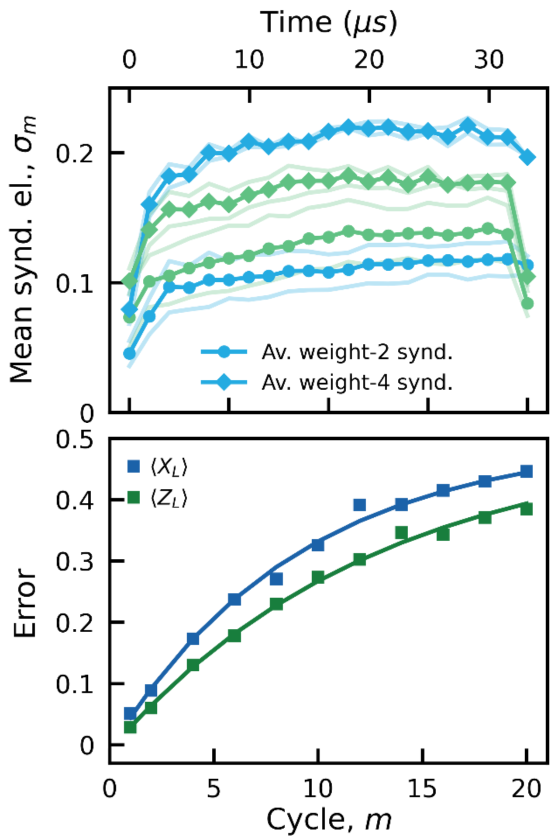

Besedin, I., Kerschbaum M. *et al.*, arXiv: 2501.04612 (2025)

Repetition-Code State-Preservation Experiment

- For repetition codes, only Z syndromes
- Error correction only for $Z_{L1},\ Z_{L2}$ observables
- error per cycle: $\epsilon_{Z1} = 0.68(3)\%$, $\epsilon_{Z2} = 0.93(11)\%$
- For X observables, we compare raw outcomes. Errors per cycle: $\epsilon_{X1} = 10.1(2)\%$, $\epsilon_{X2} = 14.0(8)\%$
- For bit flip-code: $\epsilon_{Y1} = 9.9(2)\%$, $\epsilon_{Y2} = 11.8(5)\%$
- Logical error per cycle in X observable for surface code similar to non-corrected observable in bit-flip code
- **Near-threshold regime**

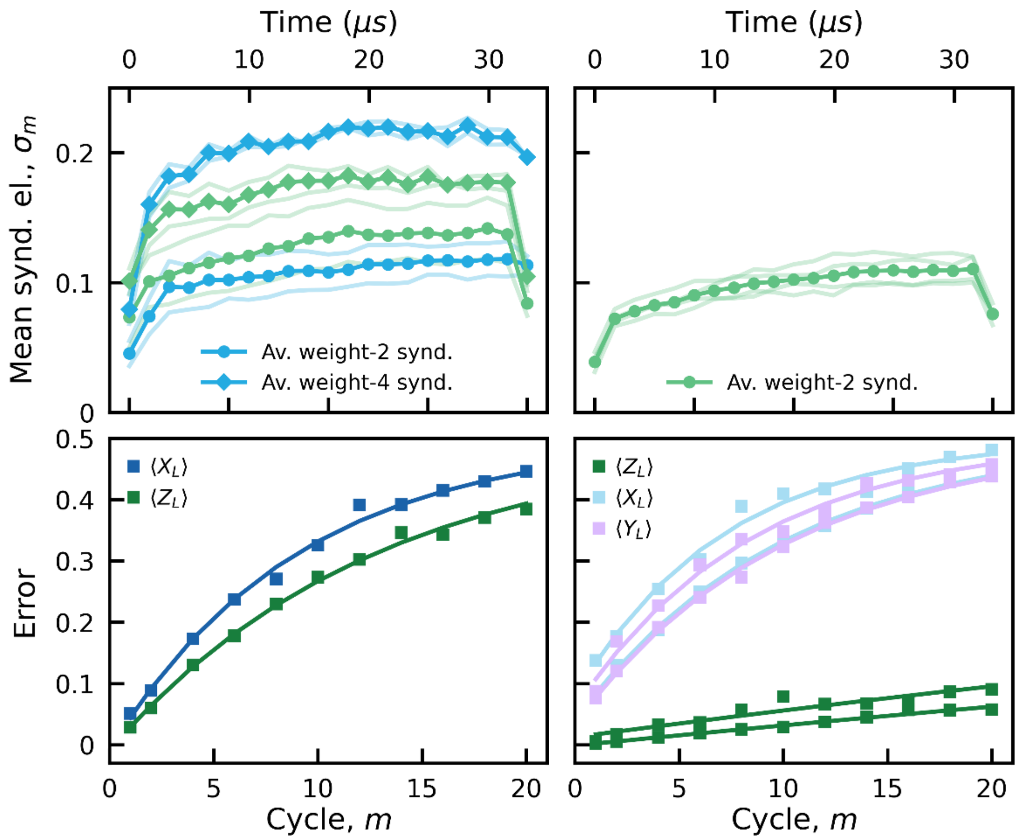

Besedin, I., Kerschbaum M. *et al.*, arXiv: 2501.04612 (2025)

Gate Sequence of Lattice-Split Operation

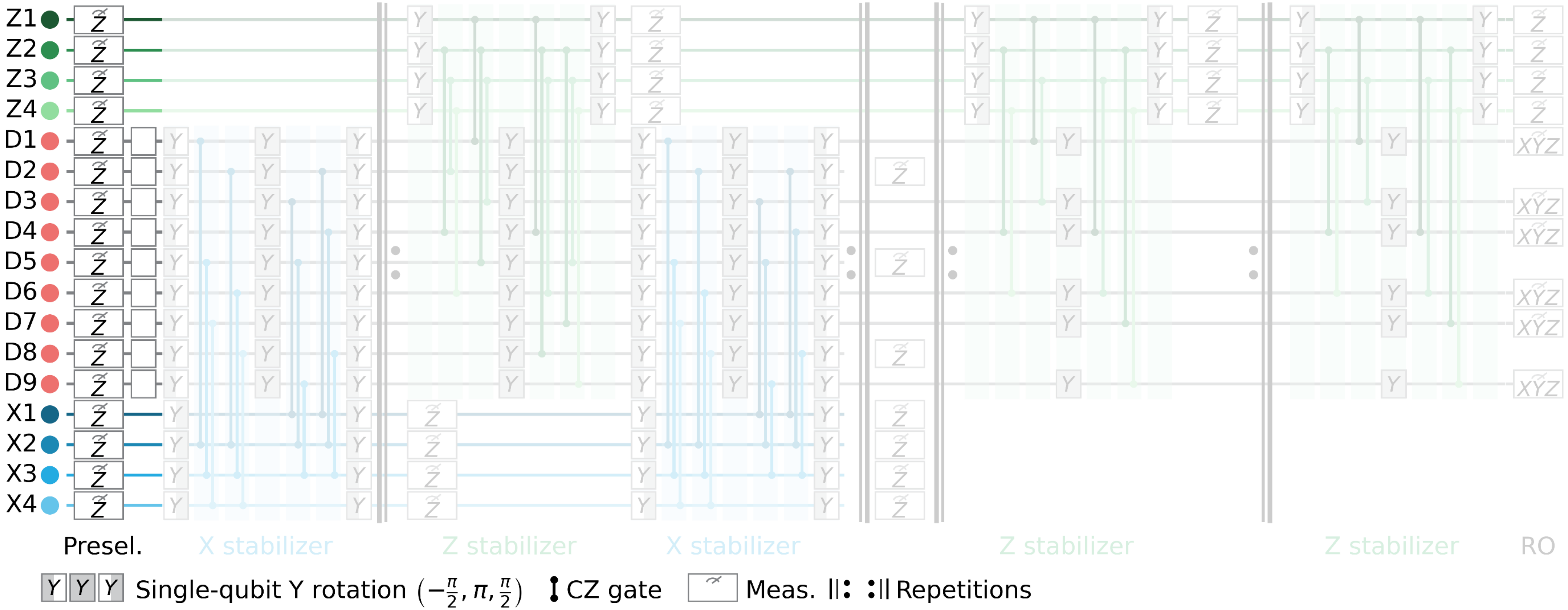

- **Qubit initialization**
- **X-syndrome extraction to initialize d = 3 qubit**
- **Three rounds of syndrome extraction**
- **Lattice split**
- **Two rounds of syndrome extraction**
- **Logical observable readout**

Logical Bell State Creation

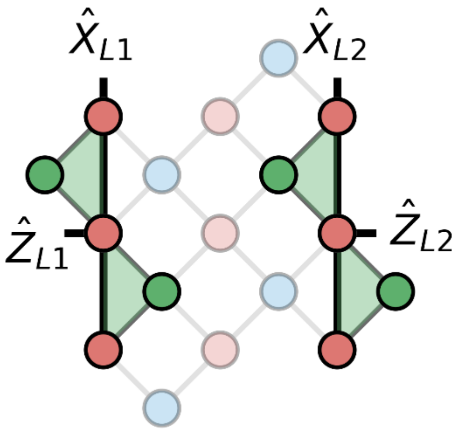

- Prepare surface-code $|0\rangle_L$ and perform lattice split
- Fault-tolerant (d = 3) with respect to **bit-flip errors**
- Non-fault-tolerant (d = 1) with respect to **phase-flip errors**

- Evaluate Logical Bell state after **Pauli-frame update**:
  - Ideally $X_{L1}X_{L2} = Z_{L1}Z_{L2} = 1$ and $Y_{L1}Y_{L2} = -1$
- ~70’000 shots per logical operator, reject leakage, and calculate **expectation values**

Besedin, I., Kerschbaum M. *et al.,* arXiv: 2501.04612 (2025)

Logical State Tomography

- Measure **all nine basis combinations of repetition code logical qubits** to perform **logical quantum state tomography**

- Use extracted syndromes to **post-select** on zero syndrome elements (no error)
  - $Z_{L1}Z_{L2}$ error <1%: **fault tolerant** with respect to **bit-flips**
  - Expectation value of $X_{L1}X_{L2}$ and $Y_{L1}Y_{L2}$ limited by repetition code

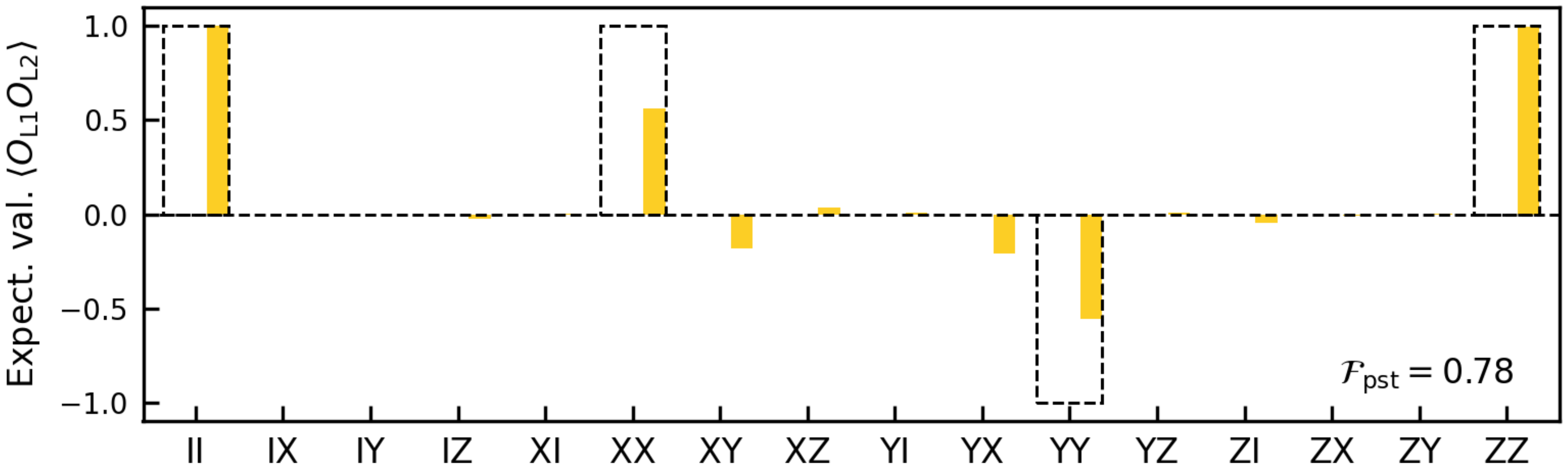

Besedin, I., Kerschbaum M. *et al.,* arXiv: 2501.04612 (2025)

Logical State Tomography

- Measure **all nine basis combinations of repetition code logical qubits** to perform **logical quantum state tomography**

Note

- Non-zero $X_{L1}Y_{L2}$ and $Y_{L1}X_{L2}$ expectation values
- Consistent with a $0.11\,\pi$ phase error on the first logical qubit state

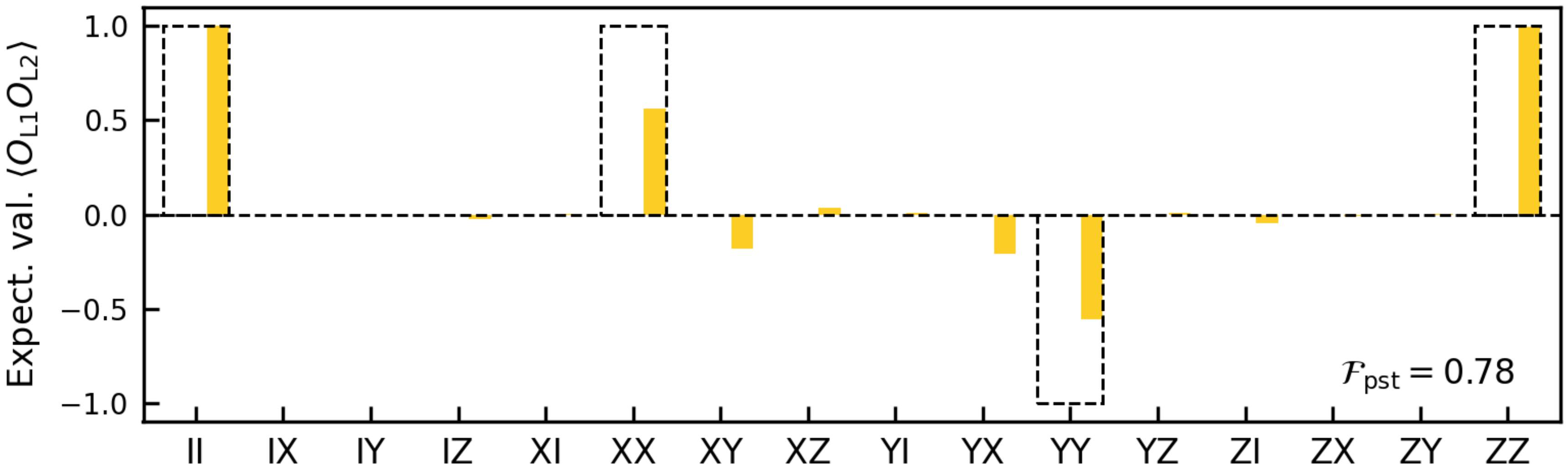

Besedin, I., Kerschbaum M. *et al.*, arXiv: 2501.04612 (2025)

Origin of Phase Error Consistent with Observations

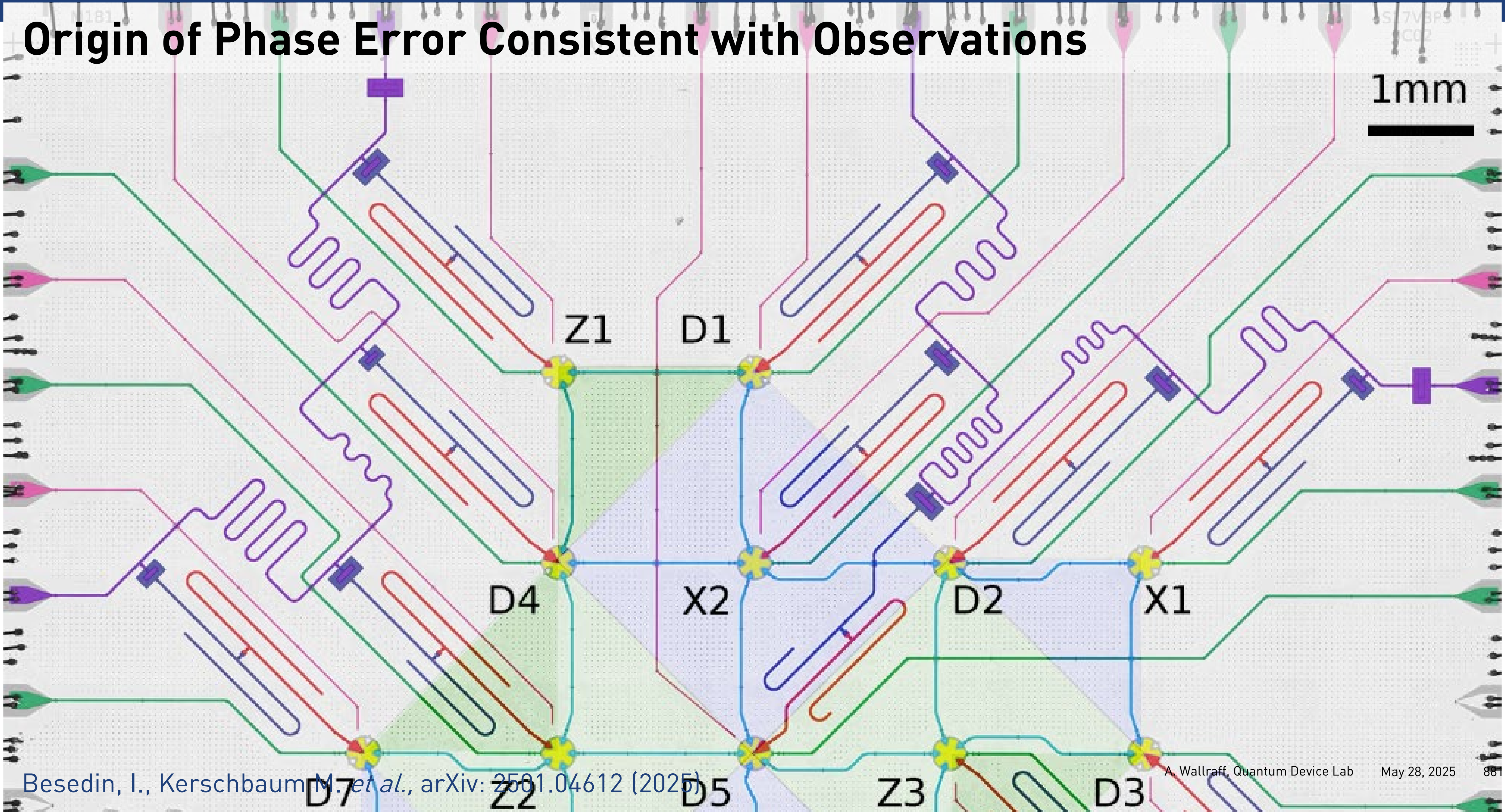

Besedin, I., Kerschbaum M. *et al.*, arXiv: 2501.04612 (2025)

Logical State Tomography

- Measure **in all nine combinations of bases of logical qubits** to perform **logical quantum state tomography**

- Use **MWPM decoder**:
  - raw Z_{L1} Z_{L2} = 0.19 is improved to 0.73
- Reasonable agreement of data with Pauli error model **simulations** based on randomized benchmarking (RB) and coherence measurements (+ coherent error on D1)

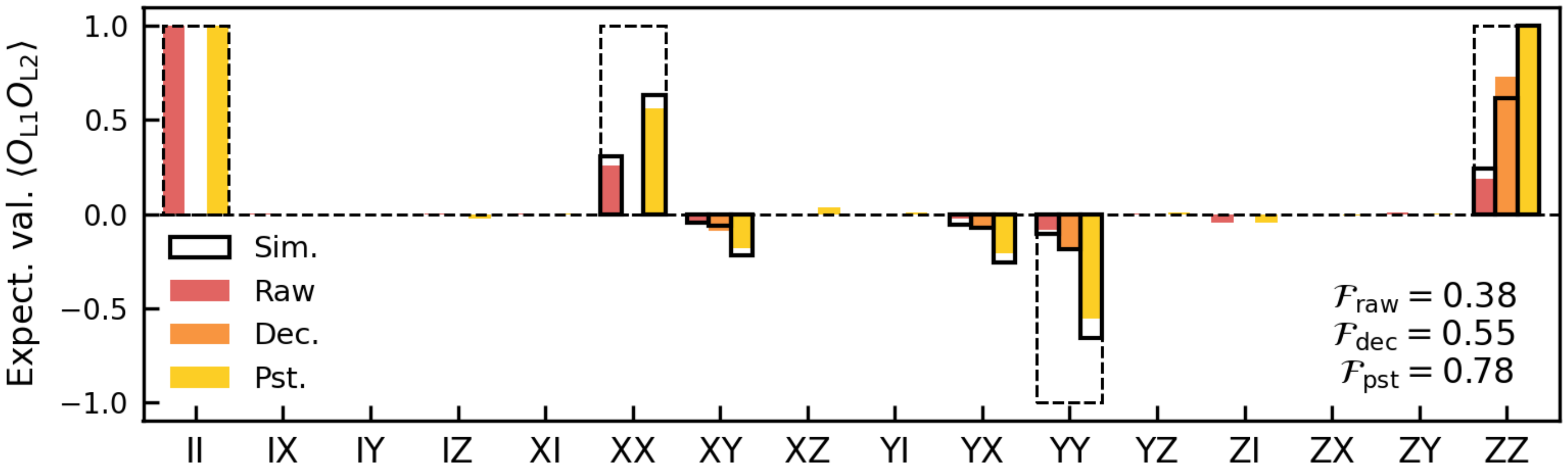

Besedin, I., Kerschbaum M. *et al.*, arXiv: 2501.04612 (2025)

Decoding Logical Operators

- Extract **weights based on correlations** in experimentally acquired syndrome data
  Spitz et al., Adv. Quantum Technol. 1 (2018)
  Remm et al., arXiv:2502.17722 (2025)

- connectivity of graph changed after lattice-split operation
  → **no strong correlations between repetition codes**
- Matched syndromes in **orange (yellow) flip Z_{L1} (Z_{L2}) operator**

- Decoded and post-selected logical density matrices

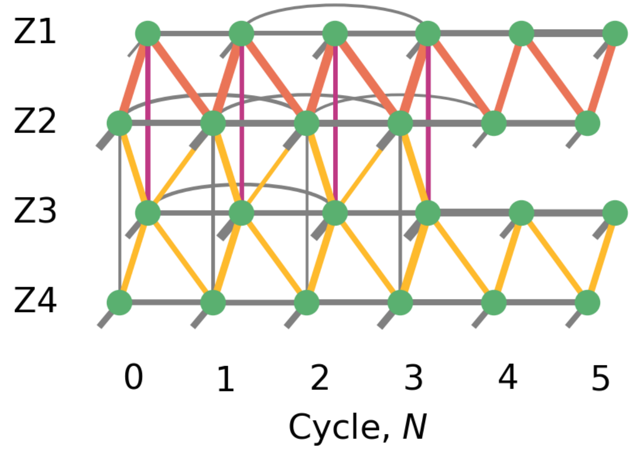

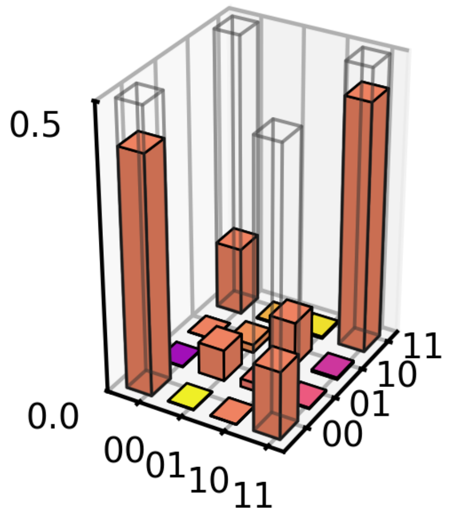

Decoded fidelity 55.3%

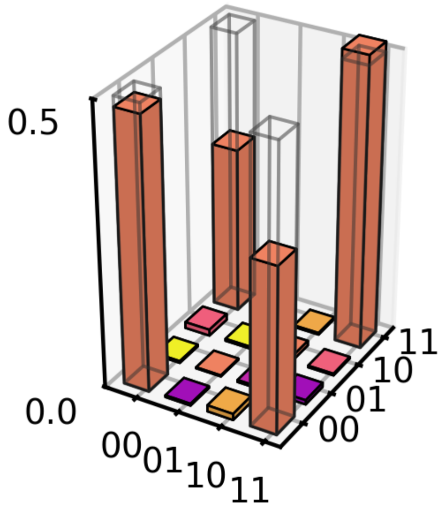

Postselected fidelity 78.8%

Besedin, I., Kerschbaum M. *et al.*, arXiv: 2501.04612 (2025)

Logical State Tomography

- Readout of X_L and Z_L observables of logical surface code qubits can be performed fault-tolerantly
- Final set of stabilizer outcomes determined from data qubit readout
- We also measure $\hat{Y}_L$ to reconstruct the full logical state (density matrix, Pauli sets)

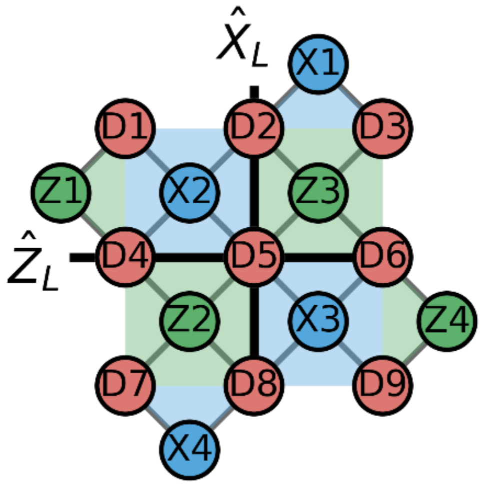

- $\hat{X}_L = \hat{X}_{D2}\hat{X}_{D5}\hat{X}_{D8}$
- $\hat{Z}_L = \hat{Z}_{D4}\hat{Z}_{D5}\hat{Z}_{D6}$
- $\hat{Y}_L = \hat{X}_{D2}\hat{Z}_{D4}\hat{Y}_{D5}\hat{Z}_{D6}\hat{X}_{D8}$

- We read out the corner data qubits in a basis that allows the weight-2 stabilizers to be determined.
- An incomplete subset of stabilizers can't be used to correct errors, but can help identifying some errors

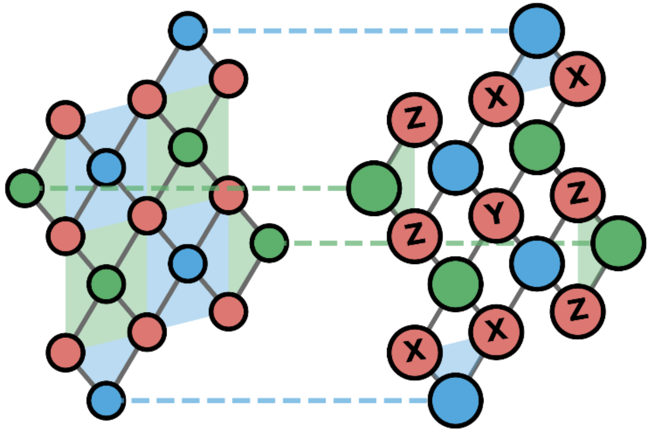

Ye, Y. et al. Phys. Rev. Lett. **131**, 210603 (2023)
L. Postler et al. Nature **605**, 675 (2022)
R. S. Gupta et al. Nature **625**, 259 (2024)

Parametrized Logical State Preparation

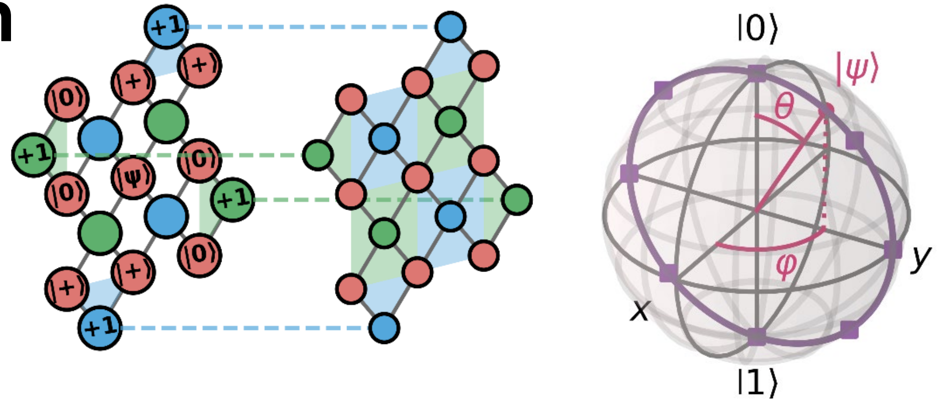

- Arbitrary state preparation scheme:
  Ye, Y. et al. Phys. Rev. Lett. **131**, 210603 (2023)
  - Central data qubit prepared in target state $|\psi\rangle$
  - Other data qubits prepared such that weight-2 stabilizers are in the +1 eigenstate
- We prepare states $|\psi\rangle = \cos\frac{\theta}{2}|0\rangle + \sin\frac{\theta}{2}e^{i\varphi}|1\rangle$

- After 1 cycle of error correction, we perform tomographic measurements, and determine the fidelity $\mathcal{F} = \langle\psi|\hat{\rho}_{\text{tomo}}|\psi\rangle$, average 83.5%
- **Postselected** average fidelity: 97.0%

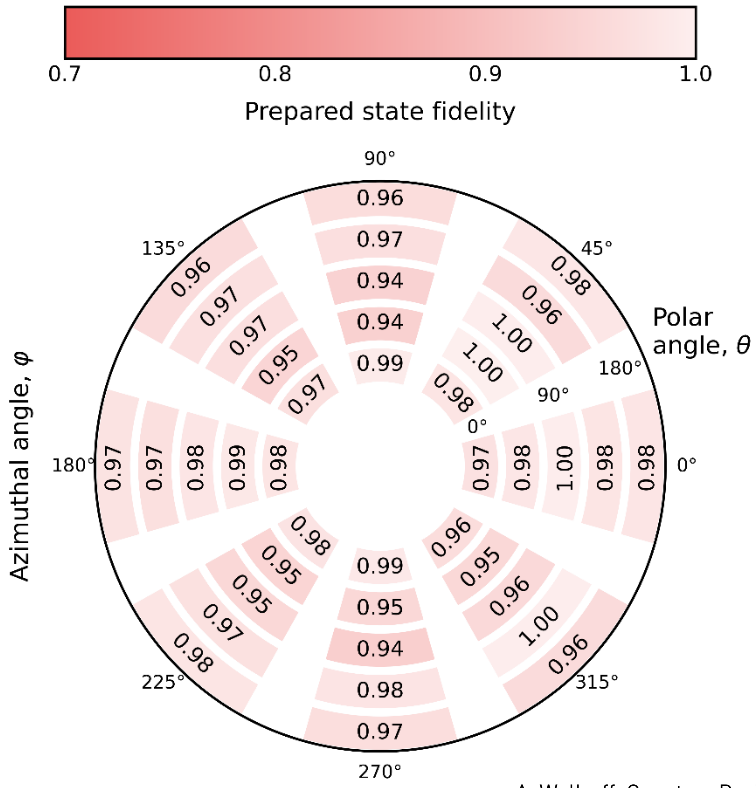

Besedin, I., Kerschbaum M. *et al.,* arXiv: 2501.04612 (2025)

Splitting of Parametrized Logical Qubit States

- Experiment combining arbitrary **logical-state preparation**, **logical-split operation** and **logical tomography**

- Consider initial states $|\psi\rangle$ in yz-plane

- Split operation after Pauli frame update:

  $$\alpha|+\rangle_L + \beta|-\rangle_L \rightarrow \alpha|+ +\rangle_{L1L2} + \beta|- -\rangle_{L1L2}$$

- Consider non-zero logical two-qubit operators:

  $$\hat{X}_{L1}\hat{X}_{L2} = +1$$
  $$\hat{Z}_L \rightarrow \hat{Z}_{L1}\hat{Z}_{L2} = -\hat{Y}_{L1}\hat{Y}_{L2}$$
  $$\hat{Y}_L \rightarrow \hat{Z}_{L1}Y_{L2} = \hat{Y}_{L1}\hat{Z}_{L2}$$

●●●● Error-corrected

○○○○ Post selected on no syndrome events

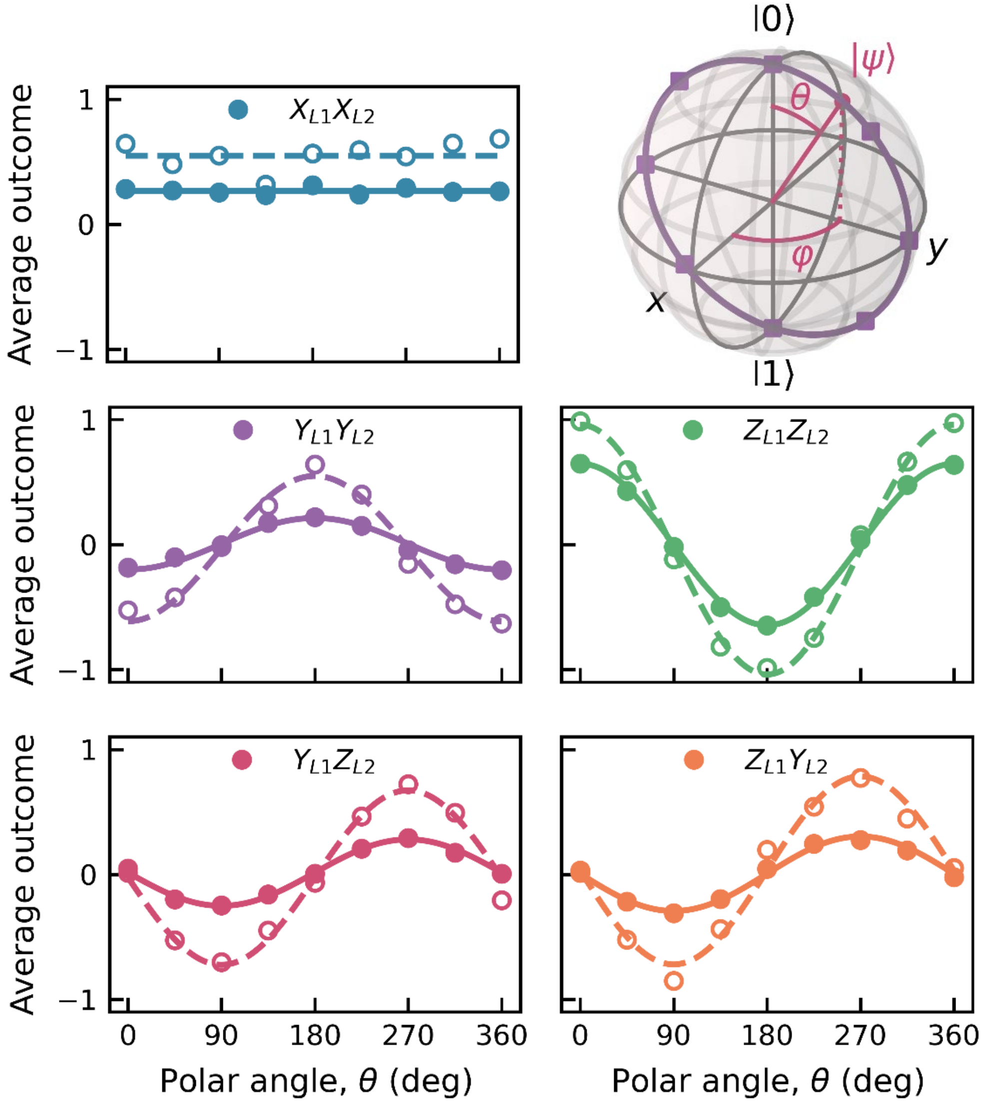

Besedin, I., Kerschbaum M. *et al.*, arXiv: 2501.04612 (2025)

Logical Quantum Process Tomography

- Split acting on logical input states $|0\rangle_L, |1\rangle_L, |+\rangle_L, |-\rangle_L, |+i\rangle_L, |-i\rangle_L$ states
- Split operation maps Pauli operators to Pauli operators
- Note: single-qubit phase rotation of 0.11π on logical qubit 1 corrected for.

- Pauli transfer matrix (PTM) representation
  - ideal values $\pm 1/2$
- Process fidelity
  - raw: $\mathcal{F} = 0.310(12)$
  - decoded: $\mathcal{F} = 0.442(12)$
  - post-selected: $\mathcal{F} = 0.80(3)$

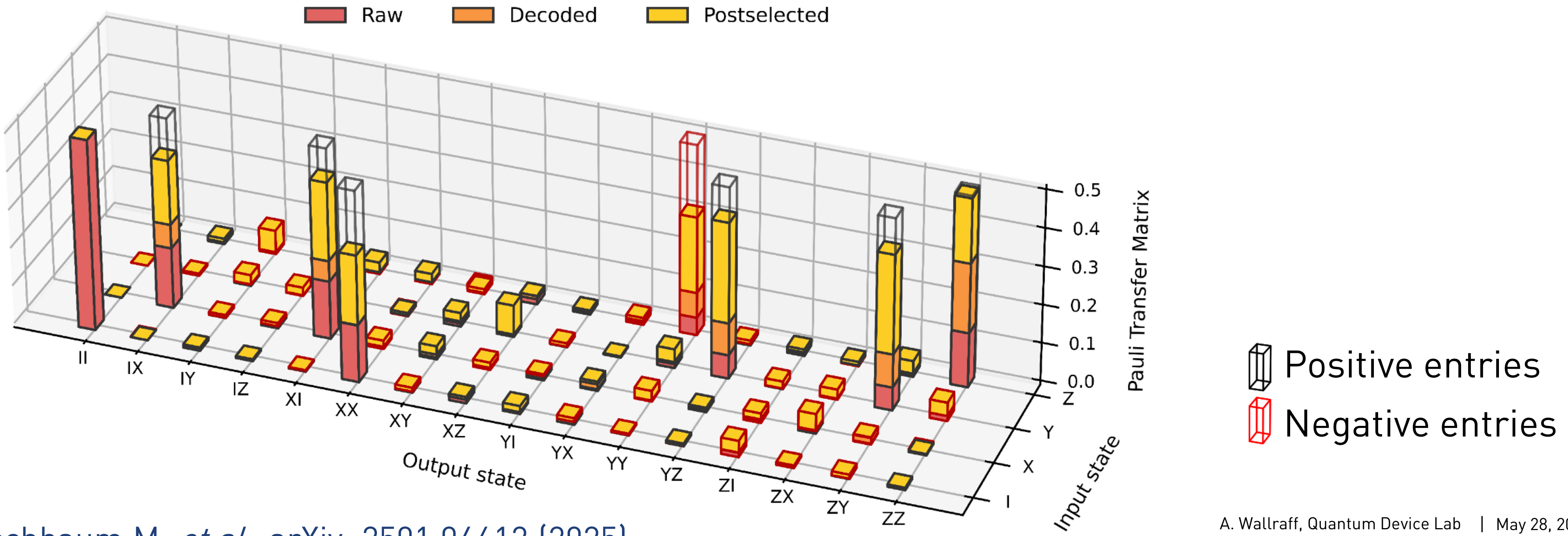

Besedin, I., Kerschbaum M. *et al.*, arXiv: 2501.04612 (2025)

Summary and Outlook

- Demonstrated **lattice surgery** on a distance-three surface code, **creating a logical Bell state** of two distance-three repetition codes
- **Increased decoded observable expectation value** compared to non-encoded variant
- Measured **logical Pauli-transfer matrix** for lattice split operation

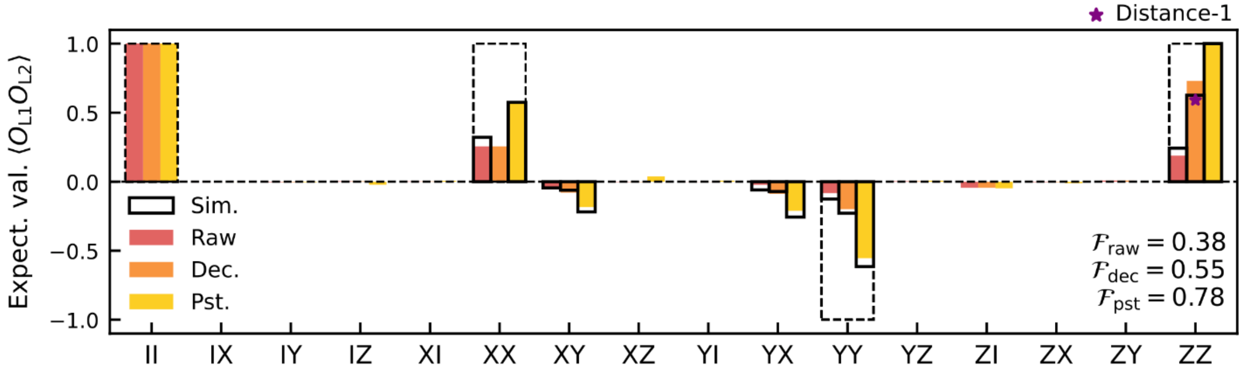

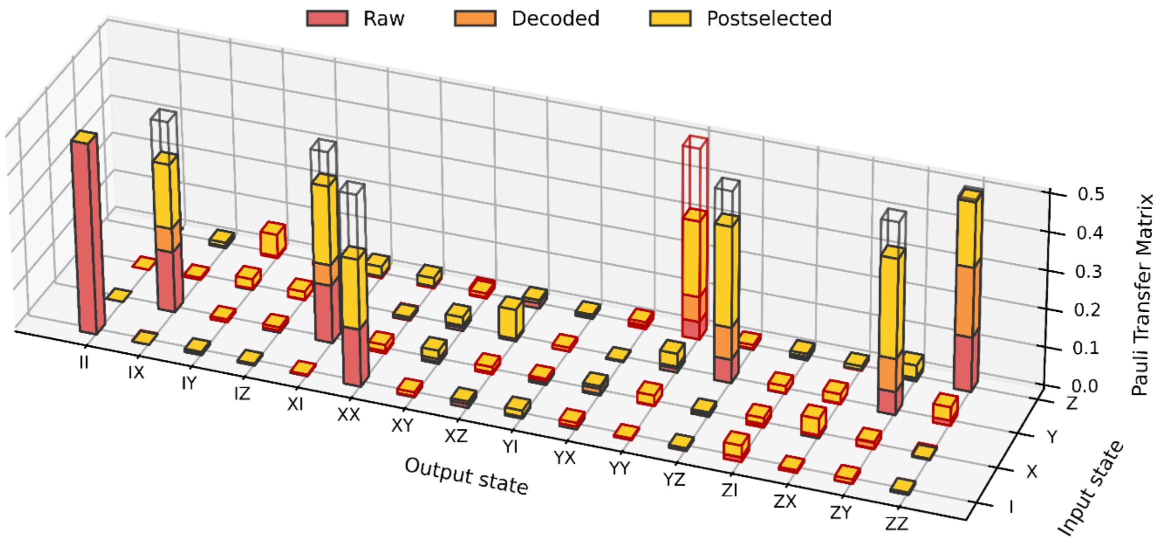

Outlook

- Deploy full scheme on two distance-three surface codes and integrate in **logical state teleportation protocol**

The Quantum Device Lab

with spring-term project students

Innovation project supported by
Schweizerische Eidgenossenschaft
Confédération suisse
Confederazione Svizzera
Confederaziun svizra
Swiss Confederation
Innosuisse – Swiss Innovation Agency

Schweizerischer Nationalfonds

IARPA
BE THE FUTURE

Want to work with us?
Looking for Grad Students, PostDocs and Technical Staff.